

Grant Number: 07600-051

Planetary Exploration Using Biomimetics

Phase I Final Report

Principal Investigator: Anthony Colozza

**OAI
22800 Cedar Point Road
Cleveland, Ohio 44142**

November 30, 2000

**Prepared for:
NASA Institute for Advanced Concepts
Atlanta, Georgia**

Table of Contents

Acknowledgements	3
Introduction	3
History of Flight on Mars.....	4
Insect Flight Aerodynamics	7
Entomopter Development	10
Environmental Conditions for Flight on Mars	14
Atmospheric Composition and Conditions	15
Dust Storms and Wind	18
Soil Composition.....	19
Mission Profile	20
Independent exploration using an entomopter	21
Exploration within the range of a central vehicle.	21
Tandem System	22
Science Objectives	24
Design	25
Power Production	26
Communications.....	27
Science Instruments.....	27
Internal Systems	28
Photovoltaic/Battery.....	29
Thermoelectric Power Generation	36
Linear Alternator System	39
Nuclear	39
Propulsion System.....	41
Propellant Selection.....	42
<i>In Situ</i> Propellant Production	51
Vehicle Configuration/Design.....	55
Performance Estimates	59
Communications.....	61
Summary	67
Bibliographic References	70
Appendix A: Mars Atmosphere Data	73

Acknowledgements

OAI and the authors of this report would like to acknowledge the contribution to this effort provided by Dr. Geoffrey Landis, Lisa Kohout and Marc Seibert of the NASA Glenn Research Center, and Dr. Phillip Jenkins and Andrew Sexton of OAI. Specifically, Ms. Kohout provided guidance and knowledge throughout the effort and Mr. Seibert provided the communications concept that is described in this report.

Introduction

Conventional flight on Mars is very difficult. Though contemplated for the past 50 years, the problems of operating a Mars aircraft using conventional aerodynamics have been sufficiently daunting that none of the various Mars Flyer programs have gone forward.

The environment on Mars makes the ability to fly much more difficult than on Earth. The main obstacle is the very low atmospheric density. This low density requires an aircraft to fly within a very low Reynolds number/ high Mach number regime. This low Reynolds number problem is compounded by the size restrictions for an aircraft, which must fit and deploy from an aeroshell, especially if it is a Mars micro-mission capsule. As a possible way around this low Reynolds number quandary, a plan is being presented to examine the concept of using an entomopter (an insect-like flapping wing, flying and crawling robotic vehicle), as the flight platform for a future Mars aircraft exploration mission.

Based on conventional aerodynamics, insects shouldn't be capable of generating sufficient lift to maintain flight, due to the size of the insect's wings and the Reynolds number they operate in. In 1994, Charles Ellington at the University of Cambridge investigated how insects generate lift to stay aloft. It was determined that a micro-scale vortex, created at the wing's leading edge during either the up or down stroke, was a source of increased lift. In addition, research conducted by the Georgia Tech Research Institute showed that the attachment of this leading edge vortex can be modified on a beat-to-beat basis, and thus control the entomopter attitude and flight path. This effect is thought to diminish as the scale approaches that of small birds (increasing Reynolds number). A Mars aircraft, with an approximate 1 meter wingspan, would be operating with a Reynolds number similar to that of terrestrial insects. Flight within the Mars environment can take advantage of this lift producing mechanism and may be an elegant architecture for producing an aircraft to fly on Mars. An additional advantage is that the Mars gravitational force is a third of that on Earth. This reduced gravity enables thinner, lighter structures to be used, which can be an important factor in the feasibility of this concept.

Recent work has been performed on terrestrial entomopter vehicles for applications such as reconnaissance and surveillance. The majority of this work has been for military applications and has been sponsored by the Department of Defense.

If achievable, an entomopter on Mars would have the ability to take off, land, and hover, a significant mission enhancement over conventional aircraft. This flight capability is a consequence of the flapping wing flight mode and the ability to control the enormous lift generating capacity of the vortex described above.

History of Flight on Mars

Mars has been a target of scientific exploration for more than twenty-five years. Most of this exploration has taken place using orbiting spacecraft or landers. Orbiters offer the ability to image large areas over an extended period of time, but are limited in their resolution. Landers can handle surface and atmospheric sampling, but are limited to the immediate landing site. Mobility is the key to expanding the scientific knowledge of Mars. The Pathfinder/Sojourner mission offered a new opportunity in that it was the first time that an autonomous mobile platform could be used for exploration. This allowed scientists the freedom to explore the surrounding terrain, maneuver to interesting sites, and perform an analysis of soil and rock composition over a broader area. In short, the scientific community has many more options. However, the surface rover is limited by the terrain it is traversing: large rocks and canyons are obstacles which are difficult for a surface rover to overcome.

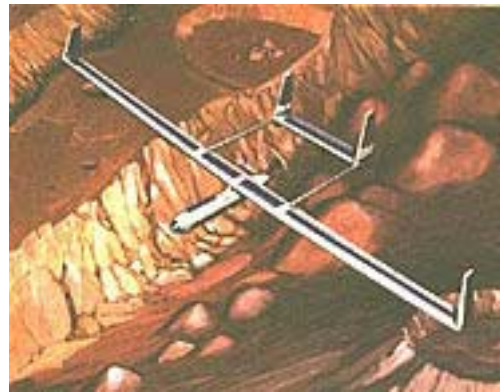
Airborne platforms can achieve science objectives that are difficult to achieve from orbit or from surface rovers. They can cover much larger distances in a single mission than a rover and are not limited by the terrain, much more easily providing imaging of very rocky or steep terrain. Airborne platforms can return images of a magnitude higher resolution than state-of-the-art orbiting spacecraft. Near infrared spectrometry, which is crucial to analyzing mineralogy on the planet, and high spatial resolution magnetometry, which may provide clues as to the origin of high crustal magnetism seen from orbit, require moving platforms. The resolution and sensitivity of these instruments is further increased by being close to the surface. Finally, atmospheric sampling can be accomplished over a far greater space, allowing scientists to study variations over a broad area.

The notion of flight on Mars has been a subject of NASA contemplation since Werner von Braun conceived a rocket plane as a means of Martian exploration in 1953. In the '50s Mars flight was purely fancy, but in the 1970s it was revisited more seriously, being spurred on by the successes of the Viking Program.

One of the most studied airborne platforms for Mars is the airplane, with initial concepts dating back to the late 1970's. Flying an airplane on Mars represents a significant challenge, mainly because of the constraints posed by the Mars environment. The lift on a wing is proportional to the atmospheric density, velocity, and wing area. The Mars atmospheric density is extremely low, approximately $1/70^{\text{th}}$ that at the earth's surface. In order to compensate for this, the wing area and/or the velocity must be increased to generate sufficient lift. Wing area, however, is limited by packing, volume, and deployment constraints. Therefore, in order for flight to be feasible on Mars, the plane must travel at higher velocities to compensate for the lack of density and the constrained

wing area. Also, the speed of sound on Mars is approximately 20% less than on Earth. Both of these factors combine to put the plane in a low Reynolds number, high Mach number flight regime which is rarely encountered here on Earth. The high velocities limit imaging camera stability and resolution. Also, given the rocky Martian terrain, it is virtually impossible for a plane to land and take-off again, thus limiting a mission to a single flight.

The NASA Dryden Research Center, Developmental Sciences, Inc., and the Jet Propulsion Laboratory (JPL) proposed unmanned aircraft designs for Mars exploration in 1977 and 1978 [1]. Their concept was a propeller-driven fixed wing aircraft fueled by hydrazine. This aircraft was based on the Mini-Sniffer high altitude aircraft. A prototype of this aircraft was constructed and some testing was performed. [Figure 1]



Mini-Sniffer High Altitude Aircraft

Solar Powered Mars Aircraft

Figure 1. Examples of aircraft concepts for Mars flight.

A decade later, JPL sponsored a Mars airplane study in which Aurora Flight Sciences proposed the electrically propelled “Jason” aircraft. About the same time, Ames Research Center and Sandia National Labs conceived a high speed aerospaceplane named AEROLUS. Unlike the earlier attempts to make a slow speed aircraft that would be deployed from an aeroshell after touchdown on the Martian surface, AEROLUS would make a direct atmospheric entry and then fly through the Martian atmosphere at hypersonic speeds. To date, neither the Jason nor the AEROLUS projects have been embraced by NASA’s Mars exploration program.

Throughout the 1980’s and early 1990’s, a number of studies were conducted looking at various approaches to flight on Mars. These studies were conducted by NASA and various universities. An example of some of this work was the solar powered Mars aircraft studied by NASA [2]. [Artist’s concept Figure 1.]

Successes with the Mars Pathfinder and Global Surveyor programs renewed interest in Mars flyers for exploration. In 1995 NASA Dryden and Ames Research Centers once again considered unmanned aerial vehicles to extend the reconnaissance range of Mars landers. The new concept was to launch a small unmanned aerial vehicle (UAV) from

the lander after it had stabilized on the surface. The UAV would provide video of the immediate vicinity of the lander (within several thousand meters) to provide feedback as to the most interesting areas for investigation by ground-based rovers. The expendable, one-flight UAV would be electrically powered with rocket assisted takeoff.

The following year in 1996, the Ames Research Center proposed an unmanned Mars aircraft in response to a NASA Announcement of Opportunity for Discovery Exploration Missions. Ames' approach was to use a propeller driven, sailplane configuration which they called "Airplane for Mars Exploration" (AME). It was not, however, selected for the Discovery mission.



JPL "Kitty Hawk" Glider



Ames "MAGE" Aircraft

Figure 2. Recent proposed Mars aircraft.

On the following NASA Announcement of Opportunity for Discovery Exploration Missions in 1998, JPL submitted a proposal for a multiple glider system (dubbed "Kitty Hawk") wherein several areas could be investigated during a single mission. Being gliders, the vehicles were obviously limited in endurance, but benefited from the lack of weight and complexity associated with a propulsion system in return for redundancy of numbers. NASA Ames also submitted a proposal to the 1998 Announcement for a motorized UAV named "MAGE". This aircraft was based on a similar hydrazine propulsion system as the Mini-Sniffer concept. Both concepts deployed from an aeroshell once it had become subsonic, approximately 12,000 meters above the Martian surface. Again, neither concept was selected for the Discovery mission. [Figure 2.]

On February 1, 1999, NASA Director Daniel Goldin announced the "Mars Airplane Micromission," which would have been the first NASA micromission program to launch on an Ariane 5 rocket. The flight would have had the first Mars airplane arriving on the Red Planet around December of 2003, coincidentally close to the hundredth anniversary of the Wright Brothers' first flight. Although conceptual designs of the plane were completed, the project was cancelled due to funding constraints.

Insect Flight Aerodynamics

As stated previously, conventional flight within the Mars environment is fairly difficult, mainly because of the very low density atmosphere. This low density atmosphere translates into flight Reynolds numbers for the wing of around 50,000 and for a propeller of around 15,000. The Reynolds number is a ratio of the inertia forces to the viscous forces for a fluid flow. As a practical matter if the Reynolds number of two vehicles are similar then the aerodynamics of the vehicles should be similar.

$$\text{Reynolds Number} = (\text{Density}) * (\text{Characteristic Length}) * (\text{Velocity}) / (\text{Viscosity})$$

With a low flight Reynolds number a conventional aircraft has a number of aerodynamic issues that severely limit its performance. The main issue is laminar separation of the boundary layer. This separation can cause loss of lift resulting in a catastrophic loss of the aircraft. To avoid this flow separation the boundary layer must be transitioned from laminar to turbulent. Within low Reynolds number flow it is very difficult (if not impossible) to transition to a turbulent boundary layer. This flow restriction is a major factor which severely limits the flight envelope and capabilities of a conventional aircraft.

While conventional flight may be difficult under such low Reynolds numbers, insects have succeeded in efficiently exploiting the low Reynolds number flight regime. Although not yet completely documented, recent work has shown how the mechanisms in insect flight are significantly different from conventional aircraft. An important mechanism for lift generation on an insect wing is vortex interaction caused by the flapping motion, which is dependent on Reynolds number. As the Reynolds number increases this lift producing mechanism diminishes. Experiments have shown that with flow on an insect wing at Reynolds numbers greater than 10^6 there is a crisis of flow over the wing caused by early boundary layer separation. As the Reynolds number decreases to around 10^4 this crisis is greatly reduced and the flow displays a smoother shape. At Reynolds numbers of 10^3 down to 10, flow separation is absent. As the Reynolds number decreases other lift producing mechanisms such as differential velocity and drag, as well as other boundary layer effects may come into play. These Reynolds number effects are a main reason for the difference in the flight characteristics between birds and insects.

A diagram of this vortex generation is shown in Figure 3. This vortex generation is not completely explained by present theory, however, it is believed to be caused by the separation of flow over the leading edge of the insect wing. A diagram of the leading edge vortex formation is shown in Figure 4. [2], [3]

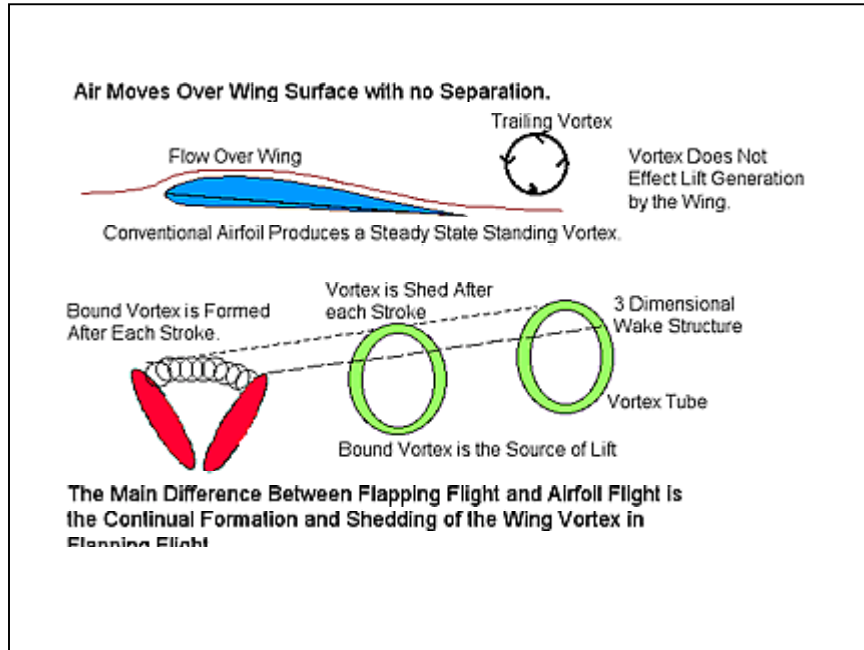


Figure 3. Conventional airfoil and insect wing lift generation mechanisms.

Flapping alone is not sufficient to generate the maximum vortex circulation possible for achieving maximum lift. This limit on reaching the maximum circulation levels is due to the flapping rate of the wings and the time delay required for the growth of the vortex circulation. It is believed that insects overcome this issue by the interaction of the insect wing with the vortex as it is shed (true in the dragon fly—the rear wing operates in the shed vortex of the front wing—not sure that all flapping things interact with the shed vortex).

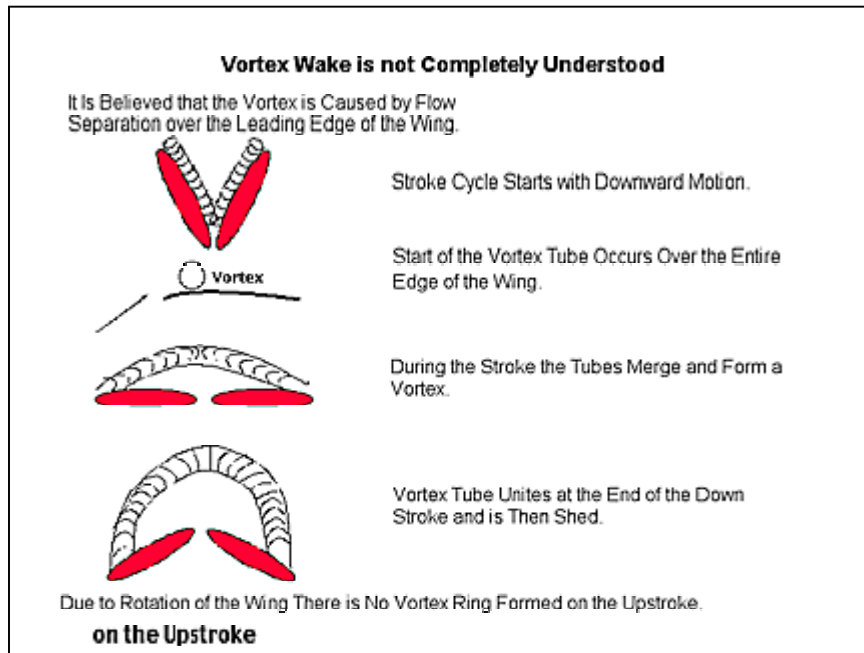


Figure 4. Flapping insect wing leading edge vortex formation.

Unlike with conventional airfoils there is no dramatic reduction in lift after the wing achieves super critical angles of attack. This suggests that flow separation prior to the vortex formation does not occur. It is believed that this resistance to flow separation during vortex formation is due to the low flight Reynolds number and the high wing flap rate of 10^{-1} to 10^{-2} seconds.

An additional lift producing mechanism which insects use is the magnus force. This is the force generated due to the rotational motion of the wing during each flap. This force is most widely know for its effect in producing a “curveball” in baseball. Insect flight control is achieved by controlling these lift producing mechanisms from wing to wing. Based on these mechanisms insects are capable of achieving lift coefficients on the order of $C_L=5$ [2]. This high lift coefficient, and the forces that are used to generate it, is what allows flight in a manner that is different from conventional aircraft or birds. It also gives insects the ability to hover, rise vertically and change direction instantly. A diagram of the lift produced through a stroke of the insects wings is shown in Figure 5. [2], [3]

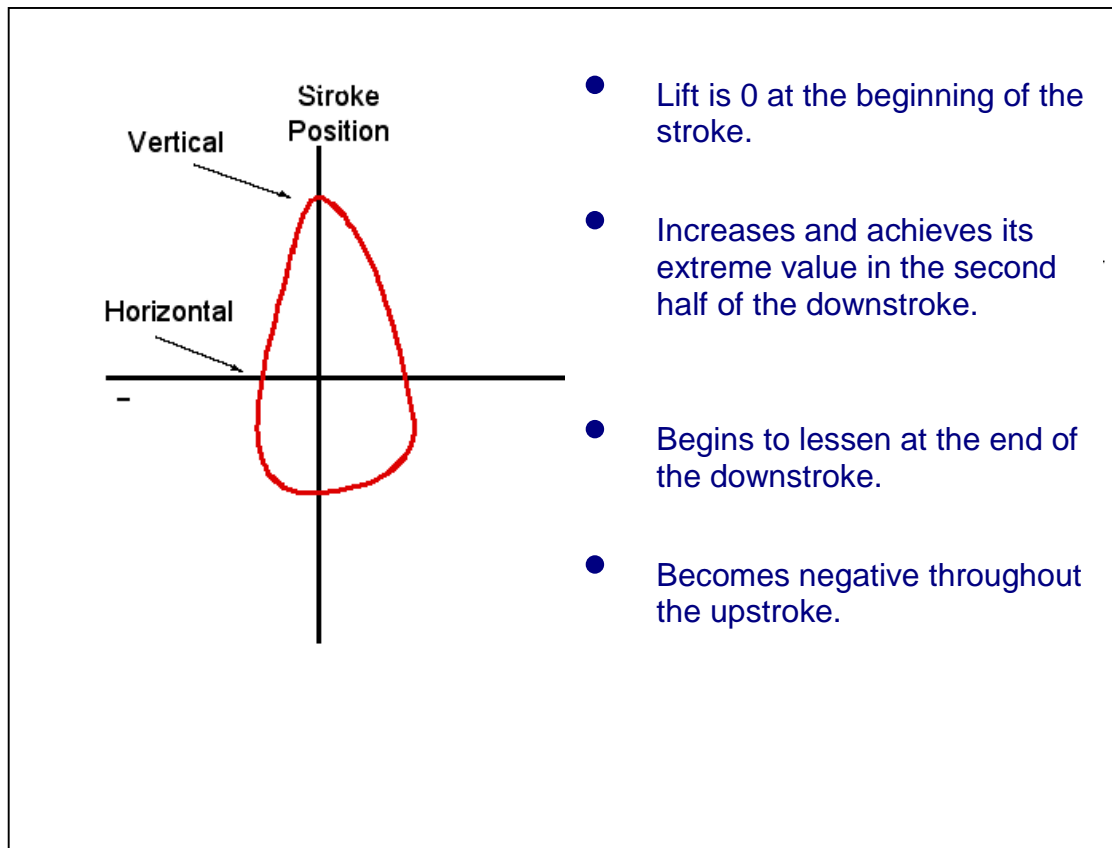


Figure 5. Insect wing lift generation profile.

Entomopter Development

The concept of an “entomopter” or insect-like flapping wing/crawling multimode aerial robot was conceived in the mid 1990’s at the Georgia Institute of Technology, where internal research and development funding was provided to demonstrate aspects of entomopter propulsion. The idea received Defense Advanced Research Projects Agency (DARPA) funding in 1998 and 1999 as a “Mesoscaled Aerial Robot” (MAR) to show feasibility for indoor applications. During the intervening years, the main propulsion unit, known as a Reciprocating Chemical Muscle (RCM), has moved through three generations of development, shrinking in size through each iteration, while increasing in reciprocation frequency.

From the first generation RCM, which could only move at reciprocation rates up to 10 Hz, through a second generation muscle able to achieve 20 Hz, the current third generation device is one quarter the size of the original prototype but produces reciprocation rates of 70 Hz, while generating stroke lengths and power outputs sufficient for flight of a 50 gram entomopter. [Figure 6] Still approximately two times larger than necessary for incorporation into a 50 gram entomopter, the RCM is currently moving into its fourth generation under funding from a U.S. Air Force Research Laboratory grant.

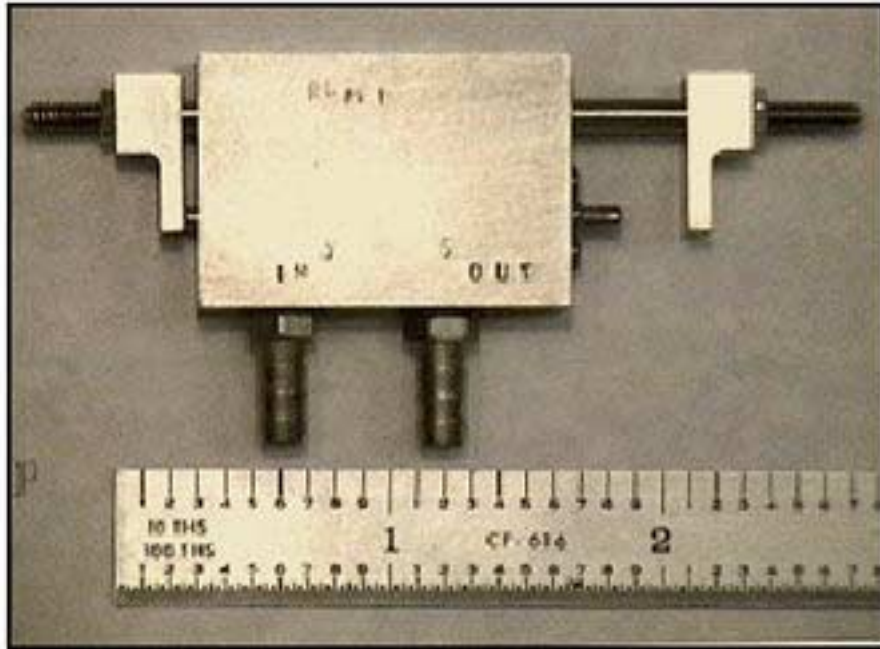


Figure 6. Third Generation Reciprocating Chemical Muscle (RCM) Testbed.

The entomopter was designed for indoor operation because there were no assets in the military inventory that could rapidly penetrate structures for reconnaissance, proactive, or relay missions. Its ability to crawl as well as fly in confined spaces made it a natural candidate for indoor applications where part of the ingress process might require movement through areas in which flight was impossible (such as under doors, or through air handling equipment). The choice of flapping wings was driven by the necessity for robust quiet flight operations in which the ability to land in confined spaces and takeoff again were desirable traits.

The development of the entomopter began by developing a prime propulsion unit that could support both flight and crawling behaviors from a limited energy source. Only then was the flight vehicle designed. Simply being able to flap wings was insufficient. The power necessary to flap the wings at rates of 25 to 35 Hz while lifting a 50 gram load could only be achieved marginally with electrical sources, so from the beginning a chemical source was considered.

The energy locked in chemical fuel sources is presently beyond that which can be stored in a battery or ultracapacitor of equal volume. The RCM was able to demonstrate that sufficient power and motion for flight was achievable from a chemical monopropellant.

The entomopter was then configured to take advantage of this type of propulsive source and went further in its level of design integration to incorporate the reuse of the waste products from the monopropellant decomposition not only to beat the wings with

sufficient force for flight, but also to perform six more necessary functions before finally being released to the atmosphere. At the scale of the 50 gram entomopter energy is at such a premium that it cannot be wasted. After the heat of reaction is used to flap the entomopter wings, the gaseous waste product is used:

- in gas bearings to reduced friction without wetted parts,
- to supply small amounts of electricity by means of thermoelectric scavenging of waste gas heat,
- to create a frequency modulated continuous wave (FMCW) ultrasonic sonar signal for hemispherical obstacle avoidance and altimetry,
- to entrain external atmospheric gasses through an ejector as a means of cooling the waste product and increasing mass flow,
- to control the lift of the wings on a beat-to-beat basis using active flow control as a means of platform stabilization and navigation, and even
- to provide directional jet thrust.

The basic entomopter design is comprised of a fore and aft wing that rotate about a central torsional fuselage at a constant beat frequency (see Figure 7). This method of wing flapping is like nothing found in nature, yet has been demonstrated in rubber band powered models. Unlike the entomopter, these models do not take advantage of resonance in their structure and are inherently inefficient. Further, they are low lift shallow wing beat devices. Nonetheless, they do fly. The efficiency of the entomopter will be far superior to its rubber band powered models, achieving greater coupling of energy from the wings into the air, coefficients of lift greater than $C_L = 5$ (C_L for conventional wings is on the order of 1), and lift generation on not only the down beat of the wing, but also on the upbeat—something that is not achieved by any flapping wing creature.

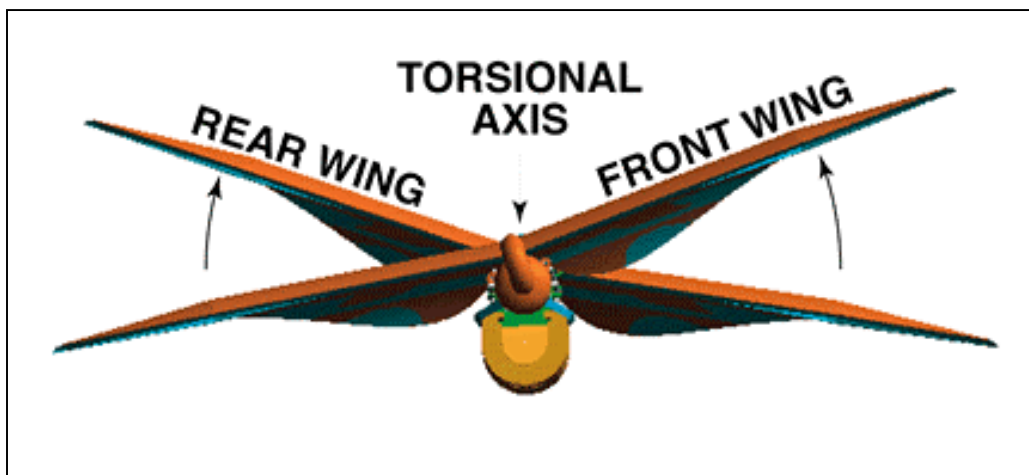


Figure 7. X-wing motion of fore and aft wings as viewed from front of entomopter

The high degree of innovation demonstrated in the entomopter design has resulted in a patent being issued by the U.S. Patent Office (Patent No. 6,082,671). A second patent for its Reciprocating Chemical Muscle is presently being processed by the Patent Office.

At its original DoD configuration and size, the entomopter will not fly on Mars... but it turns out that the Reynolds number regime in which the terrestrial entomopter will operate is essentially the same as that of a larger Mars entomopter. An entomopter of increased wing span should function efficiently in Mars' lower atmosphere with the added benefit that Mars' diminished gravity does not result in the same weight penalty were the terrestrial entomopter to be scaled up for flight in Earth's atmosphere.

So why is the entomopter particularly relevant to operations on Mars? In a global perspective, flight on Mars is significant to the development of future manned operations. However as a precursor, flight will enable large areas of the planet surface to be surveyed economically. From the standpoint of unmanned Mars surface surveyors, in the same time that a surface crawler can survey a particular area, a flying machine could cover an area that is orders of magnitude greater. The nature of the surveys will be drastically different however. The surface crawler is able to stop and sample its environment over a limited area. A traditional fixed wing or wind-driven balloon surveyor can identify widely scattered potential points of interest on the surface but lacks the ability to easily land and sample those points because of the necessary speed of flight or inability to maneuver.

A flying Mars surface surveyor that is capable of slow flight as well as multiple landings and takeoffs is of particular significance because such a capability now permits rapid wide area surveys of varying resolution, *in situ* sampling, and the potential for mission life extension by on-demand refueling.

The incorporation of Mars-based fuel production from indigenous materials adds further significance to the behavior of a Mars flyer to physically interact with the ground (and ground-based platforms), because now intelligent low speed flight missions can be discontinuous— lasting weeks or months instead of minutes or hours— and can be flown selectively when conditions are favorable.

The entomopter is just such a vehicle. Were a Mars Flyer to be based on the form and function of the entomopter, it would

- be capable of slow flight in the thin Mars atmosphere (due to the fact that its wings are still moving rapidly enough to generate sufficient lift),
- have the potential to land and takeoff again, while even crawling on the surface to position itself for sampling,
- exhibit enhanced flight control (small radius turns, slow flight and perhaps hovering) through the use of the same active flow control techniques designed for the terrestrial entomopter,
- use the same chemically fueled reciprocating chemical muscle technology for flight and ground propulsion, obstacle avoidance, and altimetry,
- benefit from the potential to use fuels manufactured *in situ* on the Mars surface by a roving companion factory or the lander from which it was originally deployed.

Environmental Conditions for Flight on Mars

The Martian environment provides a number of significant challenges to atmospheric flight, not the least of which are the lack of oxygen to support combustion for propulsion, a rarefied atmosphere, and extremely cold temperatures. Specifically, the Martian atmosphere is over 95% carbon dioxide and is less than 0.5% as dense as that of Earth. The average surface pressure is only 0.7% of Earth's atmosphere, which is roughly equivalent to Earth's atmospheric pressure at an altitude of 105,000 ft. The average temperature near the surface of Mars is -63°C , with diurnal highs and lows ranging from $+20^{\circ}\text{C}$ down to -140°C . Mars has only 37% of Earth's gravity, requiring less lift to be generated during flight. A detailed description of the environmental conditions is necessary in order to accurately assess the ability on an entomopter to fly within the atmosphere of Mars.

TABLE 1. PHYSICAL PROPERTIES OF MARS [1]

Inclination of Equator to Orbit	25.2°
Day Period	24h 39 m
Solar Radiation Intensity	Mean: 590 W/m^2 Parihelion: 718 W/m^2 Apehelion: 493 W/m^2
Gravitational Constant	3.73 m/s^2
Sidereal Year	687 days (Martian)
Surface Temperature Extremes	-143°C to 27°C

Atmospheric Composition and Conditions

TABLE 2. MARS ATMOSPHERIC COMPOSITION [1]

Gas	Percent Volume
Carbon Dioxide (CO ₂)	95.32
Nitrogen (N ₂)	2.7
Argon (Ar)	1.6
Oxygen (O ₂)	0.13
Carbon Monoxide (CO)	0.07
Water Vapor (H ₂ O)	0.03
Neon (Ne)	2.5 ppm
Krypton (Kr)	0.3 ppm
Xenon (Xe)	0.08 ppm

Mars atmospheric profiles are listed in Appendix A. This appendix consists of four atmospheric profiles generated by different sources and for different locations on Mars. The data available with each profile is not necessarily the same.

The first profile is a reference atmosphere supplied by JPL. This data was generated for a latitude of -20°. It provides data on temperature, pressure, viscosity and density from just above the surface to nearly 10 km. [2]

The second profile is a general atmospheric model that is not specific to any location. This was generated to provide a rough estimate of the atmospheric conditions at any location on the planet. It provides density, temperature, pressure and speed of sound data for elevations of -5km (below the mean surface level) to 120 km above the surface. [3]

The third profile was generated using the Mars-GRAM atmospheric simulation tool. This profile was generated for a specific location on Mars, Parana Valles (-25°, 11°). It contains information on density, temperature, pressure, speed of sound and viscosity for altitudes of 2.38 km to 20 km. [4]

The fourth and last profile was also generated using the Mars-GRAM atmospheric simulation tool. This profile was generated for a specific location on Mars Utopia Planitia (57°, 235°). It contains information on density, temperature, pressure speed of sound and viscosity for altitudes of -1.74 km to 20 km.[4]

Significant data was also collected on the Mars atmosphere during the recent Pathfinder mission. For the first 30 days, surface pressure at the landing site underwent substantial daily variations of 0.2 to 0.3 mbar, which were associated primarily with the large thermal tides in the thin Mars atmosphere. Daily pressure cycles were characterized by a

significant pressure change throughout the day period. This is shown in Figure 7 and the pressure change over a 30 day period is shown in Figure 9.

The near surface temperature on Mars is greatly influenced by the surface temperature cycle (surface heating during the day and radiative cooling at night due to the low density of the Martian atmosphere. At sunrise, the atmosphere is typically stable and cool dense air lies near the surface. As the surface warms, the air mass is heated and by early morning begins to rise. As the heating continues the atmosphere becomes unstable. This causes temperature fluctuations on the order of 15° to 20°K, which are observed during the remainder of the day. At sunset, the atmosphere cools, the instability

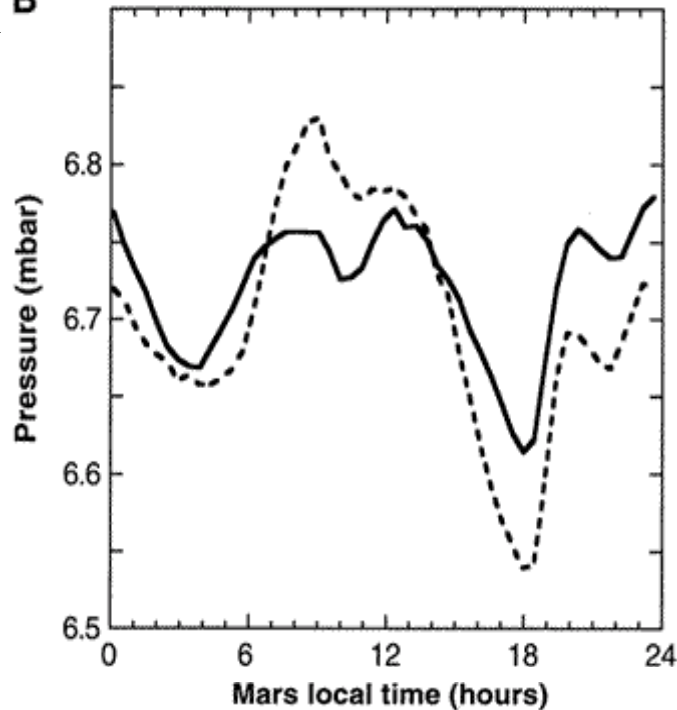


Figure 8. Daily pressure variation (Pathfinder Data). [5]

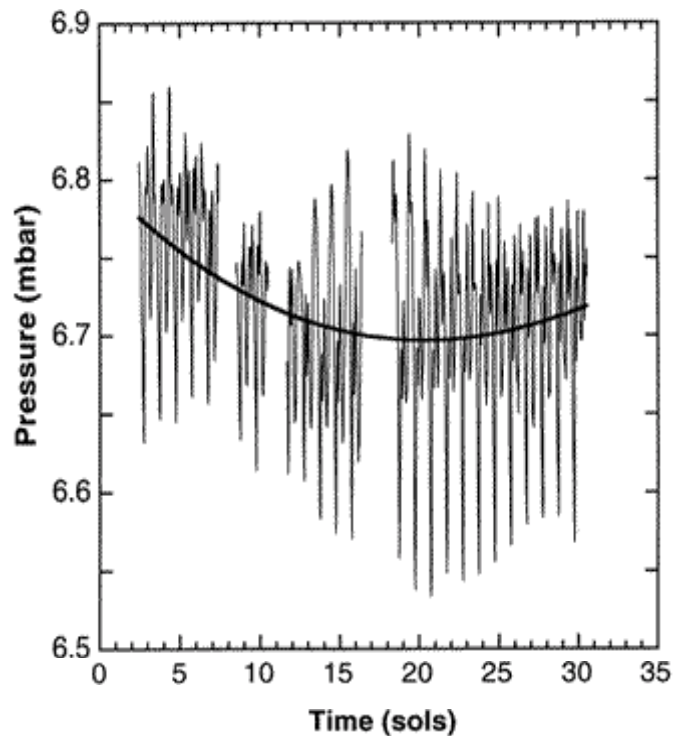


Figure 9. Pressure variation over a 1 month period (Pathfinder Data). [5]

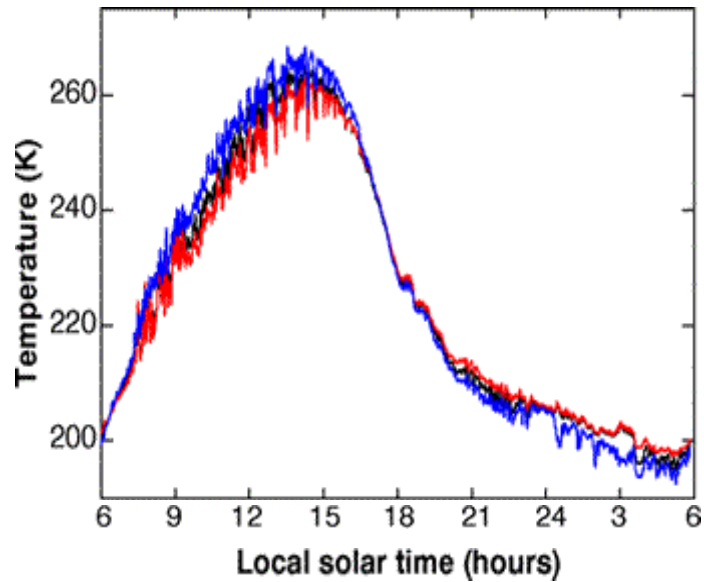


Figure 10. Atmospheric temperature variation throughout a day (Pathfinder Data) [5]

By evening, the thermal convection subsides and the instability in the atmosphere is diminished. The atmosphere becomes stable again due to surface cooling during the night time period. Any major nighttime temperature fluctuations are caused by downslope winds that disturb the surface boundary layer.

Dust Storms and Wind

The wind at or near the surface can range from 2 to 7 m/s, (based on Viking lander data). These winds have a strong diurnal and seasonal variation in both direction and magnitude. Wind speeds of up to and possibly greater than 50 m/s will occur above the surface boundary layer. This surface boundary layer is estimated to extend tens of meters above the surface. Preliminary estimates of the Pathfinder wind data suggest that wind speeds were comparable with or lower than those measured by Viking Lander-1 at the same time of year. Speeds were generally less than 5 to 10 m/s, except during the passage of dust devils, and were often less than 1 m/s in the morning hours. This may be consistent with the lower slope at the Pathfinder site. [5]

For a one month period, Pathfinder data shows that wind direction generally rotated in a clockwise manner through a full 360°. Winds were consistently from the South in the late and early morning and then rotated steadily through West, North, and East during the day period. The wind direction at nighttime was very consistent but became more variable throughout the day. The wind direction is shown in Figure 11.

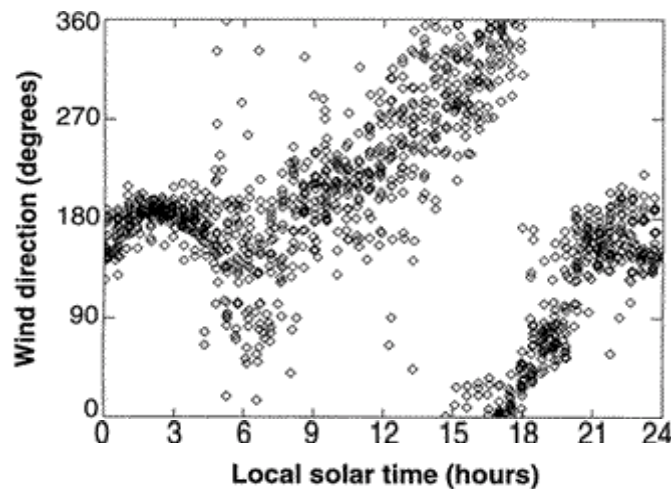


Figure 11. Wind Direction Throughout the Mars day (Pathfinder Data) [5]

Dust storms tend to occur when Mars is near perihelion in its orbit, when the solar intensity is the greatest. It is believed that the greater intensity of solar radiation coupled with variations in the topology of Mars triggers the dust storms. The storms can last up several months and the opacity of the storms can be quite high. Due to the low atmospheric density these dust storms result in only minimal distribution and accumulation of debris. More information on dust storms, gathered for the Mars micromission aircraft program is included in the bibliography.

Dust devils are short term variations in measured surface pressure, wind velocity and air temperature over periods of tens of seconds to minutes. This is shown in Figure 12. Dust devils, about 2 km width and a few kilometers high, have been observed in the tropics by the Viking orbiters.

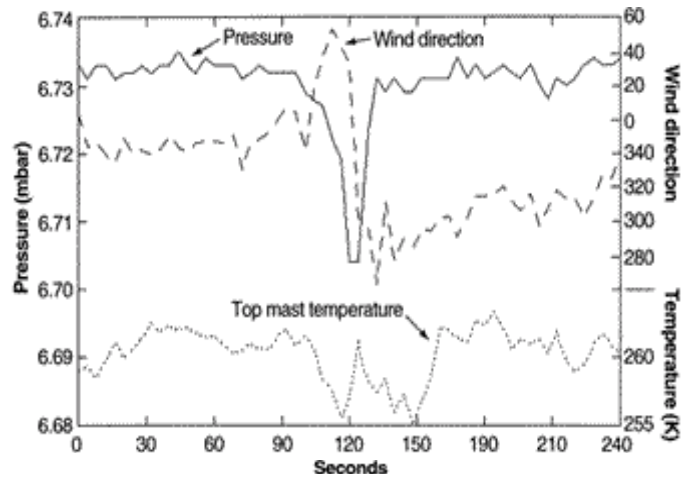


Figure 12. Measurements taken during a Dust Devil (Pathfinder data). [5]

Soil Composition

The soil composition of Mars is can be an important factor in the potential of utilizing *in situ* resources for propellant production. The data given on the soil composition was generated by the Mars Pathfinder mission.

TABLE 3. MINERAL COMPOSITION OF MARS SOIL [7]

Mineral Compound	Percent Composition by Weight
Na ₂ O	2.4
MgO	7.8
Al ₂ O ₃	8.6
SiO ₂	48.6
SO ₃	5.9
Cl	0.6
K ₂ O	0.3
CaO	6.1
TiO ₂	1.2
FeO	16.5

TABLE 4. ELEMENT COMPOSITION OF MARS SOIL [7]

Element	Percent of Soil Composition by Weight
Oxygen (O)	43.9
Sodium (Na)	3.8
Magnesium (Mg)	5.5
Aluminum (Al)	5.5
Silicon (Si)	20.2
Phosphorus (P)	1.5
Sulfur (S)	2.5
Chlorine (Cl)	0.6
Potassium (K)	0.6
Calcium (Ca)	3.4
Titanium (Ti)	0.7
Chromium (Cr)	0.3
Manganese (Mn)	0.4
Iron (Fe)	11.2
Nickel (Ni)	~0.1

Mission Profile

An entomopter on Mars would be a very capable tool for exploration. Because of the flight characteristics of this type of vehicle, exploration can be performed that would be impossible to perform with any other single platform. The way the entomopter is utilized

will also to some degree dictate its design. Therefore, for this initial design effort three potential scenarios were examined.

1. Independent exploration using an entomopter
2. Exploration within a range of a central vehicle
3. Tandem system, the entomopter works in conjunction with a rover

1. *Independent exploration using an entomopter*

In this scenario, a lander containing one or more entomopters lands on the surface. The lander is basically a transport vehicle with no other capabilities. The entomopters leave the lander and begin to explore the surrounding territory. The entomopters are independent vehicles and relay their data directly back to an orbiting communications platform or, if possible, to Earth. Depending on the type of power source, it may be possible for the entomopters to recharge (by utilizing solar energy) in order to extend mission time. This recharge capability would require the entomopter to remain stationary or sleep for a period of time. A typical mission segment might consist of a 20 to 30 minute flight followed by a 5 to 10 minute data relay session and then a 12 hour recharge time.

The main advantage of this type of mission structure is that the entomopter is not restricted to the local area near the lander. It is capable of exploring larger, more complex terrain. With recharge capability the mission duration and territory covered are limited only by mechanical failure. However, the main drawback to this scenario is that without the ability to recharge the mission duration would be short. The range of the vehicle would be twice that of a similar vehicle in Scenario 2, since it would not have to return to the lander, although it would not be capable of multiple trips.

2. *Exploration within the range of a central vehicle.*

For this scenario, a lander containing a number of entomopter vehicles would land on the surface. The entomopters would then depart this central vehicle and explore the surrounding terrain. All data and samples collected would be brought back to the central vehicle. This central vehicle would act as a refueling station for the entomopters as well as a communications link between the mission and Earth.

The main advantage of this type of mission structure is that the lander provides a number of applications which would otherwise have to be performed by the entomopter vehicle. The communications capabilities of the entomopters would not need to be great since they only need to extend over a short distance to the lander. Also the lander can provide a source of fuel for the entomopters, greatly extending their mission lifetime. This fuel can either be carried by the lander from earth or possibly made on site, depending on the type of fuel required. The ability to make fuel on site using solar power and the

atmosphere as a source would be a great benefit since it would provide a basically unlimited mission duration, limited only by mechanical failure.

The main drawback to this type of mission is that the exploration area is limited to the round trip range of the entomopter vehicles from the lander.

3. Tandem system, the entomopter works in conjunction with a rover

In this scenario a lander containing one or more entomopters as well as a rover vehicle lands on the surface. The rover and entomopters leave the lander and begin to explore. The lander is a transport vehicle and has no additional capabilities. The entomopters communicate with the rover which in turn relays the data to an orbiting communication system. The entomopters can assist the rover in terrain navigation as the group slowly moves across the surface. The mission capabilities would be similar to the first scenario, however in this case instead of a fixed lander the mobile rover is used as the home base. The entomopters would be able to dock with the rover for refueling [Figure 12], but their range would be limited to the round trip distance to and back from the rover.

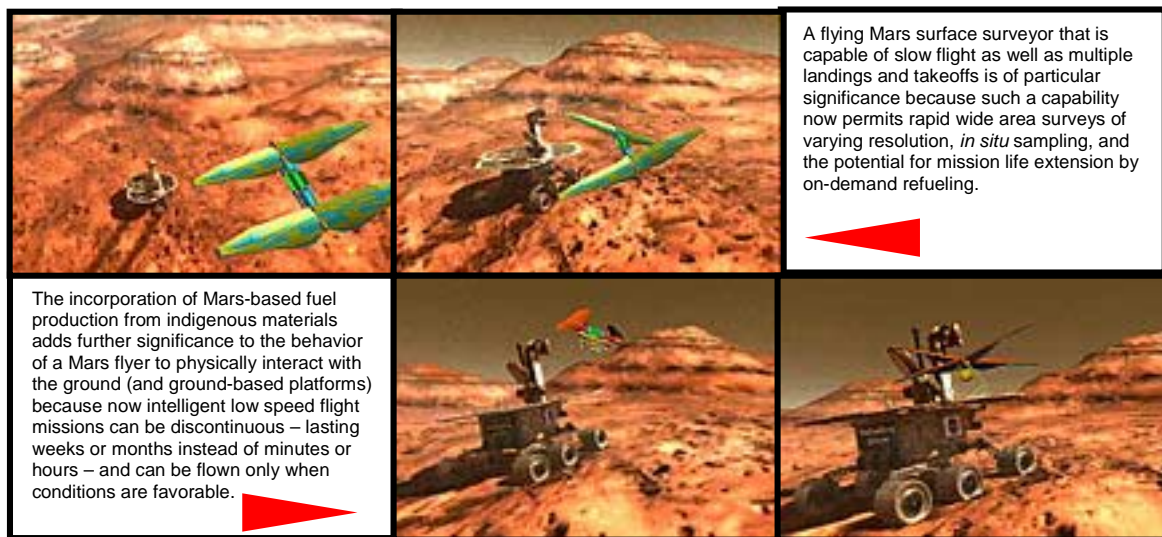


Figure 13. Entomopter acquires a roving fuel production unit and docks to it for refueling.

The main advantage of this type of system is that new territory can be explored each day by the entomopters, as their home base, the rover, slowly moves along the surface. This scenario only makes sense if recharge capability is available for the entomopters and rover. Either each vehicle is independently rechargeable or the rover acts as the refueling station. With rechargeable vehicles, the only limit on mission duration is mechanical failure.

A diagram of a potential mission scenario is shown in Figure 14. This Figure represents four entomopter flight vehicles flying to and from a fixed base station. The flight

duration profile, shown in the Figure, represents the flight and ground time for the entomopter throughout the return trip to and from the base vehicle. This is one example of flight profile. The combination of ground and flight segments can be altered and distributed differently to account for investigating varying points of interest along the flight path.

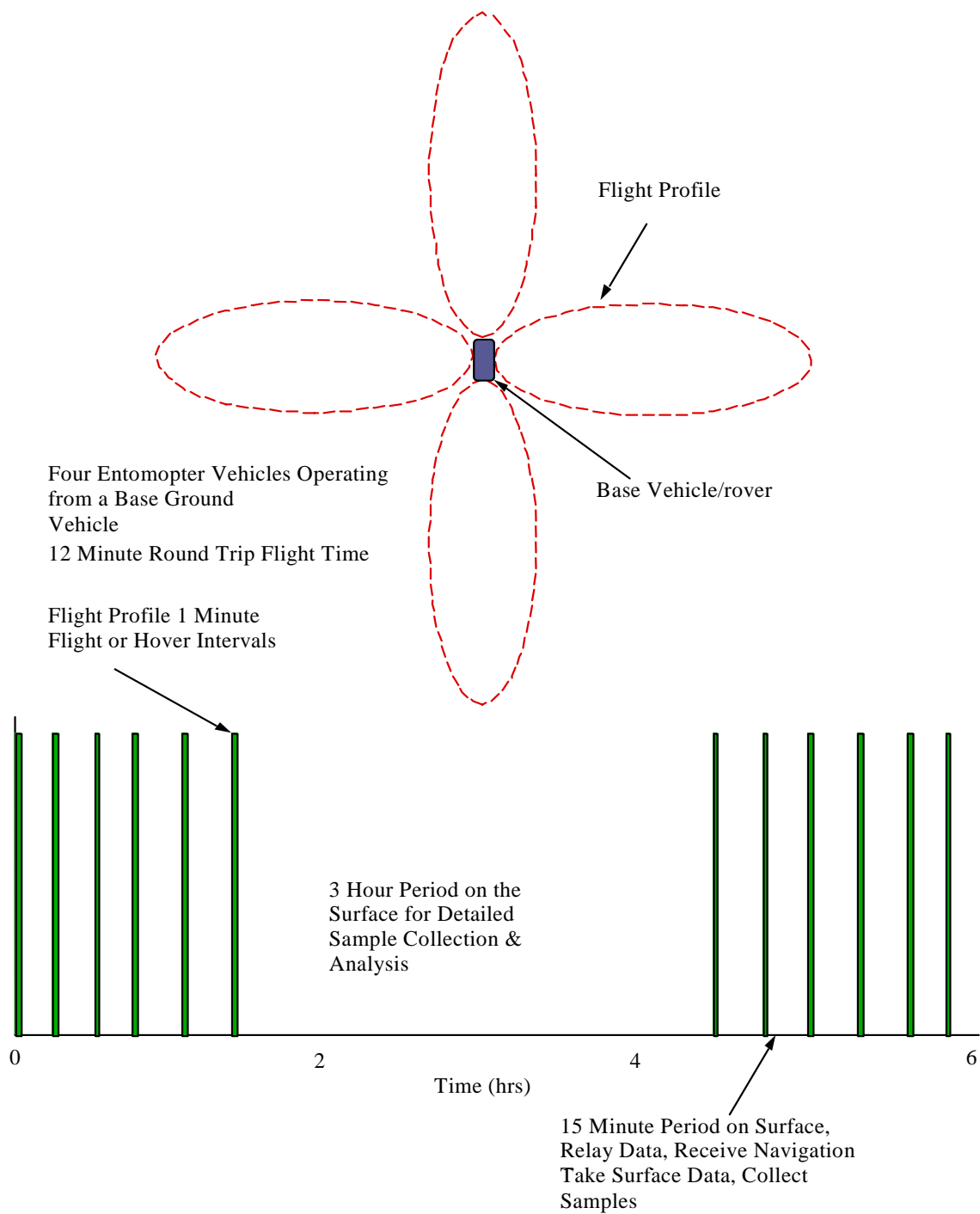


Figure 14. Diagram of Entomopter Flight Path and Duration.

Science Objectives

Using the three mission scenarios listed above a number of science objectives would be carried out by the entomopter. The missions can be structured so that each entomopter

vehicle carries only one science instrument. The amount of instrumentation carried by the entomopter will ultimately depend on its payload capacity and the weight of a given science instrument.

A definition of the requirements for the sensors and the type of science which can be performed on these missions can be found in Bibliography References 7 and 8. These references are from the Mars micromission aircraft program but there are a number of similarities between the Mars micromission aircraft science data collection and those that can be performed by the entomopter. A list of some of the science data that can be collected by the entomopter vehicle is shown in Table 5.

TABLE 5. ENTOMOPTER SCIENCE DATA CANDIDATES

Science Objective	Description
High Resolution Surface Imaging	Provide high resolution images of the Martian terrain, atmosphere, and horizon both while in flight and on the surface. Provide close up views of the surface material while on the surface. Camera weight ~78 gm, power consumption ~ 1W
Surface Mineralogy and Sampling	Collect and store samples of material from the surface. Also analyze surface material composition. Small samples would be carried back to the base vehicle for further examination. Analysis of larger, immovable object would be done on site. Composition analysis could be performed with an alpha proton X-ray spectrometer (similar to that used on Pathfinder) Pathfinder instrument specifications were 0.57 kg mass, 0.3 W power.
Atmospheric Sampling	Collect samples of the atmosphere at various altitudes. These samples would be analyzed for composition and dust content. Also atmospheric conditions will be monitored while in the air and on the surface. These conditions include temperature, pressure, and wind speed/direction.
Payload Delivery	There will also be the potential for payload delivery to the surface at various locations. The payloads would need to be micro instruments and can have a number of potential applications from beacons to micro weather stations.
Magnetic Field Mapping	A gauss meter will be used to map the local magnetic field.
Infrared and Radar Mapping	The potential exists utilizing a small infrared camera for imaging the surface in the infrared spectrum. Also a radar transmitter could be installed to allow for radar mapping of the terrain while in flight.

Design

The design of a Mars Flyer based on entomopter technology will involve the investigation of propulsion methods that are effective in the Mars atmosphere. Further, the choice of propellant to fuel the chosen method of propulsion must be compatible with the extremes of the Mars environment. A secondary, but important consideration with regard to the propellant, is its ability to be synthesized from indigenous materials readily available either on or near the surface, or in the atmosphere.

Given an appropriate propulsion system and a propellant to fuel it, the entomopter-based Mars Flyer must be able to execute a useful mission. This will entail the ability to perform self-stabilized behaviors such as takeoff, attitude maintenance, landing, refueling, navigation, and situation/environmental awareness. These innate functions are distinct from “payload” functions such as science experiments, telemetry, and communication, which may vary from one entomopter platform to the next.

The design of an entomopter-based Mars Flyer will leverage the existing body of knowledge resulting from earlier entomopter research and patents. The Mars Flyer is expected to benefit from the same features that make the terrestrial entomopter concept attractive. In particular, the multimode nature of an entomopter which is able not only to fly but crawl; its ability to fly slowly at low Reynolds numbers; its ability to generate abnormally high lift on any of its four wing sections upon command—using only the waste products of its propulsion system; and its ability to actively and remotely sense the presence of nearby objects for obstacle avoidance and altimetry, again by using the waste products of propulsion. These features are unique to the entomopter design and are distinct advantages when applied to a Mars Flyer.

These features will be incorporated into an entomopter-based Mars Flyer of larger scale (approximately 1 meter wing span) while using the reduced gravity of Mars to advantage in the choice of materials, as well as the determination of fuel and payload fractions.

Power Production

Although the entomopter engine is providing the power for propelling the vehicle, electric power is still needed to run the communications and science equipment. If the vehicle is to be used for repeated missions then this power system would need to be rechargeable or have the ability to produce power for extended periods of time. The systems that may be able to meet this requirement are the following:

- Photovoltaic/Battery system
- Thermoelectric
- Linear alternator
- Nuclear

The key to the evaluation of these systems will be whether they can meet the estimated power production requirements within the mass and volume constraint of the vehicle. The system will need to power the communications system, science equipment and on board computer systems. The overall power system design will depend on the power

needs for each of these systems as well as the load profile each requires. For the purposes of comparison, an estimate of the power requirements of each of the systems is given below. These estimates are based on an operational pattern (shown in the mission section) for each of the systems, which is considered as a "likely" mode of operation for the given system.

Communications

The transmitting power for the communications system is estimated to be 0.5 watts. The transmission from the communications system will be intermittent and depend greatly on the amount and type of data being transferred. An example of a transmission profile is given in Figure 15. The energy consumption by the communications system through one mission cycle would be 3 watt hours.

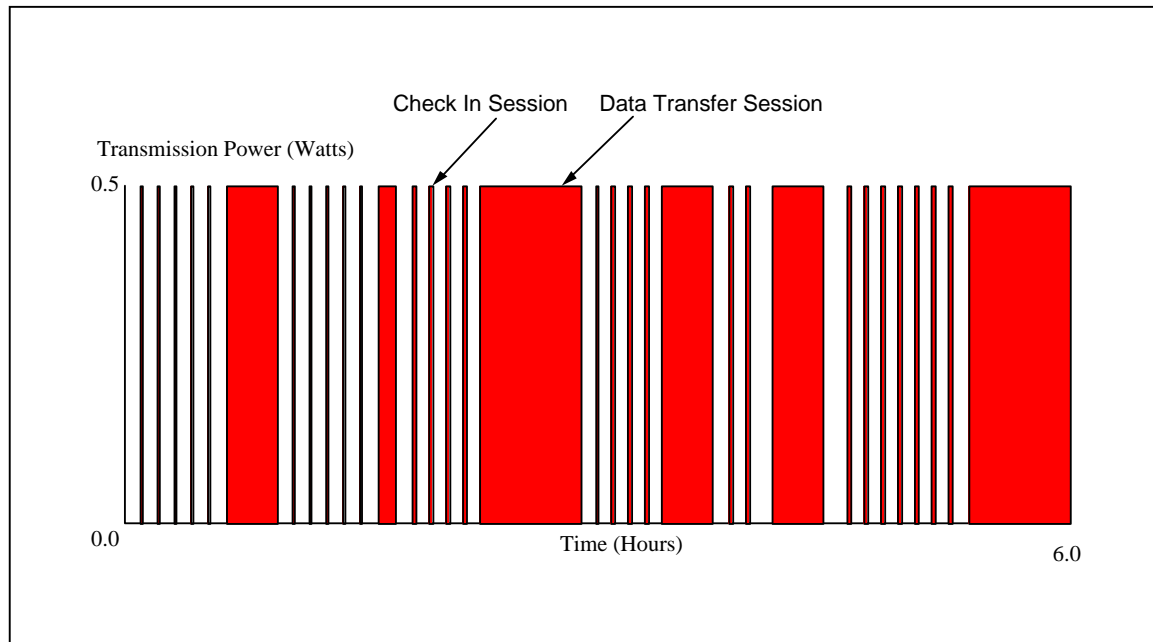


Figure 15. Typical communication power profile for one mission segment.

Science Instruments

The science instruments power requirements will depend on what type of equipment is being used and its duration of use. Also the ability to store and transmit the data collected will also effect the rate of use and therefore power consumption of the science instruments. It is assumed that while on the ground soil collection and sampling will require more power then the in flight instrumentation such as imaging. The energy consumption by the science instruments through one mission cycle is estimated as 10.7 watt-hours. An estimate of the science instrument power profile is shown in Figure 16.

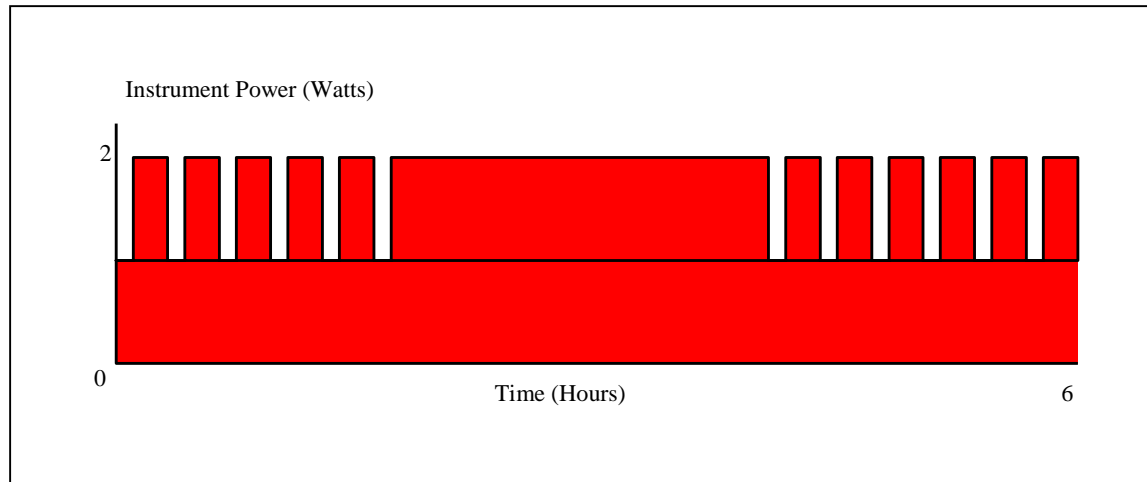


Figure 16. Typical science instrument power profile for one mission segment.

Internal Systems

The internal systems consist of any onboard computer as well as other internal systems which are used for vehicle operation. These systems would include health monitoring, avionics, and flight control. The energy consumption by the internal systems through one mission cycle would be 6 watt hours. An estimate of the internal system power profile is shown in Figure 17.

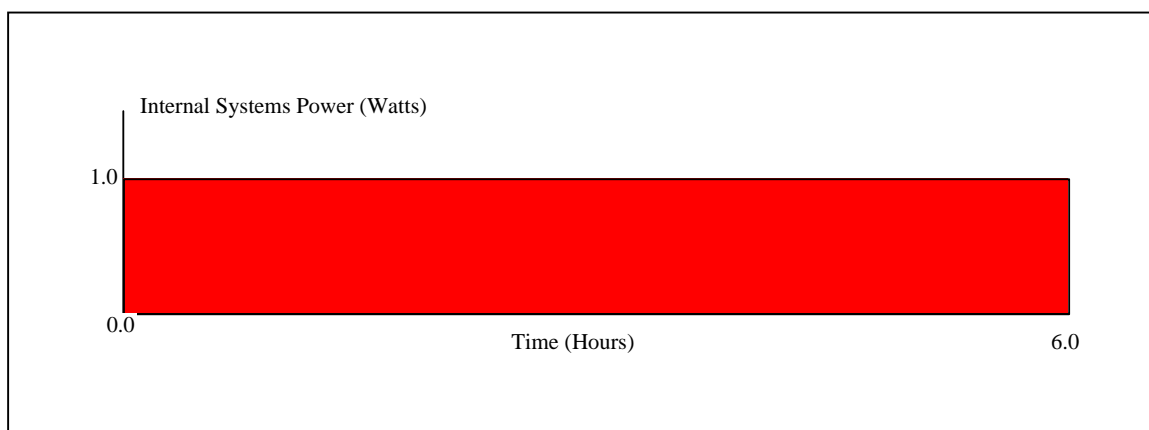


Figure 17. Typical internal systems power profile for one mission segment.

It should be noted that the mission specifications and power consumption profiles will greatly effect the power system sizing and selection. Any change in these specifications could change the conclusion as to which system is most applicable to the entomopter vehicle.

Photovoltaic/Battery

The photovoltaic (PV) system consists of a flexible thin film array mounted on the wings of the entomopter with a rechargeable battery and battery charge controller. The array supplies power directly to the loads as well as for recharging the battery. The battery charge controller monitors the rate and state of charge of the battery. The battery is used to supply power when either the array is inoperable (such as during the night period) or when the load requirements cannot be met by the array alone. A diagram of the system is shown in Figure 18.

The sizing of each of the components depends on the load requirements as well as the available power from the solar array. Some candidate solar arrays and their characteristics are listed in Table 6 [10]. The type of PV array best suited for this application is the thin film array. Thin film arrays are very light weight and flexible, can be easily molded to the entomopter's wing, and should not affect the aerodynamic performance of the vehicle. Depending on the characteristics of the solar array chosen it may be possible to use the array as the wing covering. This would reduce the structural mass of the vehicle, thereby reducing the impact of the PV array on the system. Thin film PV arrays are also very robust in their construction and present the greatest potential to withstand the acceleration/deceleration loads of the rapidly flapping wing. Because of these characteristics only thin film PV arrays were considered for this application. Figure 19 shows the advancement in performance of thin film solar cells over the last 25 years.

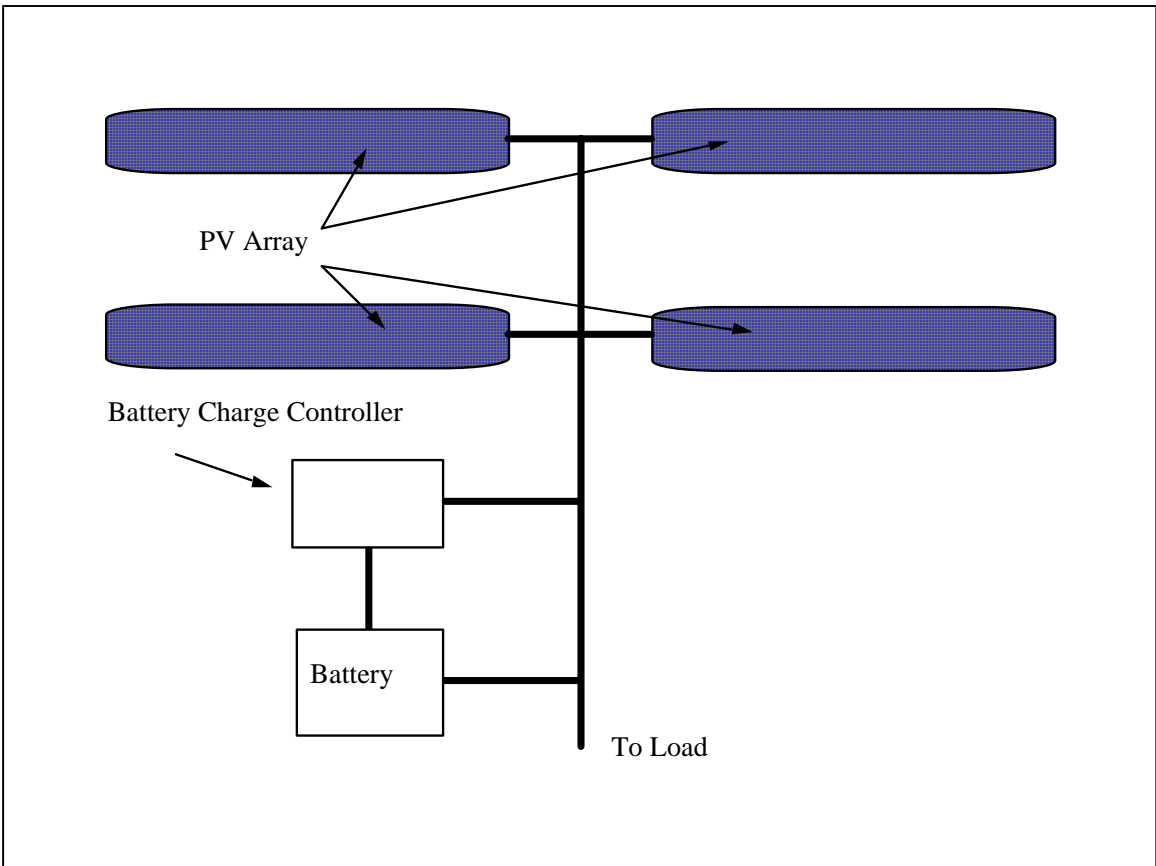


Figure 18. PV Array/Battery System Layout .

Polycrystalline Thin-Film Solar Cell Efficiencies

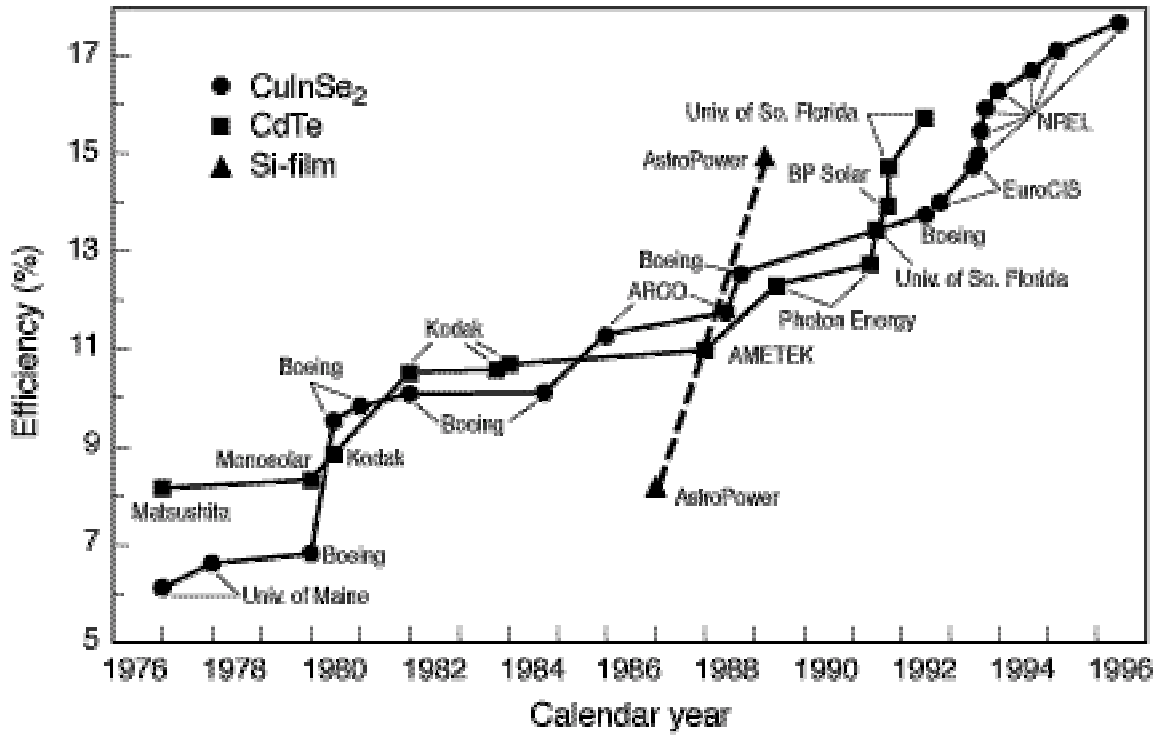


Figure 19. Thin film cell performance [10]

TABLE 6. THIN FILM SOLAR CELL TYPES AND THEIR CHARACTERISTICS

Solar Cell Type	Efficiency Range	Specific Mass kg/m ²
CuInSe ₂	11% to 6%	0.286
CdTe	8% to 15%	
Si-film	9% to 14%	

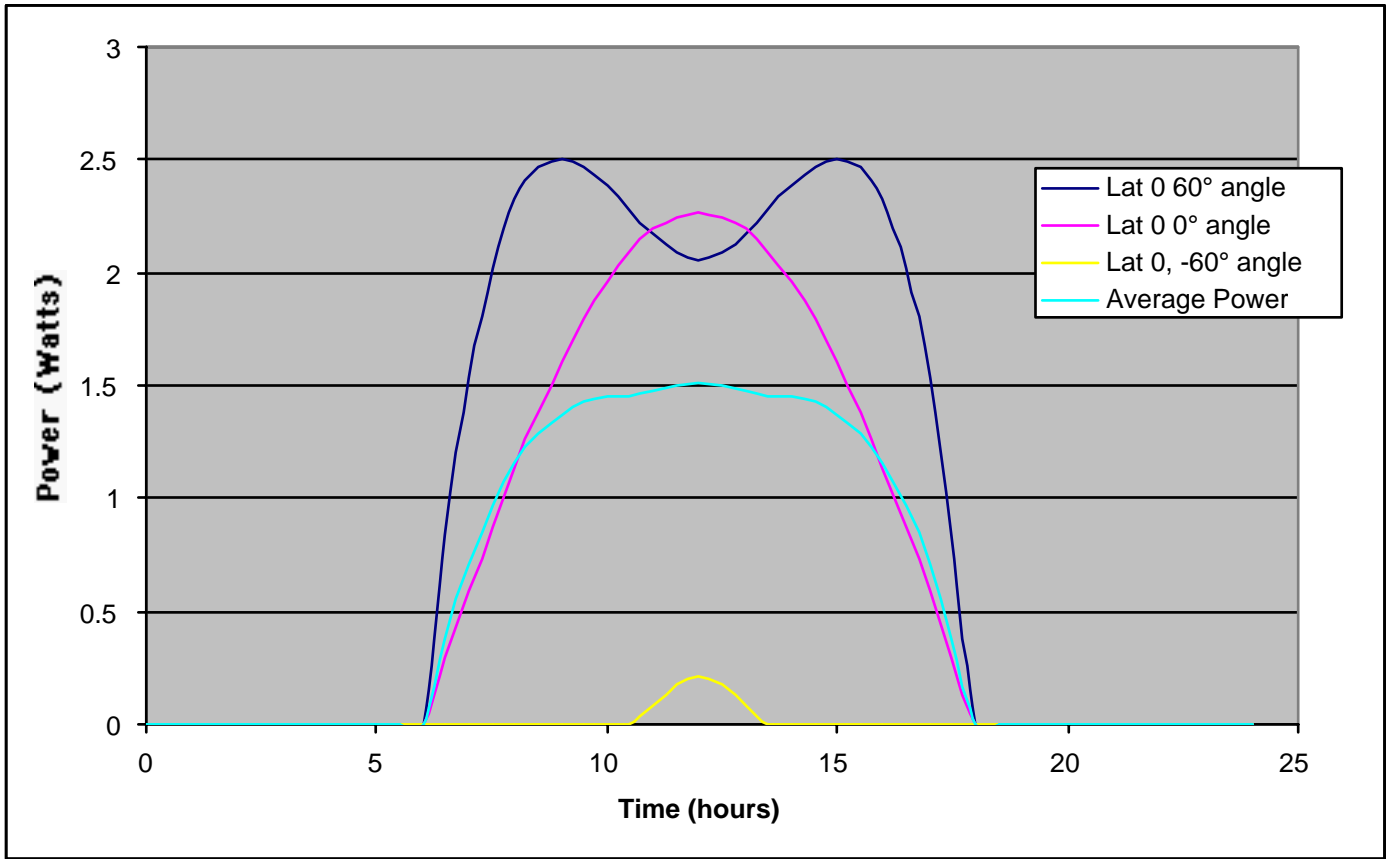


Figure 20. Output per array at the equator during the summer solstice.

The output of the solar array is shown in Figures 20 and 21. This output is for a 10% efficient array with an area of 0.05 m^2 , which represents covering one wing section with a solar array. For the total vehicle there will be 4 arrays, one located on each wing section. The output power for the total arrays can be obtained by multiplying the power level on the graphs by 4. The output is based on a solar intensity of 590 W/m^2 and an atmospheric attenuation of 15%. The mass of the solar array, based on the CuInSe_2 array, would be 0.014 kg.

Since the wings of the entomopter are constantly moving the output of the array will vary continuously. The total wing motion is 120° , $+60^\circ$ (up from the horizontal) and -60° (down from the horizontal). The curves on Figures 19 and 20 represent the output power of the wing at these two locations as well as the horizontal position. The power output is given as a function of time of day for one complete day cycle. The total useable power available per stroke is given by the average power curve. This curve represents the average power available throughout a wing stroke.

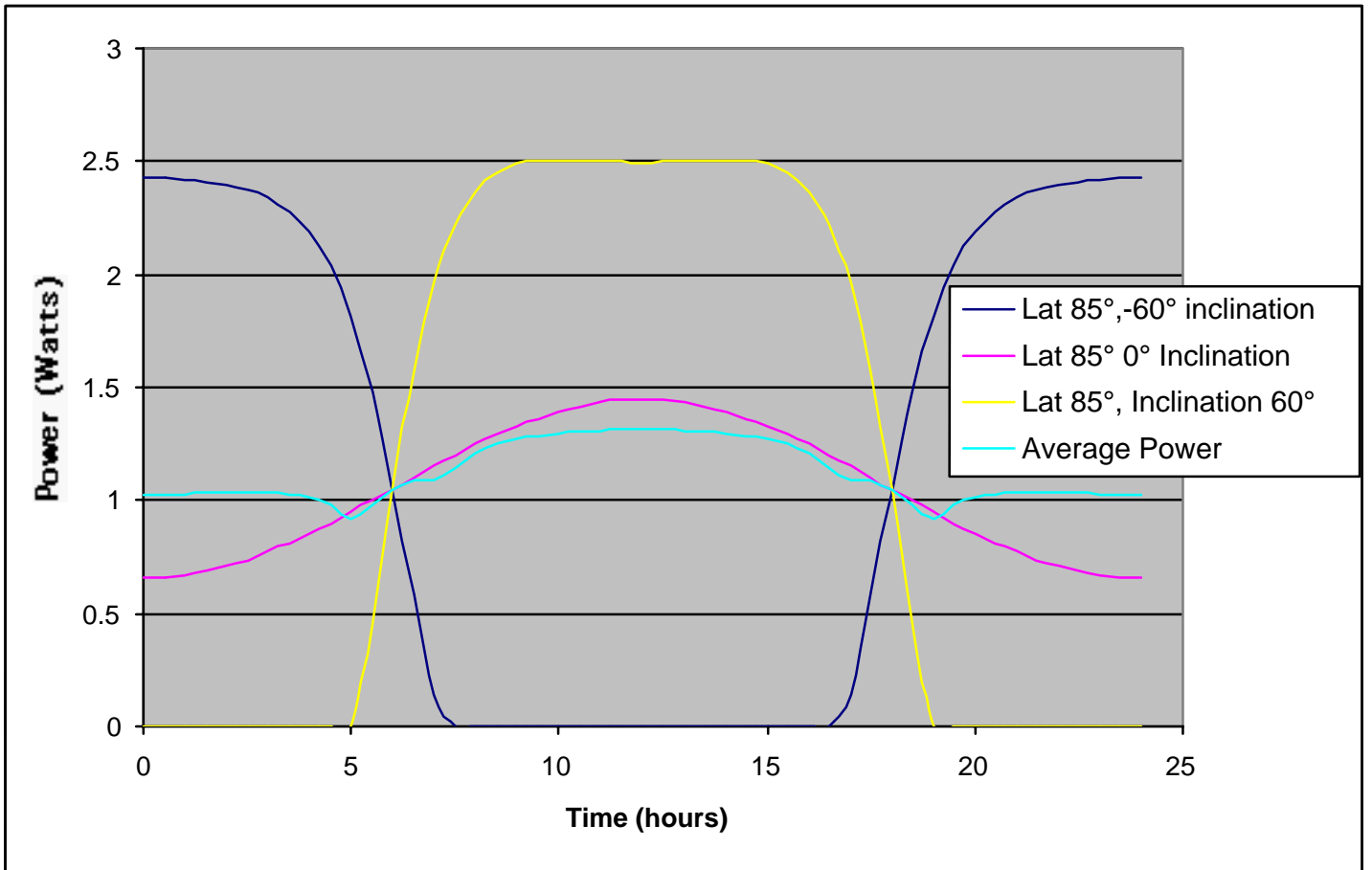


Figure 21. Output per array at 85° North latitude during the summer solstice.

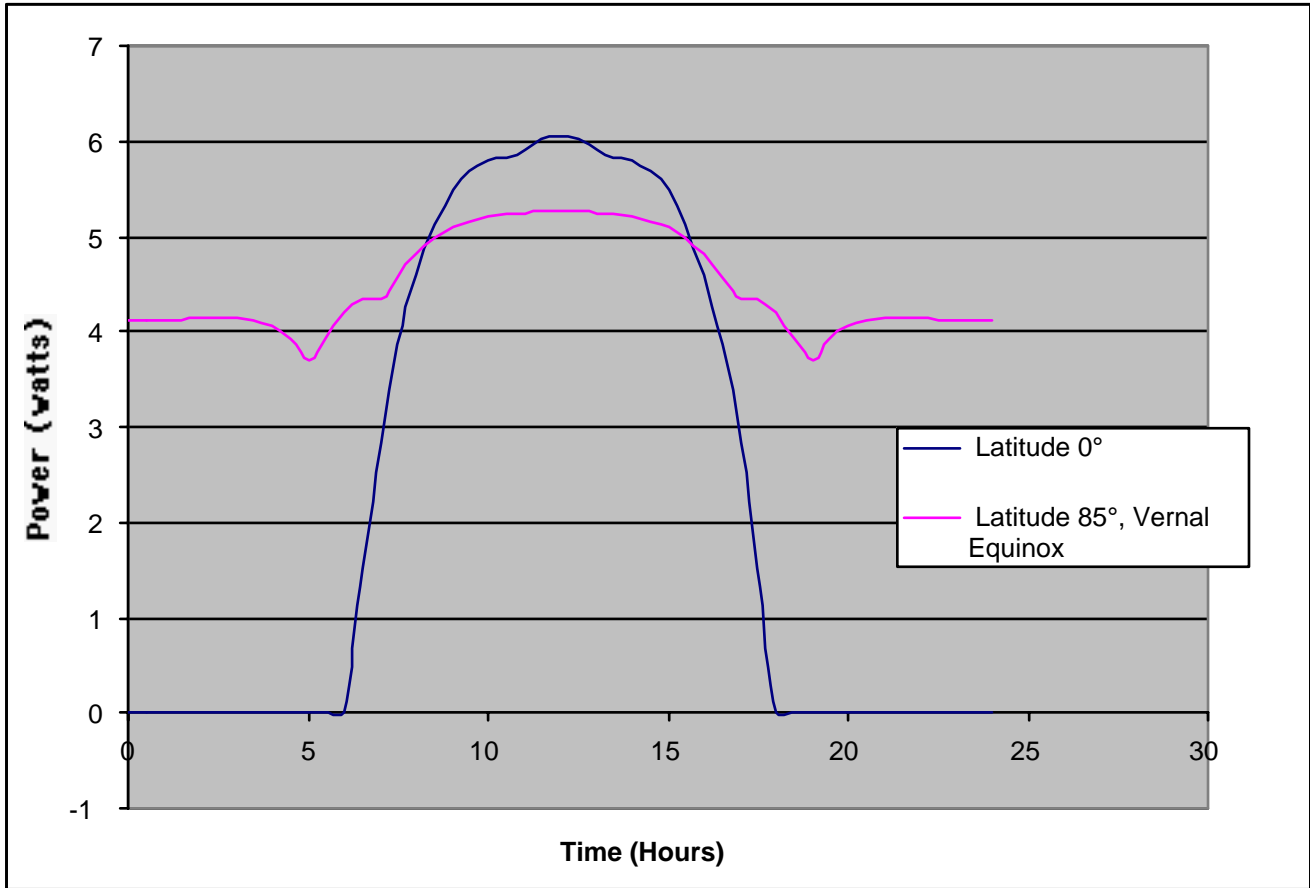


Figure 22. Solar array average output power for the Equator and 85° N Latitudes at day 170 (summer solstice Northern hemisphere)

As can be seen from Figures 20 and 21 the available power changes considerably as the latitude and time of year change. This is due to the inclination of Mars and the change in incident angle on the array from the change in latitude. For the data shown it was assumed that the entomopter was flying East to West.

The average output power per wing stroke for the total array (four panels) is shown in Figure 22. As can be seen the average output power can vary greatly depending on latitude and time of year. Figure 22 represents the extremes in average output power at the equator and near the North Pole at the time of summer solstice. The time of year, especially at higher latitudes, can greatly effect the array output. For example during the winter time at the 85° North latitude there would be no sunlight, and therefore no array output for extended periods of time. The watt hours provided by the solar array for curves shown in Figure 14 are:

Equator at Solstice	55.71 Watt-Hrs
85° North Latitude at Solstice	107.62 Watt-Hrs

This is the amount of energy available from the solar array for the given day.

The energy storage component of the system will be utilized to provide power when the solar array is either obscured from sunlight (by either being shadowed or during nighttime) or when the power demand is greater than what the array can provide. Presently lithium polymer batteries hold the most promise for a lightweight rechargeable system.

Lithium polymer battery cells can be configured in virtually any prismatic shape, and can presently be made thinner than 0.039 inch (1 mm), to fill virtually any space efficiently. This would be a great benefit in the entomopter design since it allows the battery to be placed almost anywhere in the vehicle. It also presents the possibility of making the wing the complete power system, by having the batteries within the wing and the solar cells on its surface. Specifications for present state-of-the-art lithium polymer batteries are given in Table 7.

TABLE 7. SPECIFICATIONS FOR LITHIUM POLYMER BATTERIES, ULTRALIFE BATTERY MODEL UBC543483. [11]

Cell Operating Voltage	4.15 V to 3.0 V (3.8V nominal)
Capacity	930 mAh at C/5 rate*
Maximum Discharge Rate	2C (continuous), 5C (pulse)*
Energy	3.5 Wh
Energy Density	135 Wh/kg, 250 Wh/l
Cycle Life	>300 cycles at C/2 to 80% of initial capacity (no memory effect)*
Operating Temperature	-20°C to 60°C
Charging Temperature	0°C to 45°C
Storage Temperature	-40°C to 60°C
Self Discharge	<10% per month

The C rating is a gauge of the current producing capacity and discharge time of the battery. At 1C the 930 mAh battery would produce 930 mA for 1 hour. At C/5 it would produce 186 mA for 5 hours and at 2C it would produce 1860 mA for 1/2 hour. It should be noted that as the discharge time decreases the overall capacity of the battery will also decrease.

Based on the estimated power consumption of the various systems, shown in Figures 7 through 9, the maximum power consumption is 3.5 watts and the total energy consumption for a mission cycle is 19.7 watt-hours. An estimate of the required battery capacity is 33% of the total energy required for the mission. This battery capacity allows the battery to provide power to the systems when the array is offline (shadowed). This requires a battery with 6.5 watt hours of capacity. Based on the battery data listed in Table 7, the battery mass would be 0.048 kg.

The overall system mass estimate for the array/battery system is listed in Table 8.

TABLE 8. PV/BATTERY SYSTEM MASS ESTIMATE

System Component	Mass (kg)
Solar Array	0.014
Battery	0.048
Contingency (10% for wiring, electronics etc.)	0.006
Total System Mass	0.0682

It should be noted that the system mass shown in Table 8 represents values based on state-of-the-art components. With future advancements in these components this may be significantly reduced. And, any variation in the assumptions used to generate these numbers can also greatly effect these results.

Thermoelectric Power Generation

The basic principle behind thermoelectric power generation is that if two different metals, semimetals or semiconductors are joined at one end and separated along their length a current will be produced in each metal strip as long as there is a temperature difference between each side of the junction. The configuration of a thermoelectric power generator is shown in Figure 23.

The heat source provides a high temperature source from which heat will flow through the converter. For the entomopter application heat can be generated either through the combustion of the propellant or from an isotope heat source. A heat sink must also be used to dissipate the excess heat and maintain the cold side of the thermoelectric at a temperature below that of the hot side. It is this temperature difference which produces the direct current electrical power. Thermoelectric generators can be made for power levels ranging anywhere from 10^{-6} watts to 10^2 watts. Semiconductor material is by far the best choice for the construction of a thermoelectric generator. These materials can presently achieve efficiencies on the order of 5 to 10%.

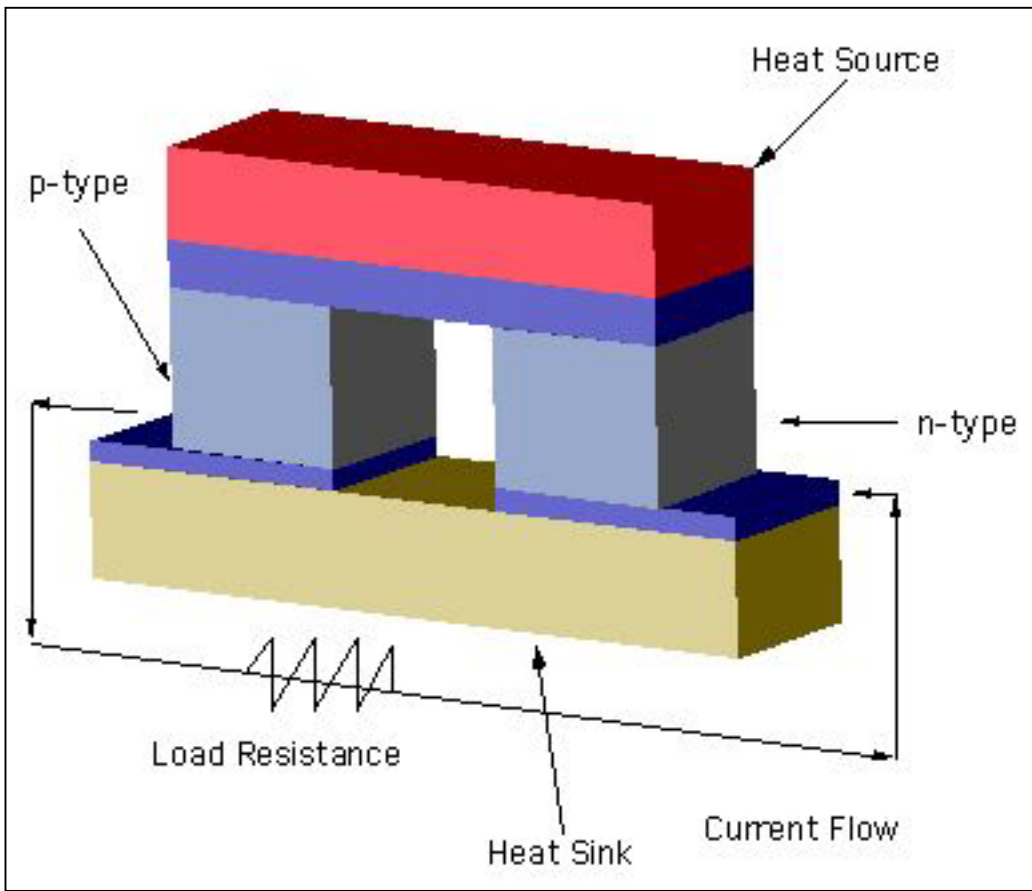
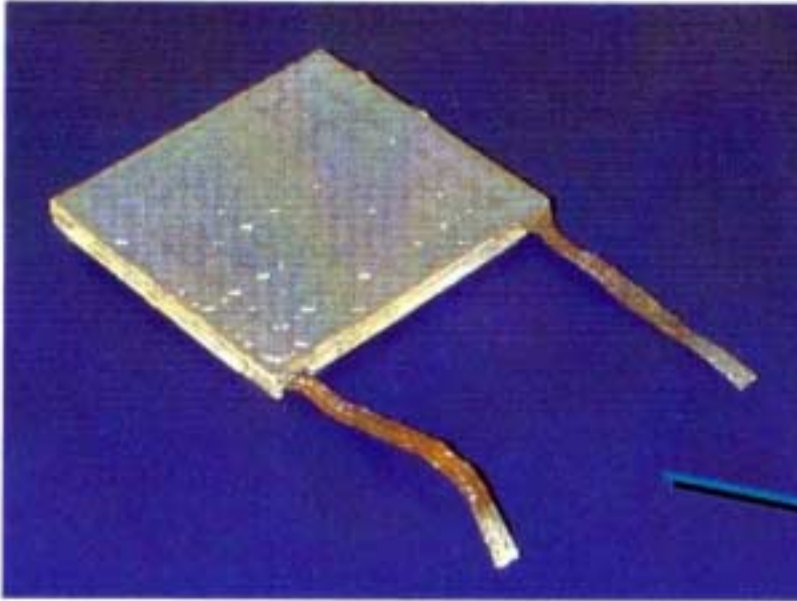


Figure 23. Operational diagram of a thermoelectric generator.

For use on the entomopter the thermoelectric would need to be very light weight and compact. A micro-thin-film thermoelectric, under development through DARPA[12], would be the ideal candidate. State-of-the-art thin film thermoelectric devices, shown in Figure 24, have efficiencies in the 5% range. However, projections for future efficiencies are up to 20%. These thin film thermoelectric devices can be integrated onto the combustion chamber wall and utilize the excess heat produced during combustion to produce electricity. Experimental models are capable of generating 20W of power from a 1 cm³ combustion engine.



Thermoelectric Module

Figure 24. Photo of a thin film thermoelectric [12]

From the estimates for thin film thermoelectric devices, sufficient power for the entomopter's systems should be available whenever the engine is operating. However, the engine operation time is a small fraction of the complete mission time. Therefore an auxiliary source of power would be needed. The best choice for this power source is a rechargeable lithium battery, similar to that used with the PV system. The operational time of the thermoelectric is limited to 15 minutes over the 6 hour mission. This would provide a total of 5 watt hours of energy. Assuming that 4 watts need to be available to the vehicle while the thermoelectric is running that leaves 16 watts or 4 watt-hours available for storage. Therefore a battery would be needed with a storage capacity of 14.7 watt-hours (19.7 watt-hours for the total mission - 4 watt hours excess produced by the thermoelectric - 1 watt-hour provided by the thermoelectric and used during flight). Based on the lithium battery specifications given in Table 7 the battery mass would be 0.108 kg. This battery mass alone is greater than the mass for the complete PV-Battery power system. Based on this comparison, the engine-powered thermoelectric would not be the ideal choice for the entomopter power system.

Another approach to using a thermoelectric is to utilize a radioisotope heat source instead of the combustion exhaust gases. This would eliminate the need for a supplemental battery to provide power when the engine is not running. A standard radioisotope heater unit (RHU) can be used as a baseline for the heat source. The specifications of the RHU are given in Table 9.

TABLE 9. SPECIFICATIONS FOR RADIOISOTOPE HEATER UNIT [13]

Isotope Material	PU-238
Mass (Fuel Source)	3.02 gm
Operating Temperature	310 °K
Watts (thermal)	1Wth

To meet the mission requirements the RHU-thermoelectric system would need to produce 3.5 watts to meet the maximum power needs plus a 0.5 watt contingency. This contingency is needed since there is no backup battery or other power source that could compensate for an unexpected power drain. So the total power to be supplied by the RHU-thermoelectric system is 4 Watts. Assuming the conversion efficiency of the thermoelectric is 15% (which is about 200% better than the state-of-the-art) the thermal watts required would be 26.6 watts thermal. This translates into an isotope mass of 0.08 kg. This isotope mass alone is greater than the PV-battery system mass. Even by eliminating the contingency power the isotope mass (0.07 kg) is still greater than that of the PV-battery system.

Linear Alternator System

A linear alternator system uses the motion of the engine to generate electricity directly and has the potential for producing the greatest amount of power per unit weight (power density) as electrical energy will be converted from that locked in a high energy density fossil or chemical fuel source. However, this will extract work from the exhaust gases by placing an additional load on the engine and will impact endurance. Although it will exhibit a higher overall power density, it will be less energy efficient overall than the thermoelectric system which provides power by utilizing the waste heat within the exhaust gases. Also, the alternator will be operating only when the engine is running and would therefore still require a supplemental battery similar to the exhaust powered thermoelectric. Based on these issues, the linear alternator would not be the best choice for the entomopter vehicle under the mission conditions.

Nuclear

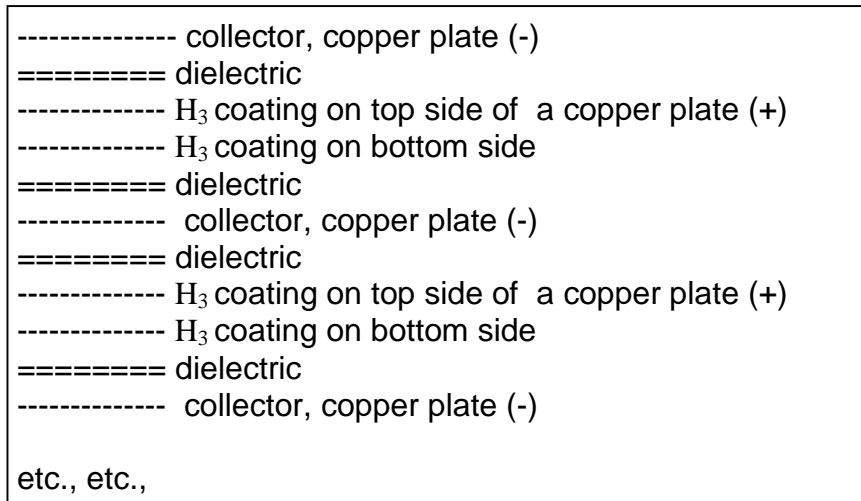
Direct conversion of nuclear emissions may provide special long endurance low current “keep alive” electrical power for the entomopter. At times, wind speeds in excess of 50 m/s can exist within 10 to 20 meters above Mars’ surface. These are often associated with dust storms which can last up several months and can significantly obscure insolation during the daylight hours [5]. Under these circumstances, an entomopter might be grounded for an extended period. In addition, during this period there may be insufficient daylight to make solar panels reliable due to suspended particles in the

atmosphere. There is even the potential that a fine dust could settle on the stationary solar panels, decreasing their efficiency while the entomopter waits out the storm.

One solution is to have a nuclear power generator that provides long term electrical energy that is independent of external sources or internally stored fuels necessary for propulsion. One such nuclear generator can be conformally contained within the entomopter wing area with minimal weight penalty.

Basically, a layer of dielectric material between a beta emitter such as tritium and a collection plate can provide small but reliable amounts of electricity for extended periods of entomopter "sleep". This would keep all vital cognitive systems alive and can even be stored up and multiplied for a higher power burst of power such as a periodic transmission.

The collection plate can be any good conductor. The dielectric must be thin enough to let the beta particles pass through, yet thick enough to prevent arcing between the collector and the beta emitting plate. The H₃ (tritium) layer must be mounted on a conductive plate (such as copper) which can be electrically isolated from all other plates as shown below:



The negative plates are then connected in parallel as are the positive plates. These basic units can be formed by sputtering thin layers of material as a sandwich onto the wings. Units connected in parallel will increase current output while units connected in series results in a higher voltage output.

This method of converting decay energy to electrical energy is inherently inefficient because only one electron is captured on a plate per beta particle emitted and all the rest of the kinetic energy is wasted, but it is attractive because it is very simple.

Fifty percent of the energy is lost in this process because the material supporting the H₃ absorbs any particles emitted in that direction before the very low energy beta particle can penetrate it. If the material supporting the H₃ were very thin, the particles may pass

through, but it could not be structurally rigid. H₃ beta particles have 6 keV average energy and can pass through only 4 mm of air on Earth, and approximately 0.003 mm of material having 1 g/cc density.

One could increase the curie content and increase the output proportionally, up to the point that the H₃ coating material starts to absorb the H₃ beta particles emitted from it, but then a plateau would be reached. When this plateau is reached would depend on the coating material and H₃ concentration used.

A more energetic beta emitter than tritium would only allow the use of a thicker coating and hence more curies on a given surface area, because the beta particles would require more energy to pass through the coating. However, this still results in only one electron liberated for each beta emitted, and therefore only one electron volt of potential energy developed, regardless of the initial energy of the beta particle. A shorter life beta emitter would allow one to use a higher specific activity coating, but would still only result in one electron per beta particle emitted.

Preliminary calculations using tritium as a power source to create a beta battery for an entomopter application indicate that if one curie of H₃ is sputtered onto a plate, 3.81 cm x 15.24 cm or 58 cm², with a matching plate located above it of the same size and having a 1 mm gap of air or vacuum between them, 0.174 microwatts of electrical energy will be produced. Such a low risk radioisotope unit could be configured to produce 3 nanoamps at 58 volts, or 30 nanoamps at 5.8 volts (or other combinations depending upon the configuration). This assumes that fifty percent of the beta particles are emitted towards the collector and that 100% of them reach it and are collected. Although the total theoretical power available is 35 microwatts, this method wastes fifty percent of the energy because of the geometry, and only 1/6000 of the kinetic energy is converted to electrical potential energy.

If these 58 cm² units were distributed over a 22.86 cm by 91.44 cm Mars Flyer wing, this would represent a total area of 2090 cm². Since the entomopter requires two such wings to fly, the total available area is actually 4181 cm². This would result in 12.53 microwatts of total continuous power available. This is sufficient for reliable onboard electronics “keep alive” purposes and would provide this function for longer than the expected lifetime of the entomopter.

Propulsion System

The propulsion system used in the entomopter is a Reciprocating Chemical Muscle (RCM). This device converts a metered chemical monopropellant into reciprocating motion with throw, frequency, and power necessary for flight. The waste gas from the decomposition of the monopropellant is used in the operation of the RCM, and is used six times further before being expelled from the entomopter. This reuse of waste gases is critical to the efficiency of the RCM and the overall endurance of the entomopter because

it obviates the need for secondary power supplies used in obstacle avoidance, stability and control while in flight, and navigation.

Details of the operation of the RCM are the subject of a U.S. patent that is currently in process, so to prevent a disclosure in the public domain, only a general description of this technology can be given in this open literature report.

The RCM meters a monopropellant into a reaction chamber where the monopropellant is allowed to decompose rapidly and exothermically. Gaseous products produced in this decomposition process provide a source of pressure and heat to drive the entomopter wings, active flow control system for lift modulation of the wings, gas bearings, ultrasonic ranging systems, mass flow amplifier, thermoelectric generator, and thruster. The metering of the monopropellant and the distribution of the resulting energy is regulated by a process control computer. The RCM process control computer regulates the fuel metering, and hence the RCM reciprocation frequency under various loads based on various feedback sensors. It also communicates with the higher level onboard cognitive processes to enact desired vehicle behaviors by controlling the gas flow to the wings to modify lift and change the attitude or direction of the vehicle during flight. Analogous behaviors are exhibited during ground locomotion.

Experimental laboratory prototype RCM units have been refined to the point that they exhibit the range of motion and power necessary for flight in a terrestrial entomopter of 50 grams total weight. The entomopter-based Mars Flyer can use a scaled up version of the RCM technology. It has particular advantage in the oxygen devoid Mars atmosphere because the use of an oxydizer is not necessary.

Further, the scaled up embodiment will afford easier heat rejection through a thermoelectric heat exchanger than is possible in the miniature terrestrial version. Although the ambient temperatures on Mars are generally lower than experienced on Earth, the heat exchange advantage will be diminished by the rarefied Mars atmosphere. On the other hand, larger (heavier) heat exchange elements can be used without penalty because of the reduced gravity on Mars.

Propellant Selection

The design of the entomopter requires the generation and expansion of gas in order for the vehicle to operate. This gas can be generated either by combustion, a catalytic reaction or sublimation of a material. The gas is necessary to drive the reciprocating piston that drives the wing motion. However it is also needed for various other aspects of the vehicle design, these include, ultrasonic emissions for altimetry and obstacle avoidance, air bearings supply, lift augmentation blowing, and jet thrust. Because the gas generation is an integral part of the operation of the vehicle the propulsion source must be a fuel based system.

The fuel selection will be based on the following criteria:

1. Ability of the fuel to meet the environmental conditions of the mission.
2. Ability of the fuel to provide the required amount of gas for the operation of the entomopter .
3. The potential of the fuel to be made on the Martian surface out of the indigenous materials present in the atmosphere and soil.

The ideal fuel will be a liquid monopropellant. A monopropellant is desirable since it reduces the complexity of the storage and delivery system for the fuel. And, being in liquid form, it minimizes the storage volume and provides for easier containment.

The operational constraints on the fuel require it to be capable of being stored for extended periods of time (up to 2 years) with little or no degradation and be capable of withstanding the deep space environment during transit as well as the environment on the surface of Mars. The main environmental issue during transit and on the Mars surface is temperature. Assuming that there is no active thermal control or heating available, the fuel must be capable of withstanding temperatures down to -40°C for extended periods of time. If the fuel can remain liquid at these temperatures then the propellant delivery system can be greatly simplified and the need for power and weight consuming heaters eliminated. This also reduces the overall risk of the mission, by eliminating a failure source occurring from improperly thawed fuel or a failed heater.

An overall list of potential fuels (and fuel oxidizer combinations) is listed in Tables 10 through 12. [14,15]. Their ability to meet the requirements listed above are evaluated and ranked regarding their applicability toward the mission.

TABLE 10: FUELS AND THEIR PHASE CHANGE TEMPERATURES

Fuel	Boiling Point (°C)	Freezing Point (°C)	Potential Oxidizers	Density (gm/cm ³ at 20°C)
Hydrogen (H ₂)	-253	-259	Oxygen, fluorine	0.071 (at -253°C)
Ammonia (NH ₃)	-33.4	-77.7	Oxygen, fluorine, Nitrogen Tetroxide, Chlorine Trifluoride	0.611
Hydrazine (N ₂ H ₄)	113.4	1.5	Oxygen, fluorine, Nitrogen Tetroxide, Chlorine Trifluoride	1.008
Monomethyl Hydrazine (N ₂ H ₆ C)	89.2	-52.5	Nitrogen Tetroxide, Chlorine Trifluoride, Inhibited Red Fuming Nitric Acid	0.874
Unsymmetrical Dimethyl Hydrazine (N ₂ H ₈ C ₂)	63.8	-57.2	Oxygen, fluorine, Nitrogen Tetroxide, Chlorine Trifluoride	0.792
RP-1 (C _{11.74} H _{21.83})	185	-40	Oxygen, Inhibited Red Fuming Nitric Acid	0.801
Methane (CH ₄)	-161	-183.9	Oxygen, fluorine	0.415 (at -164°C)
Propane (C ₃ H ₈)	-42.2	-187.1	Oxygen, fluorine	0.585 (at -44°C)
Diborane (B ₂ H ₆)	-92.6	-164.8	Oxygen Difluoride	0.435 (at -92.6°C)

TABLE 11: OXIDIZERS AND THEIR PHASE CHANGE TEMPERATURES

Oxidizer	Boiling Point (°C)	Freezing Point (°C)	Density (gm/cm ³)
Oxygen (O ₂)	-183	-218.8	1.143
fluorine (F ₂)	-188.1	-219.6	1.505
Nitrogen Tetroxide (MON3) (N ₂ O ₄)	21.2	-11.2	1.45
Chlorine Trifluoride (CLF ₃)	11.8	-76.6	1.825
Inhibited Red Fuming Nitric Acid (IRFNA) (0.835HNO ₃ 0.140NO ₂ 0.020H ₂ O0.005HF)	~60	~ -62.2	1.56
Oxygen Difluoride (OF ₂)	-145	-223.9	1.521
Nitrogen Tetroxide (MON25) (N ₂ O ₄)	-9	-54	1.45

TABLE 12: MONOPROPELLANTS AND THEIR PHASE CHANGE TEMPERATURES

Monopropellant	Boiling Point (°C)	Freezing Point (°C)	Density (gm/cm ³)	Combustion Temperature (°C)	Specific Impulse (Isp)
Hydrogen Peroxide(0.9H ₂ O ₂ 0.1H ₂ O)	141.1	-11.5	1.39	757	148
Ethylene Oxide (C ₂ H ₄ O)	10.6	-112.8	0.87	1004	199
Nitromethane (CH ₃ NO ₂)	101.2	-29	1.14	2193	245
n-Propyl Nitrate (C ₃ H ₇ NO ₃)	110.5	-101.1	1.057	1078	210
Hydrazine (N ₂ H ₄)	113.4	1.5	1.008	633	199
Hydrazine Propellant Blend (HPB) HPB-1808 (18% HN, 8% water)	100	-20	na		230
61% Hydroxylammonium Nitrate (NH ₃ OH)NO ₃ (HAN) 14% Glycine (H ₂ NCH ₂ CO OH)	100	-35	na		190

The following systems have the greatest potential remaining liquid throughout the mission with little or no active heating.

Fuel:

Hydrogen

Hydrogen is a stable, non corrosive, non toxic material. However in order to be useable for this mission it must be kept in a liquid state. This requires cryogenic storage which would significantly increase the complexity of the mission.

Ammonia

Ammonia is a stable compound that can be stored in Teflon, 18-8 stainless steel, aluminum, or polyethylene. It is mildly toxic but can be fatal in concentrated exposure. The main issue with its use for this mission is that it is in the gaseous state under mission conditions.

Hydrazine

Although its most common use is as a monopropellant, hydrazine can also be used as a bipropellant. It has the same general properties as the monopropellant version, but its performance is significantly improved when utilized in combination with an oxidizer.

Monomethyl Hydrazine

Monomethyl hydrazine is fairly stable at lower temperatures, however it becomes unstable above 260°C (500°F). It can be stored in 18-8 stainless steel, aluminum, or Teflon. It is toxic. Its liquid temperature range is well within the requirements for the mission environment.

Unsymmetrical dimethyl-hydrazine (UDMH)

Unsymmetrical dimethyl-hydrazine is stable at low temperatures but becomes violently unstable at temperatures above 260°C (500°F). It can be stored in most materials including mild steel, 18-8 stainless steel, aluminum, Teflon, and polyethylene. It has a lower level of toxicity than hydrazine but more than that of ammonia. Its liquid state temperature range is well within that of the mission requirements.

RP-1

RP-1 is a fuel developed for space applications. It is stable up to 370°C (700°F) and is compatible with all common metals as well as, neoprene, asbestos, fluorocarbons, and epoxies. Its toxicity is comparable to that of kerosene. The liquid temperature range for RP-1 is within the operating range for the mission, but, the freezing point is at the

estimated low temperature for the mission. To insure that RP-1 doesn't freeze during the mission some active thermal control would probably be required.

Methane

Methane is stable and compatible with all common metals as well as neoprene, asbestos, fluorocarbons and epoxies. It is essentially non toxic. The main issue with it is its low boiling point, requiring it to be used as a gas or stored cryogenically. Due the the small volume of the proposed entomopter, storing the fuel as a gas would significantly limit the flight duration. Also, using it as a cryogenic liquid would greatly increase the mission complexity.

Propane

Propane essentially has the same properties as methane. It is stable and compatible with all common metals as well as neoprene, asbestos, fluorocarbons and epoxies. The issues with its use are the same as those of methane.

Diborane

Diborane is a gas at room temperatures and will slowly decompose. At higher temperatures it decomposes rapidly. It is compatible with most metals and some organic materials. It has moderate toxicity. The issues with using diborane are significant. It would need to be stored as a cryogenic liquid in order to provide for sufficient mission duration as well as minimize the decomposition rate. Because of these issues it would not be suitable for the proposed entomopter mission.

Oxidizer:

Oxygen

Oxygen is highly reactive and non toxic. It is non-corrosive and is very stable in storage. The main issue with its use is that it would be in the gaseous form under the mission conditions, which will significantly limit the volume of oxygen which can be stored. Liquid oxygen can be used, however, creates significant issues regarding the storage and manufacture of a cryogenic liquid.

Fluorine

Fluorine is highly reactive with almost any material. It can be stored in 18-8 stainless steel or copper but monel is preferred. It is very important that all materials that come into contact with fluorine are thoroughly cleaned so that there are no contaminating particles for the fluorine to react with. There are no non metallic materials which are completely unreactive with fluorine. It is also highly toxic and corrosive to body tissue. Like oxygen it is a gas at mission temperatures, and it would need to be stored cryogenically in order to be used in the mission.

Nitrogen Tetroxide

Nitrogen tetroxide is a stable compound. It is not highly reactive and can be stored in mild steel, stainless steel, aluminum, Teflon and polyethylene. Its toxicity is comparable to that of chlorine. Various formulations of nitrogen tetroxide are available, varying the percent of nitric oxide in the formulation, which can effect the freezing point for the propellant. The mixtures of nitrogen tetroxide shown in the table above have varying amounts of nitric oxide: MON 25 (25% mixed NO) has a significantly decreased freezing point over MON 3 (3% mixed NO). This ability to lower the freezing point of nitrogen tetroxide makes it applicable to the mission environment, and would eliminate the need for thermal control of the propellant.

Chlorine Trifluoride

Chlorine trifluoride is a stable oxidizer that can be stored in 18-8 stainless steel, nickel, and monel: most common metals can be used if free of contaminants. It is highly toxic with a toxicity comparable to fluorine. Its liquid state temperature range is more than sufficient to meet the mission requirements.

Inhibited Red Fuming Nitric Acid (IRFNA)

IRFNA is subject to decomposition at elevated temperatures and its decomposition rate is directly related to temperature. It can be stored in 18-8 stainless steel, polyethylene, and Teflon. It is toxic and corrosive to body tissue. The liquid temperature range of IRFNA is sufficient to keep the oxidizer in a liquid state throughout the proposed mission duration.

Oxygen Difluoride

Oxygen Difluoride is stable at normal room temperature but becomes increasingly unstable at elevated temperatures. It can be stored in 18-8 stainless steel, copper, aluminum, monel and nickel. Nonmetallic materials are generally not compatible. It is highly toxic and corrosive to body tissue. The main issue is that it is a gas at mission temperatures. In order to be useable it would need to be stored cryogenically, thus adding significant risk and complexity to the overall mission.

Monopropellant:

Hydrogen Peroxide

Hydrogen Peroxide has a flight heritage dating back to the 1930's, although recently the technology has been dormant. It is seeing a revival of sorts, primarily as an oxidizer in a bipropellant combination, but also as a monopropellant. The main advantage of hydrogen peroxide is that it is nontoxic. However, the freezing point is higher than what is necessary to perform the mission without thermal control. There are a few options for dealing with the freezing issue. A passive thermal system may be used to maintain the temperature above freezing. This may be possible since its freezing point is within 30°C of the expected environmental conditions. Another advantage of this propellant is that as it is the fuel presently used by GTRI in their entomopter designs, there is a significant experience and history with its use in this type of vehicle. Hydrogen Peroxide decomposes in the presence of a catalyst such as carbon, steel or copper. For storage it doesn't react with certain materials such as aluminum, tin, glass, polyethylene or Teflon.

Ethylene Oxide

Ethylene oxide remains liquid over a temperature range which is more than adequate to meet the mission requirements. It is generally stable but the polymerization rate is increased in the presence of some materials. Storage materials it is compatible with include 18-8 stainless steel, aluminum, mild steels, copper, nylon, and Teflon. This material is relatively toxic and must be handled with caution.

Nitromethane

Nitromethane's temperature range is nearly within the range required by the mission. It would require some insulation or thermal control to assure it would not freeze. It doesn't react with 18-8 stainless steel, aluminum, or polyethylene. These materials can be used for storage. The main issue with its use is that it may detonate under conditions of confinement, heating and mechanical impact, any of which can possibly be experienced during this mission. Also, it is relatively toxic and must be handled with caution.

n-Propyl Nitrate

n-Propyl Nitrate is capable of remaining liquid well within the temperature range of the mission. It is relatively stable and insensitive to mechanical or thermal shock. It can be stored in containers made of either 18-8 stainless steel, aluminum, polyethylene, Teflon, nylon, Orlon, Dacron or Mylar. This material has no serious toxicity problems, which allows for easy handling.

Hydrazine

Hydrazine monopropellant has been used in spacecraft for the last 30 years, mainly for low thrust applications like satellite station keeping. Decomposition is achieved by a

catalyzed reaction with a metal oxide. Materials which are compatible with hydrazine and will not react include Teflon, 18-8 stainless steels, polyethylene, and aluminum. The main issues with using hydrazine are that it is highly toxic and has a high freezing point (approximately 1.5°C). Because of this high freezing point significant heating would be required throughout the mission in order to maintain the propellant in its liquid state.

Hydrazine Propellant Blend (HPB)

HPB represents a family of monopropellant formulations composed of hydrazine, hydrazinium nitrate (HN), and water. The addition of NH and water serve to depress the freezing point and increase the performance of plain hydrazine. Several HPBs were developed and tested in the 1960's and 1970's primarily for military applications. HPBs are receiving renewed attention as a low freezing point monopropellant. Presently NASA is sponsored HPB development work at Primex Aerospace.

HAN

HAN is a family of monopropellants composed of an oxidizer rich salt, a fuel component and water, and have been under development by NASA the last decade. HAN based monopropellants offer a high density, low freezing point, nontoxic alternative to hydrazine.

Propellant Candidates

One of the main requirements for the propellant selection is for the propellant to be in liquid form during storage. If possible this would mean that the propellant be maintained in this state throughout the mission with a minimum amount of thermal control, minimizing the complexity of storing, transporting and manufacturing the propellant and greatly simplifying the entomopter and support vehicle design. Therefore, based on this requirement, most of the propellants listed and described in the previous section are not applicable to the entomopter mission.

Table 13 lists the potential bipropellant combinations and monopropellants which would be applicable. Also given is the Isp of each propellant. Isp is the Specific Impulse of the propellant. It is a gauge of the amount of thrust you get per mass out for a specific propellant. This can be used to gauge the energy contained within the propellant. The higher the Isp the greater the energy released during combustion.

TABLE 13. PROPELLANT CANDIDATES BASED ON TEMPERATURE AND OPERATIONAL STATE REQUIREMENTS

Propellant	Oxidizer / Fuel Ratio	Isp	Combustion Temperature (°C)
Fuel: Monomethyl Hydrazine Oxidizer: Nitrogen Tetroxide	2.20	288	3122
Fuel: Monomethyl Hydrazine Oxidizer: Chlorine Trifluoride	3.00	283	3318
Fuel: Monomethyl Hydrazine Oxidizer: IRFNA	2.50	274	2848
Fuel: UDMH Oxidizer: Nitrogen Tetroxide	2.70	286	3162
Fuel: UDMH Oxidizer: Chlorine Trifluoride	2.85	278	3306
Fuel: RP-1 Oxidizer: IRFNA	4.90	263	2881
Monopropellant: Hydrogen Peroxide	na	148	757
Monopropellant: Ethylene Oxide	na	199	1004
Monopropellant: Nitromethane	na	245	2192
Monopropellant: n-Propyl Nitrate	na	209	1077
Monopropellant: HPB	na	200	----
Monopropellant: HAN	na	---	----

In Situ Propellant Production

The ability to refuel the entomopter once on the surface of Mars is a vital component to the proposed mission scenario. To achieve this goal the propellant used within the entomopter must be capable of being produced out of the materials available at the Martian surface. A list of the elements and compounds is given in the environmental section for both the soil and atmosphere.

From the listing of elements and compounds available it can be seen that there is very little hydrogen available on Mars. The only compound containing hydrogen is the trace water vapor within the Martian atmosphere and this constitutes only 0.03% of the atmosphere makeup. However all the propellants listed in Table 13 require hydrogen. Therefore it will need to be assumed that unless a water source is found on Mars that the hydrogen needed to produce the selected fuel will need to be brought from Earth.

The remaining elements that make up the fuels listed in Table 13 are present on Mars with the exception of fluorine. The lack of fluorine as well as the scarcity of chlorine eliminates the following four propellants as potential candidates for fueling the entomopter: Monomethyl Hydrazine and Chlorine Trifluoride, Monomethyl Hydrazine

and IRFNA, UDMH and Chlorine Trifluoride, RPI and IRFNA. Also HAN and the HPB monopropellants were eliminated due to the complexity in their chemical makeup which would be difficult to manufacture.

Since the remaining propellants all require hydrogen (which must be brought from Earth) the next step is to determine which of these propellants minimize this hydrogen requirement. Table 14 shows the percentage of hydrogen, on a weight basis for the candidate fuels.

TABLE 14. PERCENT OF HYDROGEN BY WEIGHT FOR THE VARIOUS CANDIDATE PROPELLANTS

Fuel / Oxidizer	Chemical Makeup	Percent Hydrogen by Weight
Monomethyl Hydrazine and Nitrogen Tetroxide	$(N_2H_6C)+2(N_2O_4)$	2.61%
UDMH and Nitrogen Tetroxide	$(N_2H_6C)+2.7(N_2O_4)$	1.96%
Hydrogen Peroxide	$(0.9H_2O_2+0.1H_2O)$	5.38%
Ethylene Oxide	(C_2H_4O)	9.09%
NitroMethane	(CH_3NO_2)	4.92%
n-Propyl Nitrate	$(C_3H_7NO_3)$	6.66%

Based on Table 14 the primary choice to minimize the need for hydrogen is the bipropellant UDMH with Nitrogen Tetroxide. However a bipropellant system will increase the complexity of the overall mission: it will require two separate production plants, one for the fuel and one for the oxidizer as well as separate storage and fueling ports. Once the details of the production system are determined, an evaluation will need to be made as to whether the reduction in hydrogen mass required for a given mission duration is off-set by the increase in mass necessary to produce a bipropellant versus that of a monopropellant.

Until these system concerns are evaluated, which will take place under the phase 2 portion of the contract, the propellant selection will be narrowed to 4 potential candidates, 2 bipropellants and 2 monopropellants: Monomethyl Hydrazine fuel and Nitrogen tetroxide oxidizer, UDMH fuel and Nitrogen Tetroxide oxidizer, hydrogen peroxide, and nitro-methane. Ethylene Oxide and n-Propyl Nitrate were eliminated as potential fuels due to the relatively higher percentage of hydrogen content. These remaining four fuels will be evaluated in further detail under the Phase 2 portion of the program.

The production of these fuels will require the ability to produce nitrogen, carbon, and oxygen from the atmosphere present on Mars. The composition of the atmosphere and

soil is listed under the environmental section. For the most part these elements can be extracted from the atmosphere. The carbon and oxygen can be obtained by breaking apart the CO₂ within the atmosphere and the nitrogen can be obtained by separating it out directly from the atmosphere.

The oxygen and carbon can be produced in a fashion similar to that planned for the Mars 2001 (now 2003) Surveyor Lander [16]. In this scheme the atmosphere will be initially compressed using a sorption compressor. This type of compressor contains no moving parts, achieving its compression by alternately cooling and heating a sorbent bed of materials. These materials adsorb CO₂ at low temperatures and release them at high temperatures. If the correct material can be found this same process can be used to separate out nitrogen from the atmosphere.

Once the CO₂ is removed from the atmosphere the carbon and oxygen will then need to be separated. This can be accomplished by using a zirconia solid-oxide generator. The zirconia acts as an electrolyzer at elevated temperatures. At temperatures in excess of 750°C it will strip off oxygen ions from the CO₂. If a current is applied to the zirconia material it will also act as an oxygen pump and pass the oxygen atoms through its crystal lattice, thereby separating the oxygen from the CO₂.

Based on these processes the main constituents of the propellants should be capable of being generated. The next process would be to produce a reactor and process that can recombine these elements into the proper compounds to construct the desired propellant. This process design of manufacturing the propellants out of their component elements is beyond the scope of this Phase I work. This process design will be thoroughly investigated during the Phase II portion of the work.

It is also worth mentioning two additional non-conventional propellant concepts that can potentially be used as fuel for the entomopter. The first is to utilize the atmosphere CO₂ directly as an oxidizer. CO₂ can react with various metals and act as the oxidizer for these reactions. The potential reactions that can utilize CO₂ as an oxidizer are listed in Table 15.

TABLE 15. COMBUSTION OF VARIOUS METALS WITH CO₂ [17]

Metal	Reaction	Ignition Temperature
Mg	$Mg + CO_2 = MgO + CO$	340°C
Li	$2Li + CO_2 = Li_2O + CO$	851°C
Al	$2Al + 3CO_2 = Al_2O_3 + CO$	>2000°C

The experimental work outlined in Bibliography Reference 17 demonstrated that CO₂ would combust with the metals listed in Table 15. In this experimental work the CO₂ pressure was kept at 1 atmosphere (Earth) with a flow rate of 0.5 m/s. On Mars this would require a 100 to 1 compression ratio of the atmosphere to provide the same

combustion environment. Additional work would need to be performed to determine the burning properties at lower CO₂ pressures. If lower pressures could be used this would significantly reduce the compression ratio. Even if significant compression is required it may be possible to achieve this through the motion of the drive engine piston, similar to that of a conventional internal combustion engine. However there are a number of issues associated with the used of this type of fuel. Mainly, the solid metal oxides will condense within the combustion cylinder and potentially clog the engine, as well as be a source of wear on the piston. The design and evaluation of a CO₂ burning engine is beyond the scope of this Phase I effort. Any detailed examination of this type of engine will be performed under the Phase II portion of the program.

The main products of the combustion reactions listed in Table 15 are condensed metal oxides and CO. Of these Mg is the easiest to ignite and has the highest burn rate, which is necessary to produce the required gas pressure for operation of the vehicle.

Magnesium oxide, which makes up about 7.8% of the soil, is present in significant enough quantities to consider mining the soil for the magnesium that is needed. If the magnesium is capable of being effectively separated out of the soil it will probably need to be dissolved in solution to make it useable as a propellant [18,19]. One potential candidate would be methanol (CH₃OH). However the use of this type of fluid would require a supply of hydrogen as well as the ability to separate out carbon and oxygen from the atmosphere. This diminishes the attractiveness of a system that utilizes the CO₂ directly out of the Martian atmosphere. Based on results given in Bibliography References 18 and 19 there are other significant issues with using methanol or any other fluid as a carrier for the magnesium. One was that the magnesium would tend to settle out of the mixture requiring frequent mixing. A second was that the carrier fluid would need to evaporate before ignition of the magnesium would take place. There may be other carrier fluids that might work better than methanol. However, a different approach, utilizing a gas as the carrier, might be utilized.

A gas would eliminate the problems of evaporation and mixing as well as the issues associated with the production of the carrier fluid. The ideal gas to use would be the Martian atmosphere itself. It may be possible to devise a mixing chamber onboard the vehicle that would be used to mix the magnesium and atmosphere (CO₂) prior to being injected into the combustion chamber. The atmosphere could be pumped in at a rate that would stir up the magnesium particles and form a suspension of magnesium powder within the tank. The magnesium could be gravity fed into this mixing chamber at a rate that would maintain the correct concentration of magnesium within the chamber (similar to the sands falling through an hourglass). The rate of magnesium powder that enters this mixing chamber could be controlled by changing the size of the orifice through which the magnesium powder passes. This suspension could then be injected into the combustion chamber. This scheme would not require any gas production and would utilize a fairly simple control scheme of adjusting the atmosphere injector and opening to the magnesium powder tank. The mixing chamber would need to be large enough to allow the

magnesium to be suspended at the correct mixture ratio prior to being injected into the chamber.

Vehicle Configuration/Design

The basic terrestrial entomopter configuration is applicable to Mars flight if properly scaled. The terrestrial entomopter having a wing span of approximately 15 cm operates in the same Reynolds number regime in the lower Mars atmosphere as a scaled up entomopter with wing span of approximately 92 cm. In both cases, the entomopter has a twin wing configuration in which the wings flap 180° out of phase at a constant autonomic rate. On Earth, this flapping frequency ranges between 25 and 30 Hz.

The entomopter-based Mars Flyer is assumed to scale proportionately for the purpose of this analysis. Future analytical and empirical investigations in Phase II will be required to refine this assumption. The basic entomopter is shown in Figure 25.

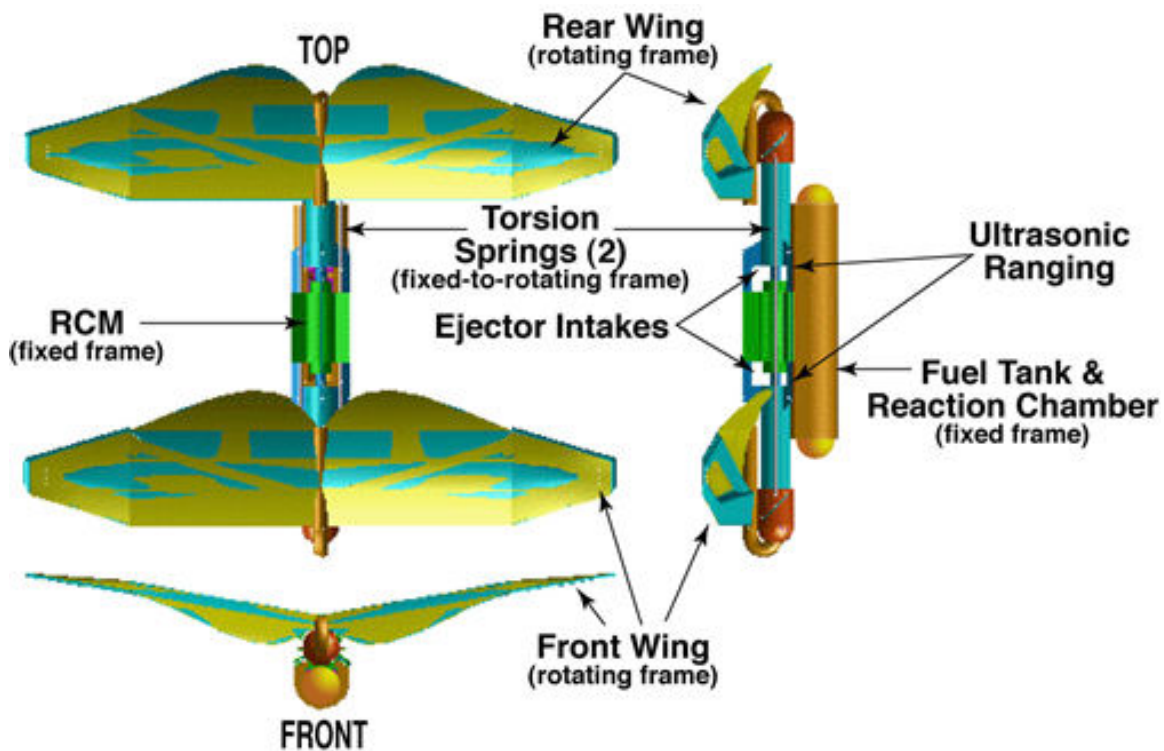


Figure 25. Entomopter-based Mars Flyer configuration.

Currently several leg configurations exist for the terrestrial entomopter, depending upon its mission. Long unjointed legs have been designed for positioning of sensors after landing, whereas short cilia-like legs are envisioned for locomotion through highly restricted areas such as conduits and pipes. The use of longer legs for the Mars Flyer is expected, however, this too is a subject for future study. The purpose of legs on Mars would be to position sensors after landing, to reposition the entomopter for a more favorable launch, and to grapple with ground-based rovers or the Mars lander during

refueling operations. The primary form of locomotion is intended to be flight and the legs are for limited surface mobility, not extended ambulation.

The entomopter wing is a thin air foil with a sharp leading edge and moderate camber. The leading edge of the wing is sharp in order to enhance the creation of the lift enhancing leading edge vortex during flapping. The separation location for this leading edge vortex is controllable and is used to modulate the lift of the wing on a beat-to-beat basis. Because the coefficient of lift of each wing section is thus controllable, the wings need not beat at varying rates or angles of attack in order to maintain attitude and heading of the vehicle. Thus, the entomopter is designed to function autonomically at a single optimal wing beat frequency. This feature facilitates the incorporation of resonance into the wing beating kinematics. In fact, this resonance is essential for any flapping wing device to operate efficiently. The flapping mechanism for the entomopter provides a resonant single-piece construction that takes advantage of torsional resonance in the entomopter fuselage to recover flapping energy as is common to flying insects which temporarily store potential energy in either the muscles or exoskeletal parts (resilin).

The entomopter wing will be designed to produce lift on both the downstroke *and* the upstroke. Instead of relying on wing twist under muscular control (a complex action requiring an extra degree of freedom in the wing hinge), the wings will be stiffened with materials that react differently to opposite loads. The flexure of the wing ribs (similar to those shown in Figure 26) will cause the wing to deform relative to the leading edge spar (which drives the wing up and down) such that it maintains an angle of attack and camber which provides positive lift on the downstroke.

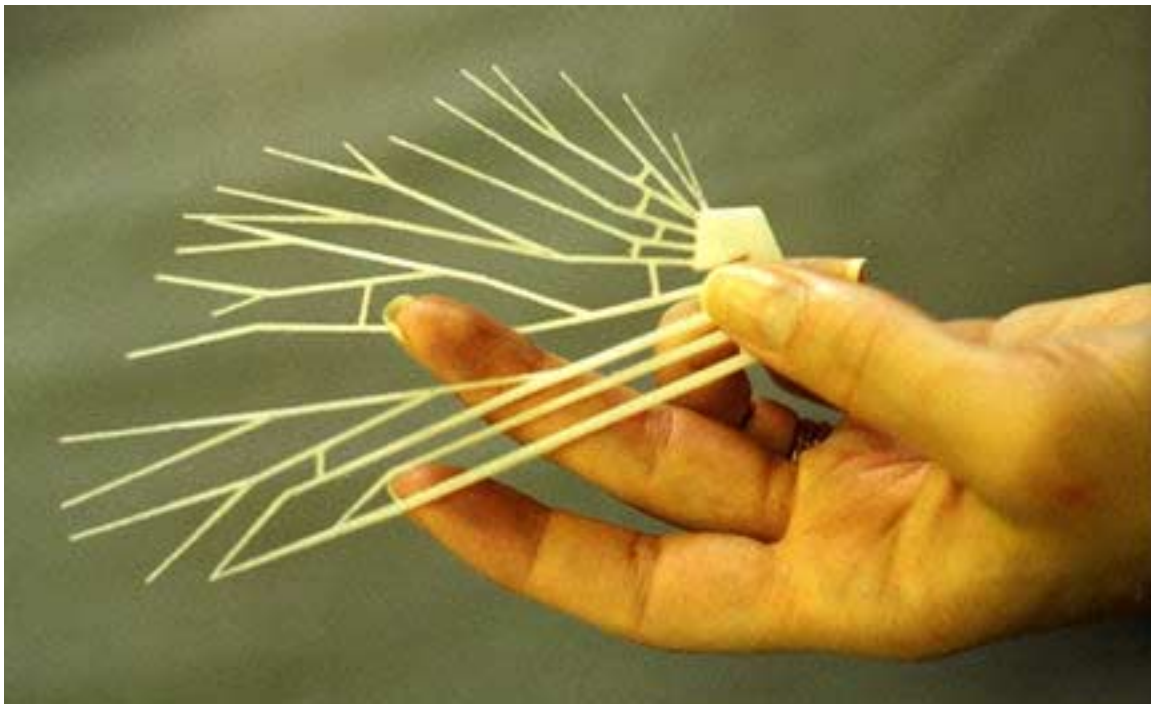


Figure 26. ABS plastic wing ribs from Fused Deposition Modeling machine.

Upon the upstroke, these same ribs will deform under an opposite load to create an angle of attack and camber relative to the leading edge spar that also has an upward lift vector on the inboard section of the wing for at least a portion of the up beat. The interstitial material between the wing ribs serves as the aerodynamic lifting surface, but relies on the wing ribs to give it form. This is depicted in Figure 27.

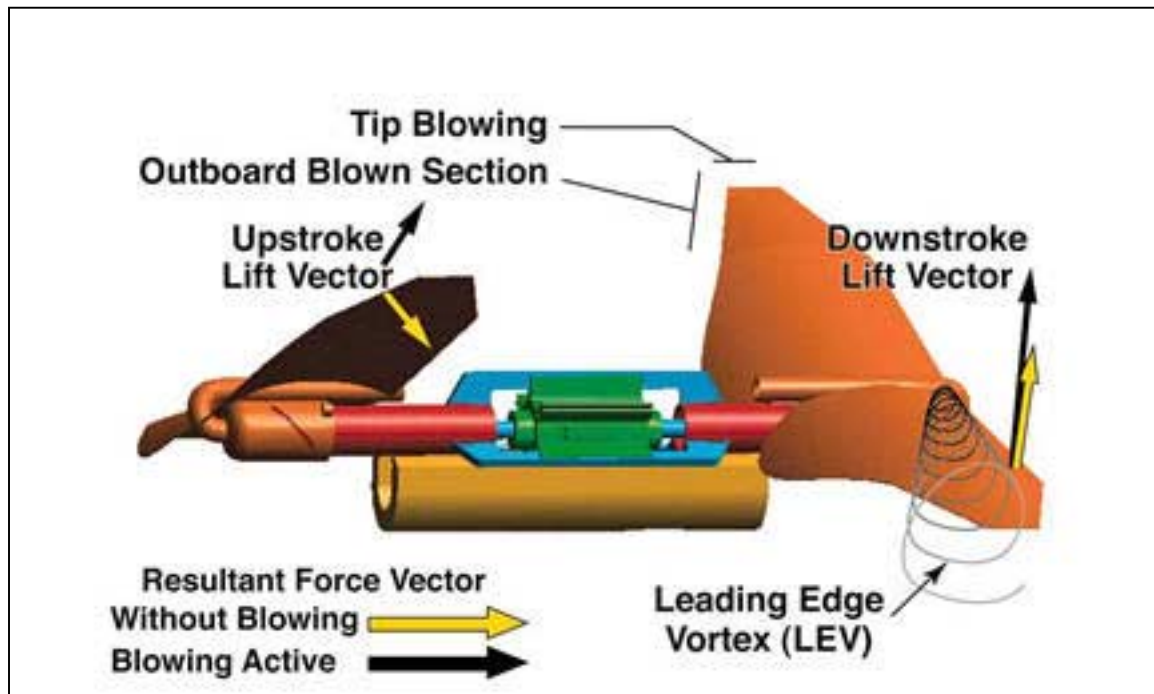


Figure 27. Lift vectors on the upthrust and downthrust wing halves.

In circulation controlled airfoil development work conducted for NASA, generation of positive lift was measured at very large *negative* angles of attack (approaching -70 degrees), and was produced by very high supercirculation caused by the trailing-edge circulation controlled blowing [23, 24]. Coupling the deformation of the wing on the upstroke with intelligent application of circulation control will allow lift to be generated not only on the entire down beat, but on the up beat as well, resulting in an efficiency greater than that of a conventional insect wing. Beyond the up beat lift that can be created, the overall coefficient of lift (C_L) of the wings can be augmented by pneumatic blowing to achieve values that are 5 to 8 times higher than the theoretical maximum achievable by a typical wing planform and camber (which has a C_L of one or less).

Because of the latency in transmissions between Mars and Earth, teleoperation of a Mars Flyer is impractical. Even supervised autonomy is of limited value. A Mars Flyer will have to be able to carry out its science mission without human intervention while being ever cognizant of its environment to assure that it avoids obstacles, hazards, and situations that would result in starvation.

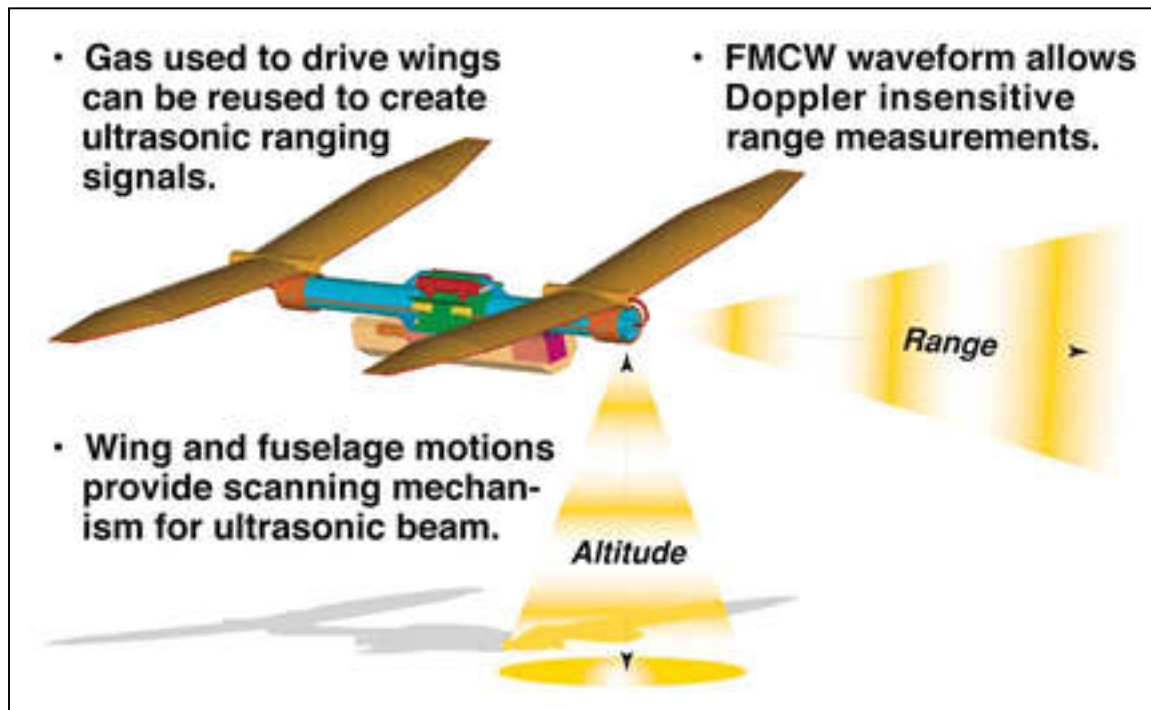


Figure 28. Integral propulsion-ultrasonic obstacle avoidance and altimetry system.

Motivation for navigation would be based on various remote sensors that will be dictated by the type of science experiments to be performed by each entomopter. For example, the search for life might entail sensors that can detect traces of water or fossil bearing rock. Other Mars Flyers might be measuring atmospheric species or performing reconnaissance for later close inspection by ground-based rovers. In each case, the Mars Flyers would use preprogrammed search patterns initially. When measuring a volume as in the case of atmospheric sampling, the entire flight might be preprogrammed. When searching for life, a preprogrammed search pattern would be abandoned in favor of following gradients based on the frequency of occurrence of evidence (motivational behavior). During the landing process, obstacles on the surface must be negotiated (avoidance behavior), and the entomopter must select a spot from which it can launch itself back into the air as it transitions from ground locomotion to flight.

Due to the occurrence of storms on Mars, the entomopter-based Mars Flyers might have to seek shelter on the surface by landing in a self preservation behavior. In all cases however, the Mars Flyers would have to be able to find their way back to the lander or rover in order to replenish depleted fuel supplies as they exhibit a feeding behavior also driven by a self preservation motivation.

The ability to fly autonomously is possible because of the ability of the entomopter to modulate its coefficient of lift for each wing section on a beat-to-beat basis, thereby

controlling attitude. This feature also permits the vehicle to change heading for navigation. Implicit is the presence of an onboard inertial system having stability that is either of duration commensurate with the flight mission length, or that is updated by an external reference analogous to GPS.

Performance Estimates

As a baseline for performance comparison, we are using a 1m wing span conventional fixed wing vehicle (one wing set) with aspect ratio of 5.874 (same as the terrestrial entomopter wing design) flying near the Mars surface at a speed of 100 meters per second. Its wing area is 1.532 sq. ft. Reference atmospheric conditions on the Mars surface are: density = 0.0000279 slugs/cu. ft., atmospheric pressure = 0.11475 psia, and temperature = -20.4°F. At a typical fixed wing lift coefficient of 1.0, that vehicle can carry 2.3 lbs. gross weight (approximately 6.2 Earth lbs. as Mars gravity is 37% that of Earth). That represents a wing loading of only 1.5 lb/sq.ft. due to the low density and pressure compared to an Earth aircraft flying at perhaps 70psf to more than 100 psf.

Based on the same pneumatic aerodynamic data used for the pneumatically enhanced terrestrial entomopter (previous wind tunnel data for circulation controlled wing model with the same aspect ratio), a $C_L=5.3$ is attainable (that is steady-state data, *not* flapping, which will be larger, as discussed below). Assuming that the two-winged entomopter has the same total wing area and aspect ratio as the conventional wing, a reduced wing span of 2.12 ft per wing is achievable. At the same flight speed, such an actively flow-controlled entomopter can lift 12.2 lbs. on Mars (33.0 Earth lbs.). Alternately, if we assume the two aircraft have the same wing areas and a gross weight of 2.3 lbs. (as above), the actively flow-controlled entomopter can reduce the required flight speed from 100 m/s to 43.4 m/s, i.e. the dynamic pressure is reduced from 1.5 psf to 0.284 psf. Finally, if we assume that both air vehicles of aspect ratio = 5.874 fly the same flight speed, (perhaps a lower value of 50 m/s), with 2.3 lbs. gross weight, the actively flow-controlled entomopter can stay aloft with a total wing area of only 1.156 sq. ft. or a wing span of 1.84 ft per wing set, compared to the span of 6.0 ft and area of 6.126 sq. ft. for the conventional wing. The size reduction possibility is clear.

Using the same slot height geometry as our actively flow-controlled terrestrial entomopter, to obtain the blown $C_L=5.3$ requires $C_\mu=0.40$. (C_μ is the “blowing momentum coefficient”, representing the momentum of the gas flowing out of the slot in the wing. It is the product of the mass flow times the velocity of the gas jet flowing out of the slot.) At the flight speed of 100 m/s, $q=1.502$ psf, and the required total slot blowing weight flow = 0.0168 lb/second, the jet velocity=1765 ft/s and blowing pressure required is only 2.5 psig. This is mainly due to the very low external atmospheric pressure and temperature on Mars.

An additional valuable comparison can be made if the appropriate wing loadings and required flight speeds are considered. The terrestrial actively flow-controlled entomopter (or “pneumatic” entomopter) design with two wing sets (i.e., 4 wing panels, 2 front, 2 aft, like a dragonfly) has a wing loading of 0.728 lb/sq ft. For a 1m span Mars Flyer with 2 wing sets scaled to that wing loading and an aspect ratio of 5.874, a flight weight of 2.24 lb can be

achieved. The conventional fixed wing aircraft with the same weight and aspect ratio and one wing set must have a wing loading of twice that, or 1.46 psf. Figure 29 is a plot that shows the flight speeds required for each aircraft at those wing loadings, as well as double the wing loading for each vehicle.

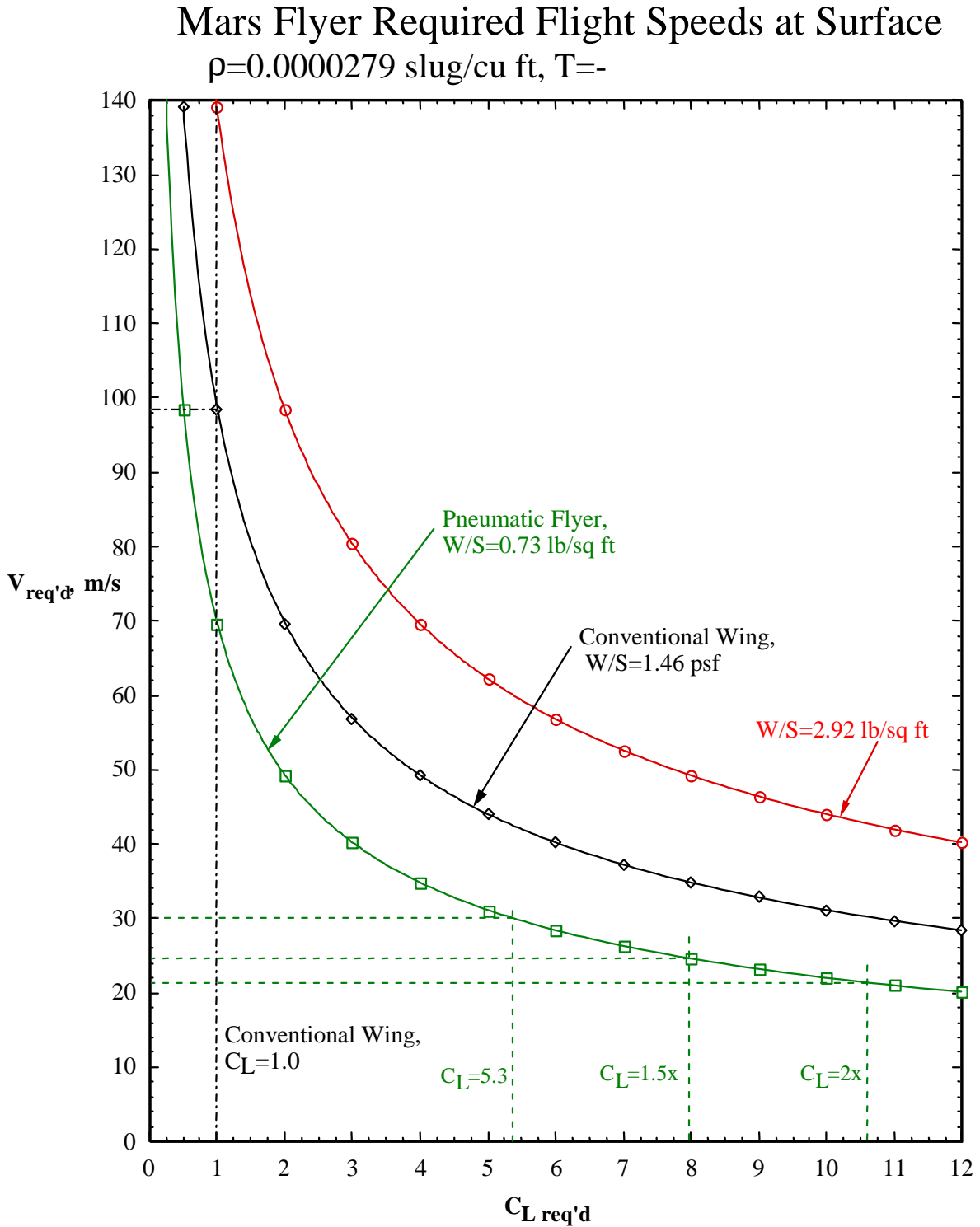


Figure 29. Entomopter-based Mars Flyer flight speed vs required coefficient of lift.

The conventional fixed wing aircraft with $C_L=1.0$ requires a speed of 98.4 m/sec to support that weight in level flight, while the same weight pneumatic entomopter with attainable $C_L=5.3$ can fly at 30.2 m/s. Collaborator in the entomopter design, Charles Ellington of Cambridge University, in his recent paper on the aerodynamics of insect-based flying machines [25] states that flapping-wing unsteady aerodynamics of insects can increase the attainable lift by a factor of 2 to 3 times the steady-state value. Unsteady data for leading-edge shed vortices of pitching helicopter rotor blades show similar trends but somewhat smaller values. So, if a more conservative factor of 1.5 to 2 is assumed, then the pneumatic entomopter can yield C_L of 7.95 to 10.6 with resulting reduced flight speeds of 24.7 and 21.4 m/s respectively.

Note that since the curves are power functions of C_L , doubling a large C_L has lesser effect on the required speed than doubling a smaller value; in this case, doubling the entomopter higher lift coefficient for unsteady effects reduces speed by only 9 m/s. Thus, the exact lift value achieved by the flapping unsteady entomopter has a relatively lesser effect compared to the base steady value, but does serve to produce a favorable effect. However, going from the lift coefficient of 1.0 in the fixed wing aircraft to even the steady-state pneumatic value of 5.3, reduces the required speed by 68.2 m/s or more than 66%! Figure 28 also shows the effect on required speed for either aircraft by doubling the weight or the wing loading. Once again, the high lift attainable by the pneumatic configuration produces a significant effect.

Even on Mars, active flow control on a 2-winged entomopter is beneficial. Certain of the assumptions have yet to be proven, such as the values of steady and unsteady lift coefficient that can be obtained with a fixed or flapping pneumatic entomopter wing converted to a Mars Flyer configuration, but the analysis performed to date shows not only the feasibility of using an entomopter-based Mars Flyer configuration, but the significant advantage in doing so.

Communications

A communications scheme based on Ultra-Wideband (UWB) technology appears to be the best choice for the entomopter vehicle. The information in this section was provided through a written report supplied by Marc Seibert of NASA Glenn Research Center. [26]

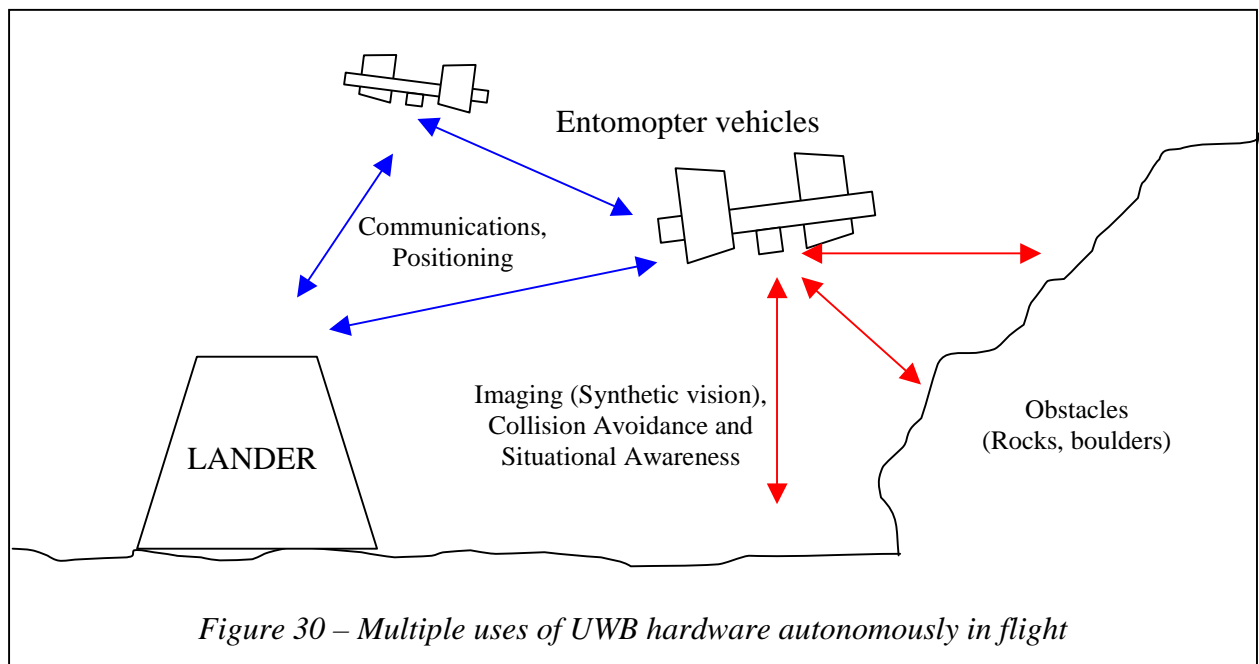
Communications are integral to successful space missions. It is imperative that communications be reliable, robust, and ensure that science is returned from the mission. For high rate communications, UWB impulse trains can be modulated many different ways with information, possibly even adaptively throughout the mission as terrain and other signal propagation factors surface. No UWB modulation techniques are yet approved for terrestrial use (except under certain DoD/NTIA agreements), but several companies including Multispectral Solutions, Inc., Anro Engineering, Aetherwire, Inc. and Time Domain, Incorporated have already developed and are testing UWB-based systems, anticipating limited approval for public use by the Federal Communications Commission [27]. In the future, such systems may be used for wireless computer and voice networks, voice communications, geolocation of “anything” on Earth, and asset tracking (via RF tags) and inter-object positioning. If UWB is approved for public use in

quantities, the benefits of the technology will become readily apparent. Future 4th or 5th generation cellular systems may be developed with this technology, enabling low-power “watch phones.” One UWB wireless network implementation already on the bench has been called “Bluetooth on Steroids.”

UWB technology is based on the process of emitting rapid sequences of extremely short (<1ns), wideband (>1GHz), and extremely low power impulses or “bursts” of radio frequency (RF) energy for a host of desired purposes. UWB waveforms have been used for a variety of classified and unclassified military applications, including independent applications for high-rate communications, intercraft and geo-positioning and/or proximity fuzes, collision avoidance for aerial vehicles, and a variety of imaging, radar, and even electromagnetic pulse warfare systems. UWB impulses are the fundamental element at the core of each of these implementations, and we believe that a multifunctional subsystem could be fabricated and used by one or more manner to perform many functions with the single subsystem with accompanying antennae [28].

UWB is an attractive technology for potentially providing Entomopter missions. The benefits of this technology are listed below and shown in the diagram in Figure 30.

1. High-rate digital communications between one or more Entomopters and a lander vehicle
2. Precise positioning information between Entomopters,
3. In-flight collision avoidance radar imaging, and precise intercraft timing synchronization



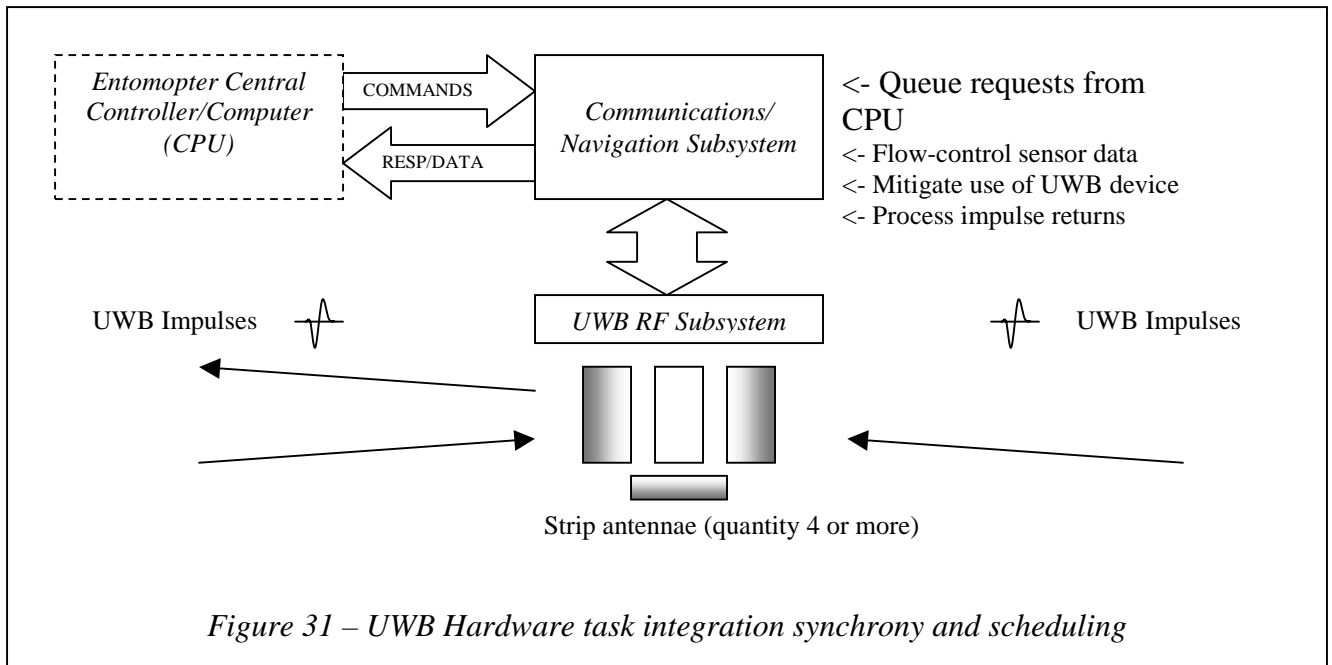
Among all the applications for which UWB has been a core technology, none of the systems appear to combine more than two functions into a single UWB subsystem. The

only space mission known to make use of UWB technology was the Apollo 17 mission in 1967 to the moon, which included a “Ground Penetrating UWB Radar,” used to characterize the lunar regolith. More recently, newer dual-use UWB subsystems have emerged for terrestrial applications, which are strongly convincing, that a single software controlled UWB micro-impulse system could be developed that can:

1. perform all four of the functions listed above concurrently using the same hardware
2. require *significantly* less power, mass and physical space than conventional systems in use, and
3. be reconfigured in real-time to perform these functions, even autonomously, by the vehicles carrying the system.

Unique space flight vehicles such as the Mars entomopter require flexible and hybrid technologies such as a multifunction UWB subsystem to achieve the tight mission architecture goals driving the mission, and effectively make use of precious power and mass budget resources.

The UWB hardware onboard the entomopter will be capable of producing a variety of impulse shapes and frames, and will be software controlled. A master communications and navigation controller onboard the entomopter would continuously reconfigure UWB hardware autonomously and “on the fly” as shown in Figure 18. Upon command or at predefined times, the communications and navigation (COMM/NAV) subsystem will issue periodic impulses that could be coded to simultaneously monitor the location of the ground, and inform the lander of it’s current geo/space-physical position (in three dimensions). The COMM/NAV subsystem will also process returns from collision-avoidance impulses, and additional impulses will be issued to improve the system’s understanding of the size of an obstacle, and so on. Also throughout the mission, specific impulse frames will be filled with communications information back to the lander (or other entomotpers) such as buffered images, meteorological data, entomopter health status, and other types of mission and flight coordination data.

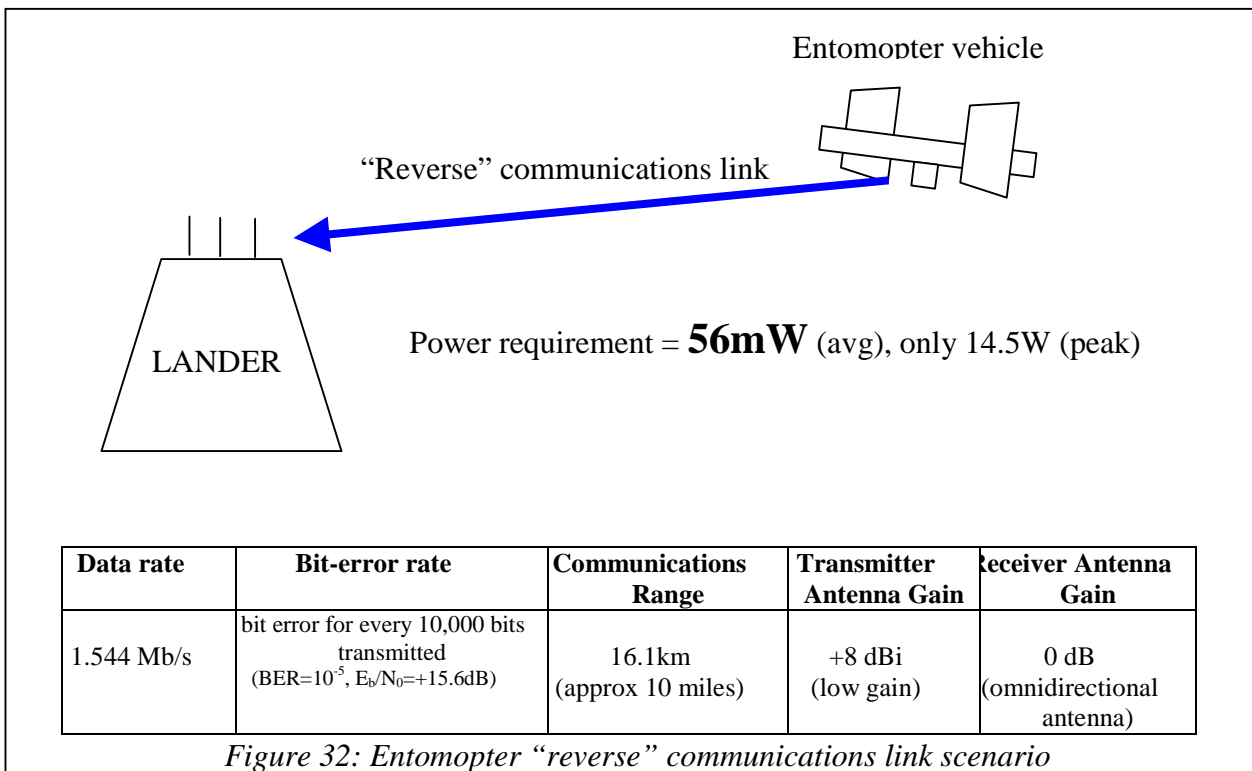


Groups of entomopters may need to hover in formation (depending on the mission), in which case the multifunction UWB subsystem would be used to coordinate the formation flight and synchronize measurement timings. Most importantly, the entomopter itself would autonomously request the use of the impulse energy in whatever ways necessary – imaging, communications, positioning or radar. Intelligent and autonomous flight dynamics must be considered and integrated into the control algorithms for the COMM/NAV subsystem as well.

To illustrate the low power benefits of the technology, consider the UWB data transmission system example in Figure 32. This high-quality channel analysis was performed by MSSSI, Inc. and represents a “reverse-link” in a mobile communications system and is an “uncoded” channel. The link would communicate up to 10 miles, and operate on only 56mW of average power (14.5W peak). Because of the duty cycle requirements of this link, the example above is 14 times more power efficient (11.5dB) than a typical current commercial device and the UWB system can transmit 10 miles at T1 data rates. In most communications circles these power figures are especially small, considering the range and quality of the channel. Error correction coding used extensively in space and other critical communications can further improve the performance of this channel (potentially to 10^{-7} or better). Note that this scenario only illustrates the “reverse” link from the entomopter. The reason for this is because this portion of the link is considered the most power-critical, and has the highest bandwidth requirement, therefore it is most advantageous to illustrate the benefits of UWB in this portion of the link. The same antennae would be used at the lander and entomopter for a

“forward” communications link (to the entomopter), potentially at even higher data rates if mission parameters require. [27]

Figure 32 shows very conservative numbers for antenna gains and expected bit errors (without forward-error correction coding), yet provides for a very high bandwidth link from the entomopter to the lander. The true bandwidth requirements for the reverse link must be defined by the actual mission parameters and the number of science data collection modules being carried onboard. For example, an entomopter carrying four active digital video cameras would require a higher bandwidth reverse communications link than would be required for an entomopter carrying only meteorological sensors. On the specific aerial system developed by MSSSI, Inc. for communications and collision avoidance, a UWB transmitter was fitted to an RC Helicopter. In the flight configuration, the UWB system measured 3" x 4" x 5" with a weight of 27.9 oz. The company notes that this was about *twice the volume necessary* for the circuit boards used, the chassis was much heavier than needed, and that the *UWB boards alone weigh only a few ounces*. In terms of performance, the system operated between 5.4 and 6.0 GHz, only required 0.2 Watts peak power (which can be increased significantly if necessary). A 0.025" wire was detected in flight at 300'. The example shown constitutes typical UWB performance characteristics for existing UWB communications systems. For an entomopter mission to Mars such specifications would be revisited, potentially resulting in increased link performance. In short, mission mass and power budget restrictions directly affect the bandwidth capability of UWB communications, and especially for communications, so UWB technology would greatly benefit a Mars mission.



Location Determination

For precise positioning applications, impulse trains can provide extremely precise positioning accuracies (<cm) at appreciable distances [28]. All mission vehicles could be programmed to regularly issue generic “I am here” type messages (even while solar charging on the ground), or, every impulse transmission from each vehicle could be processed by the lander and analyzed in time to compute the physical position of the “talker” at the instant it is “talking.” Using the first technique may constitute a more reliable means for locating vehicles, however, the second technique is the most bandwidth efficient since no extra impulses would be issued strictly for one purpose. Communications impulse energy could be analyzed for both information content *and* spatial origination. Figure 33 illustrates from a plan (top view) perspective how the antennae on one entomopter and the lander could locate each other in 3-dimensions.

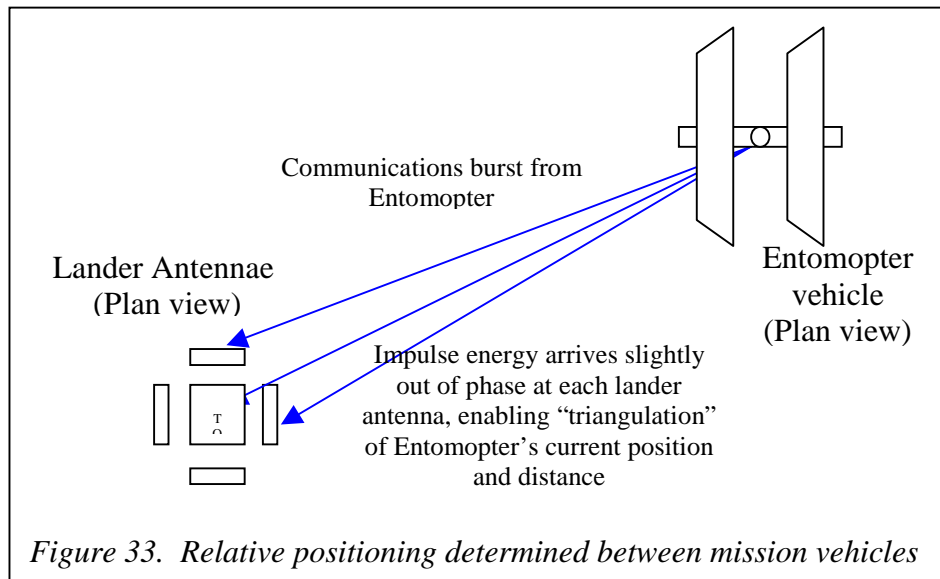


Figure 33. Relative positioning determined between mission vehicles

Radar Collision Avoidance

To suit radar, collision avoidance, and potentially “synthetic vision,” requirements in flight, the same types of impulses can be used to accurately measure scattered components in an environment better than conventional radar. UWB technology has been used for decades for ground-penetrating radar, and one company is even able to locate striations of gold 20 feet into rock. Dolphins naturally emit echolocation impulses similar to UWB waveforms to navigate in unclear waters, and have even located a meal buried a several feet under a sandy sea bottom. UWB radar also has the capability to “range gate” impulse returns, enabling them to ignore returns from close objects (like a wall, boulder, etc) and effectively “see through” these objects to image the environment on the other side.

UWB collision avoidance systems have already been employed in support of DARPA's Micro Air Vehicle (MAV) program, at least one company demonstrating a capability for an autonomous flying vehicle to detect and avoid objects as small as a 0.25" wire in the flight path. This technology could be enhanced to provide an autonomous flight vehicle with this capability, as well as a real-time synthetic view of the environment in any direction, and avoidance of other vehicles in flight. With additional special processing, such a system could be used in conjunction with the intercraft positioning processing to synchronize formation or cluster flight arrangements, and so on.

Distributed Timing, Intercraft Synchronization and Marking Experiment Events in Flight

For precise intercraft timing, a multifunction UWB subsystem can provide the means for intercraft synchronization and for experiment marking events. Similar to the techniques discussed above for communications and positioning, special impulse protocols could be used to announce an impending mark event, trigger entomopter flight coordination events, and broadcast distributed event measurement timing. For example, imagine four entomotpers used to measure upper atmosphere oxygen content in four different physical locations simultaneously. The lander master controller would designate one of the entomotpers as lead timing vehicle, and distribute mission parameters to the vehicles in one broadcast or independently. The lead entomopter would autonomously synchronize timing between the vehicles (in a manner yet to be determined), then coordinate assembly of the proper formation for the experiment and initiate the measurement gathering activity.

This type of experiment autonomy obviously relies on other navigational control capabilities in the entomopter as well, but a multifunction UWB subsystem may enable such complicated autonomy that these systems require. A basic messaging scheme an entomopter master controller and the COMM/NAV subsystem would also be required to facilitate such autonomy.

Summary

The work performed under the Phase I portion of this program addressed the feasibility of utilizing an entomopter vehicle for Mars exploration. The characteristics of entomopter flight do allow the vehicle to operate efficiently within the low density atmosphere of Mars. This is in contrast to a conventional aircraft which has significant difficulty in generating lift and thrust at the low flight Reynolds numbers encountered on Mars.

Mars has been one of the main objects of exploration in our solar system since space exploration began, and the desire to fly a vehicle on Mars has also had an extensive history dating back to the mid 1970's. The majority of the concepts for Mars aircraft never left the analysis stage and only a few had made it to the proof-of-concept or component hardware level although none have ever flown. The main reasons for these concepts not proceeding further were the difficulty in flying an aircraft in the harsh Mars environment and providing a means for significant science return.

The Martian environment provides a number of significant challenges to atmospheric flight, not the least of which is the lack of oxygen to support combustion for propulsion, a rarefied atmosphere, and extremely cold temperatures. Specifically, the Martian atmosphere is over 95% carbon dioxide and is less than 0.5% as dense as the Earth's. The average surface pressure is only 0.7% Earth's atmosphere, which is roughly equivalent to Earth's atmospheric pressure at an altitude of 105,000 ft. The average temperature near the surface of Mars is -63°C , with diurnal highs and lows ranging from $+20^{\circ}\text{C}$ down to -140°C . Mars has only 37% of Earth's gravity, requiring less lift to be generated during flight. A detailed description of the Mars environment and composition of the atmosphere and soil were compiled for the Phase I effort and are included in the Phase I Final Report.

With a conventional aircraft, even if the aerodynamic issues can be solved the mission duration would still be limited, due to a conventional aircraft's inability to land on or take off again from the rocky Mars surface.

An entomopter avoids these issues by utilizing lift generating mechanisms that differ from those of conventional aircraft. Although not yet completely documented, the mechanisms in insect flight are significantly different than that of conventional aircraft. Recent research has produced an understanding of the unique methods that nature uses to create high coefficients of lift: these have been used as starting points to develop working mechanical analogues.

The main mechanism for lift generation on an insect wing is vortex interaction caused by the flapping motion. This interaction is dependent on Reynolds number. As the Reynolds number increases this lift producing mechanism diminishes. Experiments have shown that with flow on an insect wing at Reynolds numbers greater than 10^6 there is a crisis of flow over the wing caused by early boundary layer separation. As the Reynolds number decreases around 10^4 this crisis is greatly reduced and the flow displays a smoother shape. At Reynolds numbers of 10 to 10^3 flow separation is absent. As the Reynolds number decreases other lift producing mechanisms such as differential velocity and drag and other boundary layer effects may come into play. These Reynolds number effects are a main reason for the difference in the flight characteristics between birds and insects.

A Mars entomopter would be a very capable tool for exploration, performing operations impossible with any other platform. For this initial design effort three potential scenarios were devised:

- 1) Independent Exploration using an entomopter: the entomotpers leave the lander as independent explorers. With recharge capability the mission duration and territory are limited only by mechanical failure.
- 2) Exploration within the range of a lander vehicle: the lander acts as fuel source, communications relay, and applications station. Area is limited to round-trip duration capability.

3) Tandem system, the entomopter works in conjunction with a rover: the rover acts as a moving fuel or recharging station for the entomopters, allowing incremental new territories to be investigated thoroughly.

A variety of potential science objectives were investigated and those determined to be the most promising are listed below:

- High resolution surface imaging, inflight and on the surface
- Surface mineralogy and sampling, samples returned to rover, onsite analysis with an alpha proton X-ray spectrometer
- Atmospheric Sampling, collecting at different altitudes for analysis, temperature, pressure, wind speed and direction
- Payload delivery of micro instruments, such as beacons or weather stations
- Magnetic field mapping using a gauss meter to determine the local field
- IR spectral analysis and inflight radar mapping

Based on the mission description an estimate of the power required by the vehicle during operation was produced. A summary of the entomopter system power requirement is listed below:

Communications:	3 Watt Hours per mission, 0.5 Watts max
Science Instruments	10.7 Watt Hours per mission, 2 Watts max
Internal Systems:	6 Watt Hours per mission, 1 Watt max

To meet the power requirements given above three types of power systems were analyzed, and the total mass of each system is listed below.

- Photovoltaic / Battery System: 0.068 kg
- Thermoelectric System: 0.08 kg (isotope only)
- Linear Alternator: not applicable Due to its inability to provide power during periods when the vehicle is on the ground

Based on the mass comparison, the PV/battery system appears to be the best choice for the entomopter power production. Another approach that was addressed to enhance the chosen system, was that a source of long duration low current “keep alive” power may be available from direct conversion of nuclear emissions, to compensate for extended obscuring dust storms, which can last for months. A nuclear generator can be conformally incorporated into the wing with minimum weight penalty, resulting in >12 microwatts for reliable onboard electronics for “keep alive” purposes.

The propulsion systems used in the entomopter is a Reciprocating Chemical Muscle (RCM), which converts the energy stored in a monopropellant into reciprocating motion, with throw, frequency, and power necessary for flight. The gaseous waste product from the decomposition of the monopropellant is used six times further before being expelled. This reuse of waste gases is critical to the efficiency of the RCM and overall endurance of the entomopter.

The RCM meters a monopropellant into a reaction chamber where it is allowed to decompose rapidly and exothermically. Gas products then provide a source of pressure and heat to drive the wings, active flow control for wing lift modulation, gas bearings, ultrasonic ranging system, mass flow amplifier, thermoelectric generator, and thruster. A process control computer meters and controls distribution of the resulting energy.

After comprehensive analysis of fuel, oxidizer, and monopropellant combinations, the propellant selection was narrowed to 4 potential candidates; 2 bipropellants and 2 monopropellants:

- Monomethyl Hydrazine fuel and Nitrogen tetroxide oxidizer
- UDMH fuel and nitrogen tetroxide oxidizer,
- Hydrogen Peroxide
- Nitromethane

These will be further analyzed in Phase II of this program. All of these propellants require hydrogen, therefore it is assumed that unless a water source is found on Mars, the hydrogen needed to produce the selected fuel will be brought from Earth.

The *in situ* manufacture of these fuels will require the ability to produce nitrogen, carbon, and oxygen from Mars' atmosphere. Bipropellants increase the complexity of the overall mission, so an evaluation is needed to determine whether the reduction in hydrogen mass required for a given system is offset by the added equipment necessary to produce a bipropellant. There are a number of processes available for extracting the main constituents of the propellants. The process for their combination into fuel will be investigated during Phase II of this program.

The Mars entomopter design was based on micro vehicles designed for surveillance here on Earth. A terrestrial entomopter having a wing span of ~15 cm. operates in the same Reynolds regime as a scaled up entomopter with a wing span of ~92 cm. in the lower Mars atmosphere. In both cases the entomopter has a twin wing configuration in which the wings flap 180° out of phase at a constant autonomic rate. On earth this flapping frequency ranges between 25 and 30 Hz.

Both the terrestrial and Mars entomopter designs are multimode vehicles capable of not only flight, but limited surface locomotion by means of legs. Legs will be useful to position sensors after landing and to grapple with the rover for refueling. The primary form of locomotion is intended to be flight, and the legs are not for extended ambulation.

The entomopter wing is a thin air foil with a sharp leading edge and moderate camber, to enhance the creation of lift enhancing leading edge vortex during flapping. The separation location for this leading edge vortex is controllable and is used to modulate the lift of the wing on a beat-to-beat basis. Because the C_L of each wing section is thus controllable, the wings need not beat at varying rates or angles of attack to maintain attitude and heading. In fact, the entomopter is designed to function at a single optimal

wing beat frequency, facilitating the incorporation of resonance into wing beating kinematics. essential for efficient operation.

The wing will be designed to produce lift on both the down stroke and up stroke by stiffening with materials that react differently to opposite loads. Coupling the deformation of the wing with intelligent application of circulation control will allow lift to be generated not only on the entire downbeat, but on the up beat as well, resulting in an efficiency greater than a conventional insect wing. Beyond the up beat lift that can be created, pneumatic blowing can augment the overall C_L to achieve values 5 to 8 times than the theoretical maximum achievable by a typical wing planform and camber ($C_L < 1$). Autonomous flight is possible because of ability to control attitude and heading through modulation of the C_L for each wing section on a beat-to-beat basis. An onboard navigation system is implicit.

Comparing with the baseline of a conventional fixed 1 m. single-wing vehicle, which would fly on Mars with a speed of 100 m/s, a pneumatic enhanced Mars entomopter, with an attainable $C_L = 5.3$, could lift 33 Earth pounds and fly at 30 m/s. Utilizing the flapping wing unsteady aerodynamics of insects can increase the attainable C_L value to between 8 and 11.

The conclusion of the Phase I work is that the Mars based entomopter system is a feasible concept and there were no fundamental obstacles to its operation as an airborne Mars surface surveyor. Using an entomopter based exploration vehicle with *in situ* generated fuels could provide a flexible system for extended exploration of the Mars surface. A Mars entomopter, with a 1 meter wingspan may be an elegant and practical architecture to produce a vehicle with the ability to take off, land, and even hover, thereby providing a significant enhancement in mission capability enhancement over conventional aircraft.

Bibliographic References

1. Development Sciences Incorporated, "A Concept Study of a Remotely Piloted Vehicle for Mars Exploration," JPL Contract Number 955012, August 1978.
2. Robert Dudley, *The Biomechanics of Insect Flight: Form, Function, Evolution*, Princeton University Press, 2000.
3. Grodnitsky, D. L., *Form and Function of Insect Wings: The Evolution of Biological Structures*, The John Hopkins University Press, 1999.
4. "Space and Planetary Environment Criteria Guidelines for Use In Space Vehicle Development 1982 Revision (Volume 1)," NASA TM- 82478, January 1983.
5. Personal Correspondence with Viktor.V.Kerzhanovich, JPL, January 2000.
6. Supplied by Robert Brawn, NASA Langley Research Center for the Mars Aircraft Micormission program, March 1999.
7. Cruz, J. and Taylor, G., "Mars Airplane Package, Preliminary Baseline Mission Sites", Document 0867-02-01A, October, 1999.

8. Schofield, J.T., Barnes, J.R., Crisp, D., Haberle, R.M., Larsen, S., Magalhaes, J.A., Murphy, J.R., Seiff, A., Wilson, G., "The Mars Pathfinder Atmospheric Structure Investigation/Meteorology (ASI/MET) Experiment.
9. Cruz, J., "Mars Dust Storms", Mars Airplane Package Document 0807-03-01A. October, 1999.
10. Rieder, R., et al., "The Chemical Composition of the Martian Soil and Rocks Returned by the Mobil Alpha Proton X-Ray Spectrometer: Preliminary Results from the X-Ray Mode, *Science* 278: 1771-1774, 1997.
11. Dr. McKay, C.P. Chair, Mars '03 Airplane Micromission Science Definition Team, "Mars '03 Airplane Micromission Science Definition Team Final Report", Document 0907-01-01A, September, 1999
12. Cutts, J.A., Bauer, J. Blaney, D.L., Lemke, L.G., Smith, S., Stetson, D.S., Kerzhanovich, V.V., "Prepared in support of the Mars Architecture Study", August 1998. (for latest update see <http://telerobotics.jpl.nasa.gov/aerobot/reports/reports.html>)
13. Zweibel, K. "Thin Films: Past, Present, Future", National Renewable Energy Laboratory Document, April, 1997.
14. Ultralife Batteries Inc., Lithium Polymer Specifications, July 2000.
15. Dr. Wing Fai Ng, "Thermoelectric-Based Micro-Air-Vehicles", Mechanical Engineering Department, Virginia Tech, 1998.
16. Angelo, J.A. and Buden D., "Space Nuclear Power", Orbit Book Company, 1985.
17. Handbook of Tables for Applied Engineering Science, 2nd Edition CRC press, 1973. Overview of Propulsion Systems for a Mars Aircraft
18. Colozza, A.J., Miller C., Reed, B., Kohout, L., Loyselle, P., " Overview of Propulsion Systems for a Mars Aircraft," NASA report February, 2000.
19. Kaplan, D.I. et al., "In-Situ Propellant Production on Mars: The First Flight Demonstration", 30th Lunar and Planetary Science Conference, March 1999.
20. Yuasa, S. and Isoda, H., "Carbon Dioxide Propulsion for a Mars Airplane," AIAA-89-2863, 25th Joint Propulsion Conference, 1989.
21. Wickman, J.H., "In-Situ Mars Rocket and Jet Engines Burning Carbon Dioxide," AIAA 99-2409, 35th Joint Propulsion Conference, June 1999.
22. Wickman, J.H., "In Situ Martian Rocket and "Air Breathing" Jet Engines", NASA SBIR Phase II Final Report, Contract NAS8-97048, November, 1998
23. Englar, Robert J., Marilyn J. Smith, Sean M. Kelley and Richard C. Rover III, "Development of Circulation Control Technology for Application to Advanced Subsonic Transport Aircraft, Part I: Airfoil Development" AIAA Paper No. 93-0644, Log No. C-8057, published in AIAA Journal of Aircraft, Vol. 31, No. 5, pp. 1160-1168, Sept-Oct 1994.
24. Englar, Robert J., Marilyn J. Smith, Sean M. Kelley and Richard C. Rover III, "Development of Circulation Control Technology for Application to Advanced Subsonic Transport Aircraft, Part II: Transport Application" AIAA Paper No. 93-0644, Log No. C-8058, published in AIAA Journal of Aircraft, Vol. 31, No. 5, pp. 1169-1177, Sept-Oct 1994.
25. Ellington, Charles. "The Aerodynamics of Flapping Animal Flight," *American Zoology*, vol. 24, 1984, pp. 95-105.

26. Seibert, M.A., "Multifunction Ultra-Wideband (UWB) Subsystem for Entomopter Simultaneous Communications, Positioning, Collision-Avoidance and Radar, NASA Glenn Internal Report, October 2000.
27. From extensive UWB examination over the past two years, and from recent conversations with Dr. Robert J Fontana, President, Multispectral Solutions, Inc., Gaithersburg, MD.
28. Fontana, R.J. Phd, "Experimental Results from an Ultra-Wide Band Precision Geolocation System" To be published in Ultra-Wideband, Short-Pulse Electromagnetics, Kluwer Academic/ Plenum Publishers, 2000.

Appendix A: Mars Atmosphere Data

JPL Reference Mars Atmosphere for -20° Latitude

Mars Atmosphere Model

	cosZ	0.7
Lat= -20	Z,deg	41.9298101

H, km	T, K	P, Pa	ρ , g/m ³	μ , Pa*s	v, m2/s	1/v
9.8750	205	273.6	6.968	1.04E-05	0.00150	667
9.6250	206	280.2	7.100	1.05E-05	0.00148	677
9.3750	207	286.8	7.234	1.05E-05	0.00146	687
9.1250	208	293.6	7.369	1.06E-05	0.00144	696
8.8750	209	300.6	7.507	1.06E-05	0.00142	706
8.6250	209	307.6	7.683	1.06E-05	0.00138	723
8.3750	210	314.8	7.826	1.07E-05	0.00136	733
8.1250	211	322.2	7.970	1.07E-05	0.00135	743
7.8750	212	329.7	8.117	1.08E-05	0.00133	753
7.6250	213	337.3	8.266	1.08E-05	0.00131	764
7.3750	214	345.0	8.416	1.09E-05	0.00129	774
7.1250	215	352.9	8.569	1.09E-05	0.00127	785
6.8750	216	361.0	8.724	1.10E-05	0.00126	795
6.6250	217	369.2	8.880	1.10E-05	0.00124	806
6.3750	218	377.5	9.039	1.11E-05	0.00122	817
6.1250	218	386.0	9.243	1.11E-05	0.00120	835
5.8750	219	394.7	9.407	1.11E-05	0.00118	847
5.6250	220	403.5	9.574	1.12E-05	0.00117	858
5.3750	221	412.5	9.743	1.12E-05	0.00115	869
5.1250	222	421.6	9.914	1.13E-05	0.00114	881
4.8750	223	430.9	10.087	1.13E-05	0.00112	892
4.6250	224	440.4	10.262	1.14E-05	0.00111	904
4.3750	224	450.0	10.487	1.14E-05	0.00108	924
4.1250	225	459.9	10.669	1.14E-05	0.00107	936
3.8750	226	469.9	10.853	1.14E-05	0.00105	948

3.6250	227	480.0	11.039	1.15E-05	0.00104	960
3.3750	227	490.4	11.278	1.15E-05	0.00102	981
3.1250	228	501.0	11.470	1.15E-05	0.00101	994
2.8750	228	511.8	11.717	1.15E-05	0.00099	1015
2.6250	229	522.8	11.917	1.16E-05	0.00097	1028
2.3750	229	534.0	12.172	1.16E-05	0.00095	1050
2.1250	229	545.4	12.433	1.16E-05	0.00093	1073
1.8750	229	557.1	12.699	1.16E-05	0.00091	1095
1.6250	229	569.0	12.971	1.16E-05	0.00089	1119
1.3750	228	581.2	13.308	1.15E-05	0.00087	1153
1.1250	227	593.8	13.655	1.15E-05	0.00084	1188
0.8750	226	606.6	14.012	1.14E-05	0.00082	1224
0.6375	228	619.1	14.174	1.15E-05	0.00081	1228
0.4500	230	629.0	14.276	1.16E-05	0.00082	1226
0.3250	231	635.7	14.365	1.17E-05	0.00081	1229
0.2375	232	640.4	14.408	1.17E-05	0.00081	1228
0.1750	233	643.7	14.422	1.18E-05	0.00082	1224
0.1300	234	646.1	14.414	1.18E-05	0.00082	1218
0.0950	234	648.0	14.456	1.18E-05	0.00082	1222
0.0675	235	649.5	14.427	1.19E-05	0.00082	1214
0.0450	236	650.7	14.393	1.19E-05	0.00083	1207
0.0275	237	651.6	14.353	1.20E-05	0.00083	1198
0.0150	238	652.3	14.307	1.20E-05	0.00084	1190
0.0066	239	652.7	14.257	1.21E-05	0.00085	1181
0.0016	244	653.0	13.970	1.23E-05	0.00088	1135

General Mars Atmosphere Model (NASA Langley)

Altitude(ell), km	Altitude(surf), km	Density (kg/m ³)	Pressure (N/m ²)	Temperature (K°)	Speed of Sound (m/s)
0.00E+00	-5.50E+00	1.44E-02	7.91E+02	2.87E+02	2.68E+02
1.00E+00	-4.50E+00	1.38E-02	7.39E+02	2.81E+02	2.65E+02
2.00E+00	-3.50E+00	1.31E-02	6.88E+02	2.74E+02	2.62E+02
3.00E+00	-2.50E+00	1.25E-02	6.40E+02	2.68E+02	2.59E+02
4.00E+00	-1.50E+00	1.19E-02	5.95E+02	2.62E+02	2.56E+02
5.00E+00	-5.00E-01	1.13E-02	5.52E+02	2.56E+02	2.53E+02
6.00E+00	5.00E-01	1.07E-02	5.11E+02	2.49E+02	2.50E+02
7.00E+00	1.50E+00	1.01E-02	4.72E+02	2.43E+02	2.47E+02
8.00E+00	2.50E+00	9.60E-03	4.35E+02	2.37E+02	2.43E+02
9.00E+00	3.50E+00	9.07E-03	4.00E+02	2.31E+02	2.40E+02
1.00E+01	4.50E+00	8.56E-03	3.68E+02	2.25E+02	2.37E+02
1.10E+01	5.50E+00	7.98E-03	3.37E+02	2.21E+02	2.35E+02
1.20E+01	6.50E+00	7.37E-03	3.08E+02	2.19E+02	2.34E+02

1.30E+01	7.50E+00	6.80E-03	2.82E+02	2.17E+02	2.33E+02
1.40E+01	8.50E+00	6.27E-03	2.58E+02	2.15E+02	2.32E+02
1.50E+01	9.50E+00	5.78E-03	2.35E+02	2.13E+02	2.31E+02
1.60E+01	1.05E+01	5.32E-03	2.15E+02	2.11E+02	2.30E+02
1.70E+01	1.15E+01	4.90E-03	1.96E+02	2.09E+02	2.29E+02
1.80E+01	1.25E+01	4.50E-03	1.78E+02	2.07E+02	2.28E+02
1.90E+01	1.35E+01	4.14E-03	1.63E+02	2.05E+02	2.27E+02
2.00E+01	1.45E+01	3.80E-03	1.48E+02	2.04E+02	2.26E+02
2.10E+01	1.55E+01	3.48E-03	1.34E+02	2.02E+02	2.25E+02
2.20E+01	1.65E+01	3.18E-03	1.22E+02	2.01E+02	2.24E+02
2.30E+01	1.75E+01	2.91E-03	1.11E+02	1.99E+02	2.23E+02
2.40E+01	1.85E+01	2.66E-03	1.01E+02	1.98E+02	2.22E+02
2.50E+01	1.95E+01	2.43E-03	9.12E+01	1.96E+02	2.22E+02
2.60E+01	2.05E+01	2.22E-03	8.26E+01	1.95E+02	2.21E+02
2.70E+01	2.15E+01	2.02E-03	7.48E+01	1.94E+02	2.20E+02
2.80E+01	2.25E+01	1.84E-03	6.77E+01	1.92E+02	2.19E+02
2.90E+01	2.35E+01	1.68E-03	6.13E+01	1.91E+02	2.18E+02
3.00E+01	2.45E+01	1.53E-03	5.54E+01	1.90E+02	2.18E+02
3.10E+01	2.55E+01	1.39E-03	5.00E+01	1.88E+02	2.17E+02
3.20E+01	2.65E+01	1.26E-03	4.51E+01	1.87E+02	2.16E+02
3.30E+01	2.75E+01	1.15E-03	4.07E+01	1.86E+02	2.15E+02
3.40E+01	2.85E+01	1.04E-03	3.67E+01	1.84E+02	2.15E+02
3.50E+01	2.95E+01	9.46E-04	3.31E+01	1.83E+02	2.14E+02
3.60E+01	3.05E+01	8.58E-04	2.98E+01	1.81E+02	2.13E+02
3.70E+01	3.15E+01	7.77E-04	2.68E+01	1.80E+02	2.12E+02
3.80E+01	3.25E+01	7.03E-04	2.41E+01	1.79E+02	2.12E+02
3.90E+01	3.35E+01	6.36E-04	2.16E+01	1.78E+02	2.11E+02
4.00E+01	3.45E+01	5.75E-04	1.94E+01	1.77E+02	2.10E+02
4.10E+01	3.55E+01	5.19E-04	1.74E+01	1.75E+02	2.09E+02
4.20E+01	3.65E+01	4.69E-04	1.56E+01	1.74E+02	2.09E+02
4.30E+01	3.75E+01	4.23E-04	1.40E+01	1.73E+02	2.08E+02
4.40E+01	3.85E+01	3.81E-04	1.25E+01	1.72E+02	2.07E+02
4.50E+01	3.95E+01	3.43E-04	1.12E+01	1.71E+02	2.06E+02
4.60E+01	4.05E+01	3.09E-04	1.00E+01	1.69E+02	2.06E+02
4.70E+01	4.15E+01	2.78E-04	8.95E+00	1.68E+02	2.05E+02
4.80E+01	4.25E+01	2.50E-04	7.99E+00	1.67E+02	2.04E+02
4.90E+01	4.35E+01	2.25E-04	7.12E+00	1.66E+02	2.04E+02
5.00E+01	4.45E+01	2.02E-04	6.35E+00	1.65E+02	2.03E+02
5.10E+01	4.55E+01	1.81E-04	5.65E+00	1.63E+02	2.02E+02
5.20E+01	4.65E+01	1.62E-04	5.03E+00	1.62E+02	2.01E+02
5.30E+01	4.75E+01	1.45E-04	4.47E+00	1.61E+02	2.01E+02
5.40E+01	4.85E+01	1.30E-04	3.98E+00	1.60E+02	2.00E+02
5.50E+01	4.95E+01	1.16E-04	3.53E+00	1.59E+02	1.99E+02
5.60E+01	5.05E+01	1.04E-04	3.13E+00	1.57E+02	1.98E+02
5.70E+01	5.15E+01	9.26E-05	2.77E+00	1.57E+02	1.98E+02
5.80E+01	5.25E+01	8.24E-05	2.46E+00	1.56E+02	1.97E+02
5.90E+01	5.35E+01	7.32E-05	2.18E+00	1.56E+02	1.97E+02
6.00E+01	5.45E+01	6.51E-05	1.93E+00	1.55E+02	1.97E+02
6.10E+01	5.55E+01	5.78E-05	1.71E+00	1.54E+02	1.96E+02

6.20E+01	5.65E+01	5.13E-05	1.51E+00	1.54E+02	1.96E+02
6.30E+01	5.75E+01	4.56E-05	1.34E+00	1.53E+02	1.96E+02
6.40E+01	5.85E+01	4.04E-05	1.18E+00	1.53E+02	1.95E+02
6.50E+01	5.95E+01	3.59E-05	1.04E+00	1.52E+02	1.95E+02
6.60E+01	6.05E+01	3.18E-05	9.21E-01	1.52E+02	1.95E+02
6.70E+01	6.15E+01	2.82E-05	8.14E-01	1.51E+02	1.94E+02
6.80E+01	6.25E+01	2.50E-05	7.18E-01	1.50E+02	1.94E+02
6.90E+01	6.35E+01	2.21E-05	6.34E-01	1.50E+02	1.94E+02
7.00E+01	6.45E+01	1.96E-05	5.59E-01	1.49E+02	1.93E+02
7.10E+01	6.55E+01	1.73E-05	4.93E-01	1.49E+02	1.93E+02
7.20E+01	6.65E+01	1.53E-05	4.34E-01	1.48E+02	1.92E+02
7.30E+01	6.75E+01	1.36E-05	3.82E-01	1.48E+02	1.92E+02
7.40E+01	6.85E+01	1.20E-05	3.37E-01	1.47E+02	1.92E+02
7.50E+01	6.95E+01	1.06E-05	2.96E-01	1.46E+02	1.91E+02
7.60E+01	7.05E+01	9.35E-06	2.61E-01	1.46E+02	1.91E+02
7.70E+01	7.15E+01	8.25E-06	2.29E-01	1.45E+02	1.91E+02
7.80E+01	7.25E+01	7.28E-06	2.02E-01	1.45E+02	1.90E+02
7.90E+01	7.35E+01	6.42E-06	1.77E-01	1.44E+02	1.90E+02
8.00E+01	7.45E+01	5.66E-06	1.56E-01	1.44E+02	1.89E+02
8.10E+01	7.55E+01	4.99E-06	1.37E-01	1.43E+02	1.89E+02
8.20E+01	7.65E+01	4.40E-06	1.20E-01	1.43E+02	1.89E+02
8.30E+01	7.75E+01	4.00E-06	1.09E-01	1.42E+02	1.89E+02
8.40E+01	7.85E+01	3.51E-06	9.55E-02	1.43E+02	1.89E+02
8.50E+01	7.95E+01	3.08E-06	8.39E-02	1.43E+02	1.89E+02
8.60E+01	8.05E+01	2.70E-06	7.36E-02	1.43E+02	1.89E+02
8.70E+01	8.15E+01	2.37E-06	6.47E-02	1.43E+02	1.89E+02
8.80E+01	8.25E+01	2.08E-06	5.68E-02	1.43E+02	1.89E+02
8.90E+01	8.35E+01	1.83E-06	4.99E-02	1.43E+02	1.89E+02
9.00E+01	8.45E+01	1.60E-06	4.38E-02	1.43E+02	1.89E+02
9.10E+01	8.55E+01	1.41E-06	3.85E-02	1.43E+02	1.89E+02
9.20E+01	8.65E+01	1.24E-06	3.38E-02	1.43E+02	1.89E+02
9.30E+01	8.75E+01	1.09E-06	2.97E-02	1.43E+02	1.89E+02
9.40E+01	8.85E+01	9.55E-07	2.61E-02	1.43E+02	1.89E+02
9.50E+01	8.95E+01	8.39E-07	2.30E-02	1.43E+02	1.89E+02
9.60E+01	9.05E+01	7.37E-07	2.02E-02	1.43E+02	1.89E+02
9.70E+01	9.15E+01	6.48E-07	1.78E-02	1.43E+02	1.89E+02
9.80E+01	9.25E+01	5.69E-07	1.56E-02	1.43E+02	1.89E+02
9.90E+01	9.35E+01	5.01E-07	1.37E-02	1.43E+02	1.89E+02
1.00E+02	9.45E+01	4.40E-07	1.21E-02	1.44E+02	1.89E+02
1.01E+02	9.55E+01	3.87E-07	1.06E-02	1.44E+02	1.89E+02
1.02E+02	9.65E+01	3.40E-07	9.35E-03	1.44E+02	1.89E+02
1.03E+02	9.75E+01	2.99E-07	8.22E-03	1.44E+02	1.89E+02
1.04E+02	9.85E+01	2.63E-07	7.24E-03	1.44E+02	1.90E+02
1.05E+02	9.95E+01	2.32E-07	6.37E-03	1.44E+02	1.90E+02
1.06E+02	1.01E+02	2.04E-07	5.61E-03	1.44E+02	1.90E+02
1.07E+02	1.02E+02	1.79E-07	4.94E-03	1.44E+02	1.90E+02
1.08E+02	1.03E+02	1.58E-07	4.35E-03	1.44E+02	1.90E+02
1.09E+02	1.04E+02	1.39E-07	3.83E-03	1.44E+02	1.90E+02
1.10E+02	1.05E+02	1.22E-07	3.37E-03	1.44E+02	1.90E+02

1.11E+02	1.06E+02	1.07E-07	2.97E-03	1.45E+02	1.90E+02
1.12E+02	1.07E+02	9.42E-08	2.62E-03	1.45E+02	1.91E+02
1.13E+02	1.08E+02	8.27E-08	2.31E-03	1.46E+02	1.91E+02
1.14E+02	1.09E+02	7.27E-08	2.04E-03	1.47E+02	1.92E+02
1.15E+02	1.10E+02	6.39E-08	1.80E-03	1.47E+02	1.92E+02
1.16E+02	1.11E+02	5.62E-08	1.59E-03	1.48E+02	1.92E+02
1.17E+02	1.12E+02	4.95E-08	1.41E-03	1.49E+02	1.93E+02
1.18E+02	1.13E+02	4.36E-08	1.25E-03	1.50E+02	1.93E+02
1.19E+02	1.14E+02	3.84E-08	1.10E-03	1.50E+02	1.94E+02
1.20E+02	1.15E+02	3.39E-08	9.78E-04	1.51E+02	1.94E+02
1.21E+02	1.16E+02	2.99E-08	8.68E-04	1.52E+02	1.95E+02
1.22E+02	1.17E+02	2.64E-08	7.70E-04	1.52E+02	1.95E+02
1.23E+02	1.18E+02	2.34E-08	6.83E-04	1.53E+02	1.96E+02
1.24E+02	1.19E+02	2.07E-08	6.07E-04	1.54E+02	1.96E+02
1.25E+02	1.20E+02	1.83E-08	5.40E-04	1.54E+02	1.96E+02

Mars-GRAM generated atmosphere profile for -25° Latitude, 11° Longitude

Height (km)	Density (kg/m ³)	Temperature (K)	Pressure (Pa)	Speed of Sound (m/s)	Viscosity (kg/m s)
2.38	1.25E-02	252.4	594.8	251.11	1.29E-05
2.5	1.24E-02	251.8	589.2	250.82	1.28E-05
2.75	1.22E-02	250.7	577.9	250.27	1.28E-05
3	1.20E-02	249.7	566.9	249.77	1.27E-05
3.25	1.18E-02	248.6	556	249.22	1.27E-05
3.5	1.17E-02	247.5	545.4	248.66	1.26E-05
3.75	1.15E-02	246.5	534.9	248.16	1.26E-05
4	1.13E-02	245.4	524.7	247.61	1.25E-05
4.25	1.12E-02	244.3	514.6	247.05	1.24E-05
4.5	1.10E-02	243.2	504.8	246.49	1.24E-05
4.75	1.08E-02	242.2	495.1	245.99	1.23E-05
5	1.07E-02	241.1	485.6	245.43	1.23E-05
5.25	1.05E-02	240.5	475.4	245.12	1.22E-05
5.5	1.03E-02	239.9	465.4	244.82	1.22E-05
5.75	1.01E-02	239.3	455.6	244.51	1.22E-05
6	9.90E-03	238.7	446	244.2	1.22E-05
6.25	9.71E-03	238.1	436.6	243.9	1.21E-05
6.5	9.53E-03	237.6	427.4	243.64	1.21E-05
6.75	9.35E-03	237	418.4	243.33	1.21E-05
7	9.18E-03	236.4	409.6	243.02	1.20E-05
7.25	9.01E-03	235.8	401	242.72	1.20E-05
7.5	8.84E-03	235.2	392.6	242.41	1.20E-05
7.75	8.68E-03	234.6	384.3	242.1	1.19E-05
8	8.51E-03	234	376.2	241.79	1.19E-05
8.25	8.36E-03	233.4	368.3	241.48	1.19E-05
8.5	8.20E-03	232.8	360.5	241.17	1.19E-05
8.75	8.05E-03	232.2	353	240.86	1.18E-05
9	7.90E-03	231.6	345.5	240.54	1.18E-05

9.25	7.75E-03	231	338.3	240.23	1.18E-05
9.5	7.61E-03	230.4	331.1	239.92	1.17E-05
9.75	7.47E-03	229.9	324.2	239.66	1.17E-05
10	7.33E-03	229.3	317.3	239.35	1.17E-05
10.25	7.18E-03	228.8	310.5	239.09	1.16E-05
10.5	7.04E-03	228.4	303.7	238.88	1.16E-05
10.75	6.90E-03	228	297.1	238.67	1.16E-05
11	6.76E-03	227.6	290.7	238.46	1.16E-05
11.25	6.63E-03	227.1	284.4	238.2	1.16E-05
11.5	6.50E-03	226.7	278.2	237.99	1.15E-05
11.75	6.37E-03	226.3	272.2	237.78	1.15E-05
12	6.24E-03	225.9	266.3	237.57	1.15E-05
12.25	6.12E-03	225.4	260.5	237.3	1.15E-05
12.5	6.00E-03	225	254.9	237.09	1.15E-05
12.75	5.88E-03	224.6	249.3	236.88	1.14E-05
13	5.76E-03	224.2	243.9	236.67	1.14E-05
13.25	5.65E-03	223.8	238.6	236.46	1.14E-05
13.5	5.53E-03	223.3	233.5	236.19	1.14E-05
13.75	5.42E-03	222.9	228.4	235.98	1.13E-05
14	5.32E-03	222.5	223.5	235.77	1.13E-05
14.25	5.21E-03	222.1	218.6	235.56	1.13E-05
14.5	5.11E-03	221.6	213.9	235.29	1.13E-05
14.75	5.01E-03	221.2	209.2	235.08	1.13E-05
15	4.91E-03	220.8	204.7	234.87	1.12E-05
15.25	4.80E-03	220.4	200.1	234.66	1.12E-05
15.5	4.70E-03	219.9	195.6	234.39	1.12E-05
15.75	4.61E-03	219.5	191.1	234.18	1.12E-05
16	4.51E-03	219.1	186.8	233.96	1.11E-05
16.25	4.42E-03	218.7	182.6	233.75	1.11E-05
16.5	4.33E-03	218.3	178.5	233.54	1.11E-05
16.75	4.24E-03	217.8	174.5	233.27	1.11E-05
17	4.15E-03	217.4	170.5	233.05	1.11E-05
17.25	4.06E-03	217	166.7	232.84	1.10E-05
17.5	3.98E-03	216.6	162.9	232.62	1.10E-05
17.75	3.90E-03	216.1	159.2	232.36	1.10E-05
18	3.82E-03	215.7	155.6	232.14	1.10E-05
18.25	3.74E-03	215.3	152.1	231.93	1.09E-05
18.5	3.66E-03	214.9	148.7	231.71	1.09E-05
18.75	3.59E-03	214.5	145.3	231.49	1.09E-05
19	3.51E-03	214	142.1	231.22	1.09E-05
19.25	3.44E-03	213.6	138.8	231.01	1.09E-05
19.5	3.37E-03	213.2	135.7	230.79	1.08E-05
19.75	3.30E-03	212.8	132.6	230.57	1.08E-05
20	3.23E-03	212.4	129.7	230.36	1.08E-05

Mars-GRAM generated atmosphere profile (57° Latitude, 2.35° Longitude)

Height (km)	Density (kg/m ³)	Temperature (K)	Pressure (Pa)	Speed of Sound (m/s)	Viscosity (kg/m s)
-1.74	2.82E-02	168.3	896.7	205.05	8.44E-06
-1.5	2.72E-02	168.8	865.8	205.36	8.47E-06
-1.25	2.63E-02	169.3	842.1	205.66	8.49E-06
-1	2.55E-02	169.8	819	205.97	8.52E-06
-0.75	2.48E-02	170.3	796.5	206.27	8.55E-06
-0.5	2.40E-02	170.8	774.7	206.57	8.57E-06
-0.25	2.33E-02	171.3	753.4	206.87	8.60E-06
0	2.26E-02	171.7	732.8	207.11	8.62E-06
0.25	2.19E-02	172.2	712.7	207.42	8.65E-06
0.5	2.12E-02	172.7	693.1	207.72	8.68E-06
0.75	2.06E-02	173.2	674.1	208.02	8.71E-06
1	2.00E-02	173.7	655.6	208.32	8.73E-06
1.25	1.94E-02	174.2	637.6	208.62	8.76E-06
1.5	1.88E-02	174.7	620.1	208.92	8.79E-06
1.75	1.82E-02	175.2	603.1	209.21	8.81E-06
2	1.77E-02	175.7	586.6	209.51	8.84E-06
2.25	1.71E-02	176.1	570.5	209.75	8.86E-06
2.5	1.66E-02	176.6	554.8	210.05	8.89E-06
2.75	1.61E-02	177.1	539.6	210.35	8.92E-06
3	1.56E-02	177.6	524.8	210.64	8.94E-06
3.25	1.52E-02	178.1	510.4	210.94	8.97E-06
3.5	1.47E-02	178.6	496.4	211.24	9.00E-06
3.75	1.43E-02	179.1	482.8	211.53	9.02E-06
4	1.38E-02	179.6	469.5	211.83	9.05E-06
4.25	1.34E-02	180.1	456.7	212.12	9.08E-06
4.5	1.30E-02	180.6	444.1	212.41	9.11E-06
4.75	1.26E-02	181	431.9	212.65	9.13E-06
5	1.22E-02	181.5	420.1	212.94	9.15E-06
5.25	1.19E-02	181.8	409	213.12	9.17E-06
5.5	1.16E-02	182.1	398.2	213.3	9.19E-06
5.75	1.12E-02	182.4	387.8	213.47	9.20E-06
6	1.09E-02	182.7	377.5	213.65	9.22E-06
6.25	1.06E-02	183	367.6	213.82	9.24E-06
6.5	1.03E-02	183.3	357.9	214	9.25E-06
6.75	1.00E-02	183.5	348.5	214.11	9.26E-06
7	9.77E-03	183.8	339.3	214.29	9.28E-06
7.25	9.49E-03	184.1	330.3	214.46	9.29E-06
7.5	9.23E-03	184.4	321.6	214.64	9.31E-06
7.75	8.97E-03	184.7	313.2	214.81	9.33E-06
8	8.72E-03	185	304.9	214.99	9.34E-06
8.25	8.48E-03	185.3	296.9	215.16	9.36E-06
8.5	8.24E-03	185.6	289.1	215.34	9.38E-06
8.75	8.01E-03	185.8	281.4	215.45	9.39E-06
9	7.79E-03	186.1	274	215.62	9.40E-06
9.25	7.57E-03	186.4	266.8	215.8	9.42E-06
9.5	7.36E-03	186.7	259.8	215.97	9.43E-06
9.75	7.16E-03	187	252.9	216.15	9.45E-06

10	6.96E-03	187.3	246.3	216.32	9.47E-06
10.25	6.77E-03	187.5	239.9	216.43	9.48E-06
10.5	6.59E-03	187.6	233.8	216.49	9.48E-06
10.75	6.41E-03	187.8	227.8	216.61	9.49E-06
11	6.24E-03	188	221.9	216.72	9.50E-06
11.25	6.08E-03	188.2	216.2	216.84	9.51E-06
11.5	5.92E-03	188.4	210.7	216.95	9.53E-06
11.75	5.76E-03	188.5	205.3	217.01	9.53E-06
12	5.60E-03	188.7	200	217.13	9.54E-06
12.25	5.46E-03	188.9	194.9	217.24	9.55E-06
12.5	5.31E-03	189.1	189.9	217.36	9.56E-06
12.75	5.17E-03	189.3	185	217.47	9.57E-06
13	5.03E-03	189.4	180.2	217.53	9.58E-06
13.25	4.90E-03	189.6	175.6	217.64	9.59E-06
13.5	4.77E-03	189.8	171.1	217.76	9.60E-06
13.75	4.64E-03	190	166.7	217.87	9.61E-06
14	4.52E-03	190.2	162.4	217.99	9.62E-06
14.25	4.40E-03	190.3	158.2	218.04	9.63E-06
14.5	4.28E-03	190.5	154.2	218.16	9.64E-06
14.75	4.16E-03	190.7	150.2	218.27	9.65E-06
15	4.05E-03	190.9	146.4	218.39	9.66E-06
15.25	3.95E-03	190.9	142.7	218.39	9.66E-06
15.5	3.85E-03	191	139	218.45	9.66E-06
15.75	3.75E-03	191	135.5	218.45	9.66E-06
16	3.66E-03	191	132.1	218.45	9.66E-06
16.25	3.56E-03	191.1	128.7	218.5	9.67E-06
16.5	3.47E-03	191.1	125.4	218.5	9.67E-06
16.75	3.38E-03	191.1	122.3	218.5	9.67E-06
17	3.30E-03	191.2	119.2	218.56	9.68E-06
17.25	3.21E-03	191.2	116.1	218.56	9.68E-06
17.5	3.13E-03	191.2	113.2	218.56	9.68E-06
17.75	3.05E-03	191.2	110.3	218.56	9.68E-06
18	2.97E-03	191.3	107.5	218.62	9.68E-06
18.25	2.90E-03	191.3	104.8	218.62	9.68E-06
18.5	2.82E-03	191.3	102.1	218.62	9.68E-06
18.75	2.75E-03	191.4	99.5	218.67	9.69E-06
19	2.68E-03	191.4	97	218.67	9.69E-06
19.25	2.61E-03	191.4	94.5	218.67	9.69E-06
19.5	2.54E-03	191.5	92.1	218.73	9.69E-06
19.75	2.48E-03	191.5	89.8	218.73	9.69E-06
20	2.42E-03	191.5	87.5	218.73	9.69E-06